

EXPERIMENTAL DETERMINATION OF TOOL WEAR IN ROUTING  
AND  
TRIMMING OF CFRP COMPOSITES

A THESIS SUBMITTED TO  
THE GRADUATE SCHOOL OF NATURAL AND APPLIED SCIENCES  
OF  
MIDDLE EAST TECHNICAL UNIVERSITY

BY

ZÜHAL PEKER

IN PARTIAL FULFILLMENT OF THE REQUIREMENTS  
FOR  
THE DEGREE OF MASTER OF SCIENCE  
IN  
MECHANICAL ENGINEERING

JULY 2015



Approval of the thesis:

**EXPERIMENTAL DETERMINATION OF TOOL WEAR IN ROUTING AND TRIMMING OF CFRP COMPOSITES**

submitted by **ZÜHAL PEKER** in partial fulfillment of the requirements for the degree of **Master of Science in Mechanical Engineering Department, Middle East Technical University** by,

Prof. Dr. M. Gülbin Dural Ünver  
Dean, Graduate School of **Natural and Applied Sciences**

\_\_\_\_\_

Prof. Dr. R. Tuna Balkan  
Head of Department, **Mechanical Engineering**

\_\_\_\_\_

Prof. Dr. Metin Akkök  
Supervisor, **Mechanical Engineering Dept., METU**

\_\_\_\_\_

Prof. Dr. S. Engin Kılıç  
Co-Supervisor, **Manufacturing Engineering Dept., Atılım Uni.**

\_\_\_\_\_

**Examining Committee Members:**

Prof. Dr. R. Orhan Yıldırım  
Mechanical Engineering Dept., METU

\_\_\_\_\_

Prof. Dr. Metin Akkök  
Mechanical Engineering Dept., METU

\_\_\_\_\_

Prof. Dr. S. Engin Kılıç  
Manufacturing Engineering Dept., ATILIM UNI.

\_\_\_\_\_

Assoc. Prof. Dr. Merve Erdal  
Mechanical Engineering Dept., METU

\_\_\_\_\_

Assist. Prof. Dr. Kıvanç Azgın  
Mechanical Engineering Dept., METU

\_\_\_\_\_

**Date:**

\_\_\_\_\_

**I hereby declare that all information in this document has been obtained and presented in accordance with academic rules and ethical conduct. I also declare that, as required by these rules and conduct, I have fully cited and referenced all material and results that are not original to this work.**

Name, Last Name : Zühal PEKER

Signature :

## **ABSTRACT**

### **EXPERIMENTAL DETERMINATION OF TOOL WEAR IN ROUTING AND TRIMMING OF CFRP COMPOSITES**

Peker, Zühal

M.S., Department of Mechanical Engineering

Supervisor: Prof. Dr. Metin Akkök

Co-supervisor: Prof. Dr. S. Engin Kılıç

July 2015, 99 page

In order to fulfill growing demand for lighter aircraft, Carbon fiber reinforced polymers (CFRP) have been developed, which differ from metals with regards to their machinability characteristics. The main problem in machining process is the damage caused by delamination of CFRP materials which need to be both cut and shorn of fibers at the same time, since they are remarkably abrasive in nature. This research aims at accessing the most appropriate cutting condition with less tool wear in routing and trimming operations for CFRP composite material.

In the current study, a diamond coated interlocked tool with 12 cutting edges and 10 millimeter diameter is used for routing and trimming CFRP composite materials which has unidirectional carbon fibers. The experiments are carried out by altering the spindle speed and feed per tooth value while keeping the radial depth of cut constant.

The experiments were done using 3-axis vertical machining center. At the beginning, 16 feed per tooth values were chosen in 5000 rpm to perform the machining test. The cutting forces were obtained from rotary type dynamometer during cutting operations. Tool wear and delamination measurements were done using an optical microscope.

From the test results, 3 feed per tooth values were observed at 5000 rpm in terms of tool wear and delamination. The best cutting conditions for high surface quality are obtained for high spindle speeds of 5000 rpm and low feed per tooth values of about 0.02, 0.03 and 0.04 mm/ tooth.

Keywords: CFRP composite material, diamond coated interlocked tool

## ÖZ

### KARBON FİBER TAKVİYELİ POLİMER KOMPOZİTLERİN KENAR KESME VE KIRPMA İŞLEMLERİNDE TAKIM AŞINMASININ DENEYSEL OLARAK İNCELENMESİ

Peker, Zühal

Yüksek Lisans, Makina Mühendisliği Bölümü

Tez Yöneticisi: Prof. Dr. Metin Akkök

Ortak Tez Yöneticisi: Prof. Dr. S. Engin Kılıç

Temmuz 2015, 99 sayfa

Hafif uçaklar için artan talebi karşılamak amacıyla, işlenebilirlik özellikleri açısından metallere farklı olan yapısıyla karbon fiber takviyeli polimer kompozitler geliştirilmiştir. Doğada yüksek derecede aşındırı olarak bilinen karbon fiber takviyeli polimer kompozitleri işlemedeki temel sorun, içeriğindeki liflere aynı anda kesme ve kırma işlemi yapılmak zorunda kalındığından, işleme esnasında delemasyonların oluşmasıdır. Bu çalışmadaki amaç, karbon fiber takviyeli polimer kompozit malzemelerin kenar kesme ve kırma işlemlerinde, en az takım aşınmasıyla, en uygun kesme şartlarının elde edilmesidir.

Yapılan çalışmada, tek yönlü serilmiş karbon fiber takviyeli polimer kompozitlerin kesme ve kırma işlemlerinin gerçekleştirilmesinde 10 milimetre çapında, 12 adet kesici ağızı bulunan, elmas kaplamalı birbirine geçmiş profildeki kesici takım kullanılmıştır. Deneyler, radyal kesme derinliğini sabit tutup, devir ve diş başı ilerleme değerlerini değiştirerek yürütülmüştür.

Deneyler 3 eksen dikey işleme tezgahında yapılmış olup, ilk etapta 5000 devirde 16 adet diş başı ilerleme değeri ile gerçekleştirilmiştir. Kesme kuvvetlerinin varyasyonları kesme esnasında döner tip dinamometre ile ölçülmüştür. Takım aşınması ve delaminasyon ölçümleri optik mikroskop kullanılarak yapılmıştır.

Yapılan testlerden takım aşınması ve delaminasyonlar göz önünde bulundurulduğunda, 5000 devirde 3 farklı diş başı ilerleme değeri ön plana çıkmıştır. En iyi yüzey kalitesi için en iyi kesme koşulları yüksek olarak nitelendirilebilecek olan 5000 devirde ve 0.02, 0.03, 0.04 düşük diş başı ilerleme değerlerinde elde edilmiştir.

Anahtar Kelimeler: Karbon fiber takviyeli polimer kompozit, elmas kaplamalı birbirine geçmiş profildeki kesici takım

*To my baby and husband...*

## **ACKNOWLEDGEMENTS**

I wish to express my appreciation to my supervisor Prof. Dr. Metin Akkök and co-supervisor Prof. Dr. S. Engin Kılıç for their guidance, advice and encouragements throughout the study.

I also would like to thank Assist. Prof. Yiğit Karpat and his student Samad Nadimi for their suggestions and comments during the measurements in the Mechanical Engineering Laboratory at the Bilkent University.

I am thankful to TAI for the support and cooperation during my graduate education.

I would like to show my appreciation to my team leader in TAI, Mr. Onur Bahtiyar for his helps and suggestions during the experiments in TAI.

I also appreciate my friend, Res. Assist. Ayşe Irkörücü from Ufuk University for her helps in the analysis part of my thesis.

I am indebted to my family for the love, respect and selflessness to this day.

I can never be thankful enough to God for bestowing me such a perfect husband, Cahit Gdl, whom I owe infinitely much and love eternally.

## TABLE OF CONTENTS

ABSTRACT.....	v
ÖZ.....	vii
ACKNOWLEDGEMENTS.....	x
TABLE OF CONTENTS.....	xi
LIST OF TABLES.....	xiii
LIST OF FIGURES.....	xiv
LIST OF ABBREVIATIONS.....	xvii
CHAPTERS	
1. INTRODUCTION.....	1
1.1. Importance of Composite Material Machining.....	1
1.2. Research Focus and Objectives.....	2
1.3. Thesis Outline.....	2
2. LITERATURE REVIEW.....	3
2.1. Fiber Reinforced Plastics (FRP).....	3
2.2. Machining of FRPs.....	4
2.3. Tool Wear in FRP Machining.....	7
2.4. Cutting Forces in FRP Machining.....	9
2.5. Surface Quality in FRP Machining.....	17
2.6. Chip Formation in FRP Machining.....	22
3. EXPERIMENTAL PROCEDURE.....	25
3.1. Introduction.....	25
3.2. Experimental Set Up For Tool Wear.....	26
3.2.1. Workpiece Material.....	26
3.2.2. Cutting Tool.....	29

3.2.3. Machine Tool Set Up.....	31
3.2.4. Workpiece Clamping System.....	34
3.2.5. Machining Configuration.....	34
3.2.6. Machining Parameters.....	35
3.3. Cutting Force Measurement.....	40
3.4. Tool Wear Measurement.....	46
3.5. Delamination Measurement.....	49
4. ANALYSIS OF RESULTS AND DISCUSSIONS.....	51
4.1. Introduction.....	51
4.2. Machining Configuration.....	51
4.2.1. Cutting Force Measurement.....	53
4.2.2. Tool Wear Measurement.....	62
4.2.3. Delamination Measurement.....	67
4.3. The Thickness of Workpiece Material.....	71
4.4. The Relation of Cutting Forces Between Non-damaged and Damaged Cutting Tool.....	79
4.5. Statistical Analysis of Experimental Data.....	81
4.5.1. Statistical Design Matrix.....	81
4.5.2. Normality Analysis of Factors.....	82
4.5.3. Statistical Output Analysis.....	83
4.6. Results and Discussions.....	88
5. CONCLUSIONS AND FUTURE WORKS.....	95
5.1. Conclusions.....	95
5.2. Future Works.....	96
REFERENCES.....	97

## LIST OF TABLES

### TABLES

Table 3.1 Fiber Orientation of the CFRP Material.....	28
Table 3.2 The CNC Machine Tool Specifications.....	32
Table 3.3 The Machining Parameters in 5000 rpm.....	36
Table 3.4 Kistler Dynamometer Operating Range.....	41
Table 4.1 The Results of the Experiments at 5000 rpm.....	52
Table 4.2 The Experiment Matrix Table.....	53
Table 4.3 The Fiber Orientation of the Second CFRP Material.....	72
Table 4.4 Design Setup of ANOVA Table for the Potential Factors and Response.....	82
Table 4.5 Analysis of Variance Table of Delamination for Linear Model.....	83
Table 4.6 Coefficient Table of Delamination for Linear Model.....	84
Table 4.7 Analysis of Variance Table of Delamination for Second Order Model.....	85
Table 4.8 Coefficient Table of Delamination for Linear Model.....	85

## LIST OF FIGURES

### FIGURES

Figure 2.1 Different Chip Formations [4].....	6
Figure 2.2 Tool Flank Wear Against Cutting Length [7].....	8
Figure 2.3 Flank Wear Against Cutting Length for Different Feeds [7].....	9
Figure 2.4 Feed Force vs. Cutting Length [10]	10
Figure 2.5 Cutting Forces vs. Feed per Tooth for Different Fiber Directions [13].....	11
Figure 2.6 Schematic View of Helical End Milling Tool Segmented into Disks and Convention for Cutting Forces (a) Front view and (b) Top view [17].	13
Figure 2.7 Milling of CFRP Laminates: (a) Milling forces acting on the tool; and (b) Tool eccentricity. [22].....	14
Figure 2.8 Unfiltered Force Data for: (a) 0°; (b) 45°; (c) 90°; and (d) 135° fiber direction CFRP laminates. [22].....	15
Figure 2.9 Tangential ( $F_t$ ) and Radial ( $F_r$ ) Milling Forces: (a) 0°; (b) 45°; (c) 90°; and (d) 135° fiber direction (after filtering) [22].....	16
Figure 2.10 Delamination Types [20].....	19
Figure 2.11 Systematic Scheme Given to Describe the Occurrence of Delamination [23].....	22
Figure 2.12 Chip Formation Mechanisms a) Delamination, b) Buckling and c) Bending [24].....	23
Figure 3.1 The Structure of the Unidirectional (UD) Continuous CFRP Composite Material.....	26
Figure 3.2 The Dimensions of Test Material.....	27
Figure 3.3 Diamond Interlocked Knurled Tool and Two-dimensional Image...	29
Figure 3.4 Technical Parameters of Cutting Tool.....	30
Figure 3.5 The CNC Machine.....	33

Figure 3.6 Machine Tool Spindle Speed- Torque/Output Diagrams.....	33
Figure 3.7 A View of the Workpiece Clamping System.....	34
Figure 3.8 Down (climb) Milling.....	35
Figure 3.9 Up (conventional) Milling.....	35
Figure 3.10 The Workpiece Before and After Machining.....	37
Figure 3.11 The Machining Operation and The Position of Tool During Cutting.....	37
Figure 3.12 Cutting Force Directions.....	41
Figure 3.13 Dynamometer Set up.....	42
Figure 3.14 Cutting Force Data.....	43
Figure 3.15 A View of the Optical Microscope Set up.....	46
Figure 3.16 Some of Cutting Tool Images Under the Microscope for 5000 rpm Spindle Speed.....	47
Figure 3.17 Non-damaged Cutting Tool Image Under the Microscope.....	48
Figure 3.18 Views of Edge Chipping on Cutting Tool Under the Microscope.	48
Figure 3.19 Type II Delamination on the Workpiece.....	49
Figure 4.1 The Cutting Forces for 3000 rpm.....	54
Figure 4.2 The Cutting Forces for 5000 rpm.....	55
Figure 4.3 The Cutting Forces for 7000 rpm.....	57
Figure 4.4 A Schematic View of the Cutting Forces Directions in Climb Milling	58
Figure 4.5 The Radial ( $F_r$ ) and Tangential ( $F_t$ ) Forces for 3000 rpm.....	60
Figure 4.6 The Radial ( $F_r$ ) and Tangential ( $F_t$ ) Forces for 5000 rpm.....	61
Figure 4.7 The Radial ( $F_r$ ) and Tangential ( $F_t$ ) Forces for 7000 rpm.....	62
Figure 4.8 The Images of Tool Wear at 3000 rpm.....	64
Figure 4.9 The Images of Tool Wear at 5000 rpm.....	65
Figure 4.10 The Images of Tool Wear at 7000 rpm.....	66
Figure 4.11 The Images of Delamination at 3000 rpm.....	68
Figure 4.12 The Images of Delamination at 5000 rpm.....	69
Figure 4.13 The Images of Delamination at 7000 rpm.....	70
Figure 4.14 The Workpiece Material Clamping System.....	73
Figure 4.15 The Cutting Forces Results for Second Test Material.....	74

Figure 4.16 The Cutting Tool Images for Second Test Material.....	76
Figure 4.17 The Images from Optical Microscope for Second Test Material...	78
Figure 4.18 The Cutting Force Result on the Damaged Cutting Tool at 7000 rpm.....	79
Figure 4.19 The Cutting Force Result on the Damaged Cutting Tool at 5000 rpm for the Second Workpiece Material.....	80
Figure 4.20 Interaction Effect Plot of Feed per Tooth and Cutting Distance for Delamination.....	86
Figure 4.21 Contour Plot of Feed per Tooth and Cutting Distance for Delamination.....	87
Figure 4.22 Two Fluted Cutting Tool.....	89
Figure 4.23 The Cutting Force Data with Two Fluted Cutting Tool on Original Workpiece.....	90
Figure 4.24 The Cutting Force Data with Two Fluted Cutting Tool on 0° Laminated Workpiece.....	91
Figure 4.25 The Cutting Force Data with Twelve Fluted Cutting Tool on 0° Laminated Workpiece.....	91
Figure 4.26 The Results of Experiments According to Spindle Speed and Feed per Tooth.....	93

## **LIST OF ABBREVIATIONS**

CFRP	Carbon Fiber Reinforced Polymer
FRP	Fiber Reinforced Plastics
RPM	Revolution per Minute
UD	Unidirectional
ANOVA	Analysis of Variance
df	Degree of Freedom
F value	Value of Anova



# CHAPTER 1

## INTRODUCTION

### 1.1 Importance of Composite Material Machining

Carbon Fiber Reinforced Polymer (CFRP) composites are used in a widespread manner in industries like aerospace, automotive and maritime due to their high genuine strength and stiffness. Moreover, they possess good thermal resistance, corrosion resistance, damping resistance and dimensional stability. Composites became the demanded choice of material as high strength and light weight are major criteria in aerospace industries. However, composite material machining becomes a major matter of concern in the industry because of the inhomogeneous structure of CFRP.

In order for a machined component to be reliable for its service application, the machined surface needs to be of good quality. Composites nevertheless have to go through finishing operations to provide the dimensional specifications for assembling with forth components even though they are manufactured near net shape. The finalizing processes include trimming, drilling and turning. Yet owing to the non-uniform nature of fiber reinforced composites, the machined surface of such material will be rugged and most likely to be delaminated, spalled and splintered. Machining also leads to some changes in the mechanical and chemical properties of the each part used in the composite. For that reason, the performance of a composite mainly relies on the surface condition generated by machining. Accordingly, the quality of a machined surface for its service life is highly crucial. Information about the machining characteristics of these materials is not sufficient enough, and there has not been much work accomplished to examine the effect of process parameters on

machined CFRP composite quality. This study focuses on studying the impact of process parameters like spindle and feed speed in edge trimming of a CFRP composite material on machined surface quality.

## **1.2 Research Focus and Objectives**

This study concentrates on quantifying the amount of machining damage on a CFRP composite material going through trimming operation based on delamination depth. The point is to specify the influence of process parameters such as spindle speed and feed speed on the surface quality of machined CFRP constituents. The purpose of this is to achieve the most convenient cutting condition with less tool wear in routing and trimming operations for CFRP composite material. Unidirectional carbon fiber reinforced polymer with the thickness of 3.5 millimeter is used as a workpiece material in this thesis. Diamond coated interlocked knurled cutting tool with 12 cutting edges and 10 millimeter diameter is selected to observe suitable cutting conditions during the experiments.

## **1.3 Thesis Outline**

This thesis consists of six chapters. First chapter is introduction on the importance of composite material machining in today's industries. The second chapter gives background information and literature review on machining of CFRP materials, cutting forces, chip formation mechanisms, tool wear and surface quality obtained. In the third chapter, the experimental set up for cutting force and tool wear measurements, workpiece material and machining parameters used are given. The fourth chapter, on the other hand, deals with the analysis and discussion of the results. The statistical analysis of the experimental data is also given in chapter four. In the fifth chapter, the conclusions derived and future works for the improvements of CFRP machining are given.

## **CHAPTER 2**

### **LITERATURE REVIEW**

#### **2.1 Fiber Reinforced Plastics (FRP)**

Composites are inhomogeneous materials which are composed of two phases called the matrix phase and the reinforcement phase that are intentionally joined to form structures with desired properties. Distinct boundaries between the phases are known as interface, and the phases are macroscopically distinguishable with them. The matrix phase is necessary to hold the reinforcement phase, to distribute the applied load and to protect the composite from adverse environmental conditions like heat, cold, moisture and corrosion. On the other hand, the role of the reinforcement phase is to provide strength for the composite, to conduct or resist corrosion and electricity. The materials, metal, polymer or ceramic, can be used for the matrix and reinforcement phase. In order to use the reinforcement materials in composite construction they should be in the form of flakes, particles, sheets, whiskers and fibers.

Composites are categorized in accordance with the sort of matrix materials and the form of reinforcement material used. The choice of reinforcement material should be in the manner that they carry high strength and stiffness for reinforcement increases the properties of the composite. In fibrous form reinforcement materials maintain their strength and stiffness much more than in any other form, so fibers are mostly used as reinforcement materials in composite construction; that's why they are called as fiber reinforced polymers (FRP).

Composites, which are gathered by stacking a number of thin layers of fibers and matrix, and by consolidating them into needed thickness are feasible in laminate

form in general fiber reinforced. A great variety of physical and mechanical properties can be acquired with the composite that is specific to the application purpose by managing the stacking succession and orientation of fiber in each layer, and in industrial applications, composites get the edge over metals and alloys with the help of this. The properties of fiber reinforced composites are extensively based on the lay and on the characteristic of each component of the composites i.e. the fiber-matrix interface.

Fiber reinforced composites offer high strength-weight ratio, high modulus weight ratio, high fatigue strength-weight ratio, high fatigue damage tolerance, low coefficient of thermal expansion and high internal damping [1]. These characteristics make fiber reinforced composites emerge as the major structural material in the aerospace, automotive and maritime industry where weight reductions as well as exceptional physical and mechanical properties are of major concern.

## **2.2 Machining of FRP**

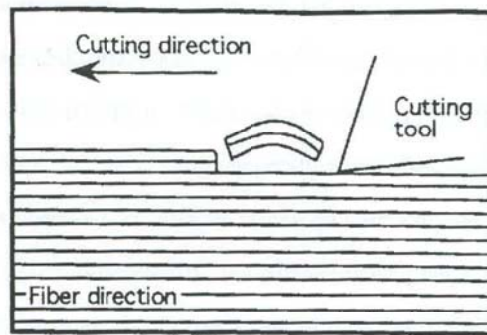
It is essential to understand the machining of FRP in greater depth in order to advance the machining process parameters. It is the curing process where the composites are generally developed to their end shape; nevertheless, they still need to undergo finalizing operations to meet their dimensional and geometrical tolerance requirements. The common finalizing stage used in industry is edge trimming. This process can be carried out with conventional router machines and with non-conventional machining processes, like electrical discharge machining, ultrasonic machining, laser machining and abrasive water jet machining [2]. Non-conventional machining processes have drawbacks like motion of a heat-affected zone and low material removal rate. As a result, conventional router and abrasive water jet machining are more preferable choices for trimming.

Machining of FRP entirely differs from machining of metals and alloys. FRPs are heterogeneous materials. Therefore, material behavior is inhomogeneous and depends on the particularizations of the fiber, matrix and the fiber orientation. Hence, this inhomogeneity causes roughness and less regularity on machined FRP surfaces compared to those of machined metal surfaces. It has been asserted that the chip

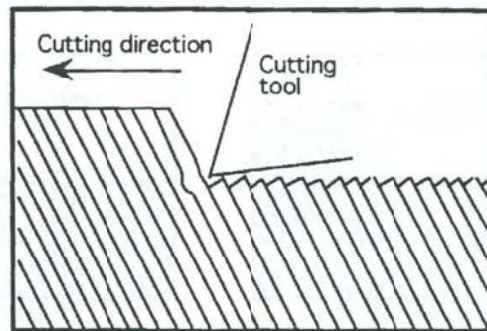
formation process and the fiber lay direction with respect to cutting direction significantly effects the machined fibrous composite surface [3]. Chip formation process in machining of FRP, which depends on three mechanisms called abrasion, plowing and cutting for producing a new surface, is completely different from machining of metals [4].

In abrasion the softer matrix is cut by the tool, and the chip is separated. In plowing, the material is pushed by the tool which in turn deforms it plastically whereas the fibers are severed while cutting it. Whether deformation, rupturing or shearing causes chip formation or not will be identified through the integration of these three mechanisms, fiber orientation and the direction of cutting. It is improper to use mechanisms that require rupturing of fibers and debonding between the matrix and fiber in the cutting of a composite laminate with fiber orientation along the direction of cutting. The reason behind this is the fracturing of fibers into pieces as the tool moves parallel to the fiber orientation.

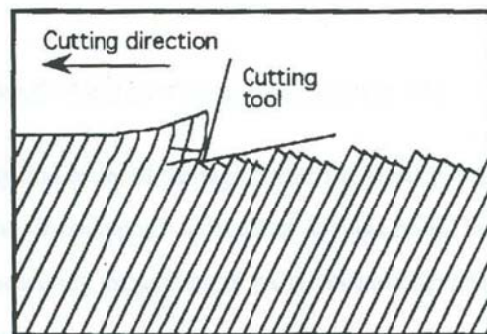
Deformation or shearing is the failure mechanism while a composite laminate is machined with fiber oriented at an angle to the cutting direction [4]. So, as the tool moves to the fiber oriented at an angle, the fiber is crushed and fractured sharply. Consequently, the fibers that are fractured bulge out from the machine surface, plies come loose, surface gets rougher, and delamination and cracks, which can be classified as large machine damages are apparent. Figure 2.1 demonstrates the rupture, deformation and shearing of a composite laminate has undergone different fiber orientation.



(a) Rupture



(b) Deformation



(c) Shearing

Figure 2.1 Different Chip Formations [4]

Hence, due to the inhomogeneity and abrasive characteristic of fibers, tool selection in machining FRP is also a major problem. Intense hardness of the fiber limits tool selection to remarkably hard and costly materials. For trimming FRP composites, polycrystalline diamonds or carbide tools are used as cutting tools since they have a prolonged tool life and are highly resistant to abrasion and crumbling [5].

The top and bottom layers have the greatest effect on machining quality in composite machining, which makes it necessary to take account layer properties while selecting the tool geometry. Tools made of polycrystalline diamond or carbide cutting materials that have multiple cutting edges are preferred to trim route glass or carbon fiber reinforced composites as they resist intermittent cutting of both hard and soft materials. Additionally, they have a long tool life and maintain their surface quality. Another important problem related to machining FRP is the generation of air borne dust that could lead to serious health problems and damage the electronic parts of the machine. Hence owing to the abrasive nature of the fiber tool, wear increases rapidly resulting in poor surface quality and hazardous dust that makes it necessary to optimize the machining process.

### **2.3 Tool Wear in FRP Machining**

The mechanical and physical properties of composites change with respect to the type of fiber, matrix material, fiber orientation, and the composition of the fiber and the matrix. For this reason, their machining behavior also changes. The cutting tool experiences pulsating loads and large-scale abrasion due to the friction of fibers on the machined work surface over the flank part of the cutting tool [6]. In the FRP machining process there is not just one type of wear, which demonstrates the condition of a tool truly. In machining of metals, flank wear is the most descriptive form of wear that specifies the condition of the tool. That is why flank wear is used extensively to indicate the tool life in FRP machining. Using a particular wear type to calculate tool life and to specify tool condition is predominantly based on the pattern of wear that is mainly observed in the course of the machining process [7].

Process parameters like spindle speed, feed rate, cutting distance, and depth of cut have an enormous effect on tool wear. Regardless of other process parameters and the type of machining, tool wear increases with an increase in cutting distance, the effect of which can be seen in Figure 2.2. [8], [9], [11], [10], [6].

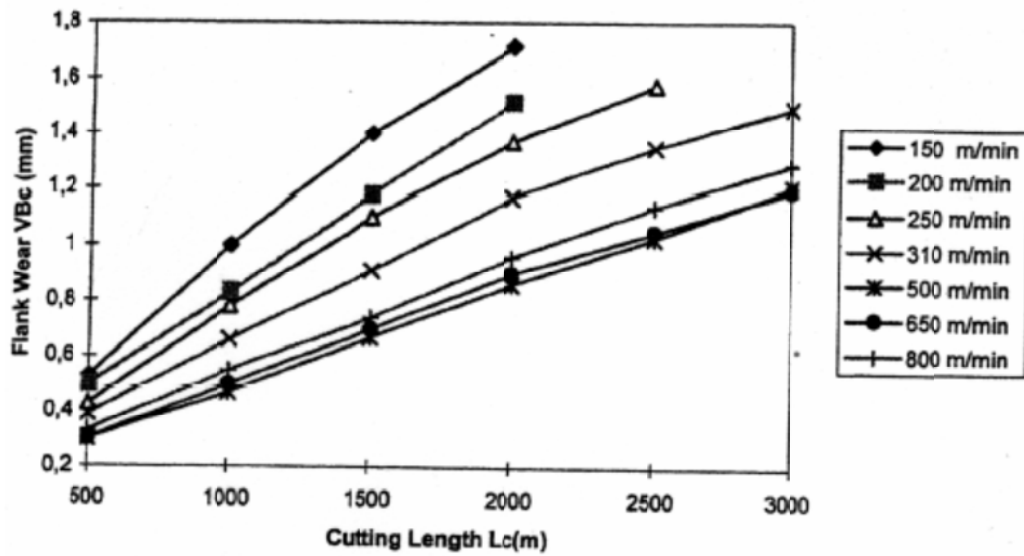


Figure 2.2 Tool Flank Wear Against Cutting Length [7]

Figure 2.2 demonstrates that flank wear mounts with rise in feed speed. Other experiments undertaken with regards to carbon fiber reinforced plastics (CFRP), and glass fiber reinforced polymers (GFRP) suggest that for turning, drilling, and milling operations, tool wear increases as feed speed goes up[9]. Studies on the turning and drilling of FRP concluded that tool wear lessens with an increase in feed per rotation. This decrease is related to the reduction in cutting resistance due oxidation induced by the increase in cutting temperature [7]. The effect of feed per rotation on tool wear for turning of FRP is shown in Figure 2.3.

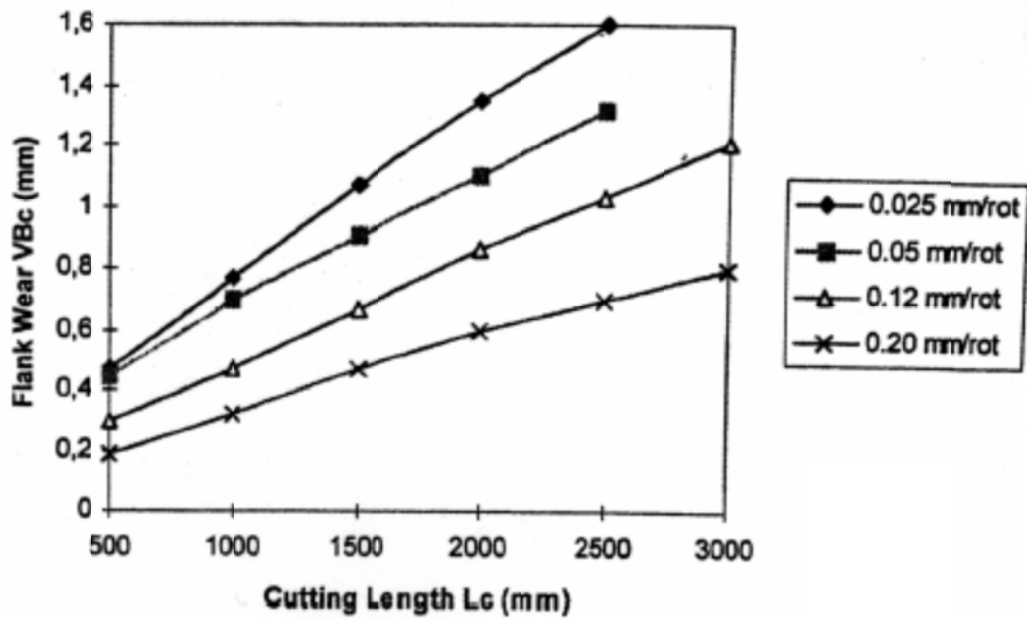


Figure 2.3 Flank Wear Against Cutting Length for Different Feeds [7].

## 2.4 Cutting Forces in FRP Machining

The performance of a cutting tool or the machinability of a work material can be assessed by evaluating the cutting forces. The cutting forces for cutting parallel and perpendicular to the fiber axis are different. Shearing takes place when cutting perpendicularly whereas buckling takes place in the former case. This variation makes the investigation of cutting forces difficult during machining. There are three constituents of cutting force observed during trimming of FRP that are feed force, normal force, and axial force. Studies indicate that feed force is generally larger than the other two components of the cutting force [11].

In a study, Ferreira et al. [10] turned a CFRP rod using cutting tools made of coated, and uncoated cemented carbide, ceramics, CBN, and PCD. The results showed that with an increase in cutting length and feed force also went up. The effect of cutting length on feed force is shown in Figure 2.4 [10].

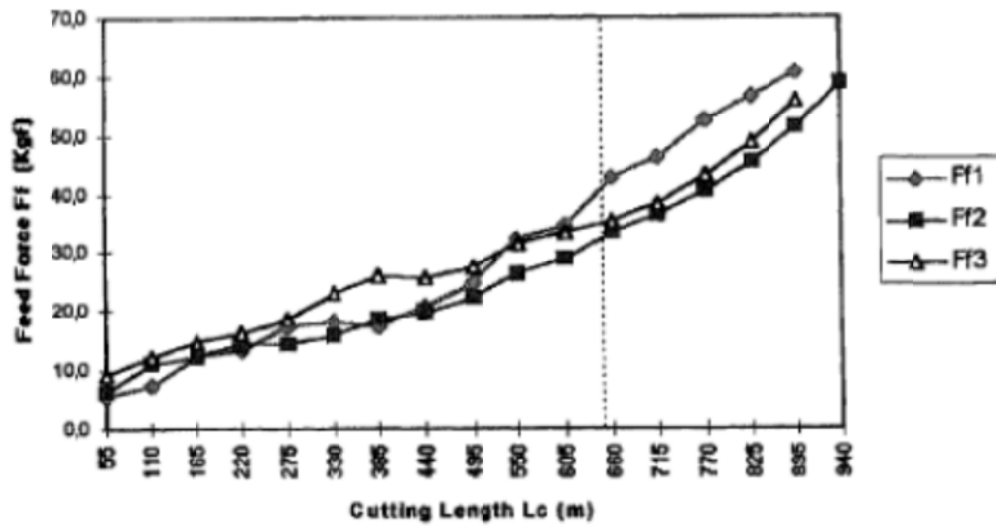


Figure 2.4 Feed Force vs. Cutting Length [10]

Puw et al. carried out a study in the milling of CFRP to examine the effect of feed rate on cutting forces. The experiment was undertaken at different spindle speeds (1500, 3000 rpm), and feed rates (50, 150 mm/min). Results of the study suggest that all the three components of cutting force rise with feed per tooth irrespective of the fiber orientation. The results are presented in Figures 2.5 a, b & c [13].

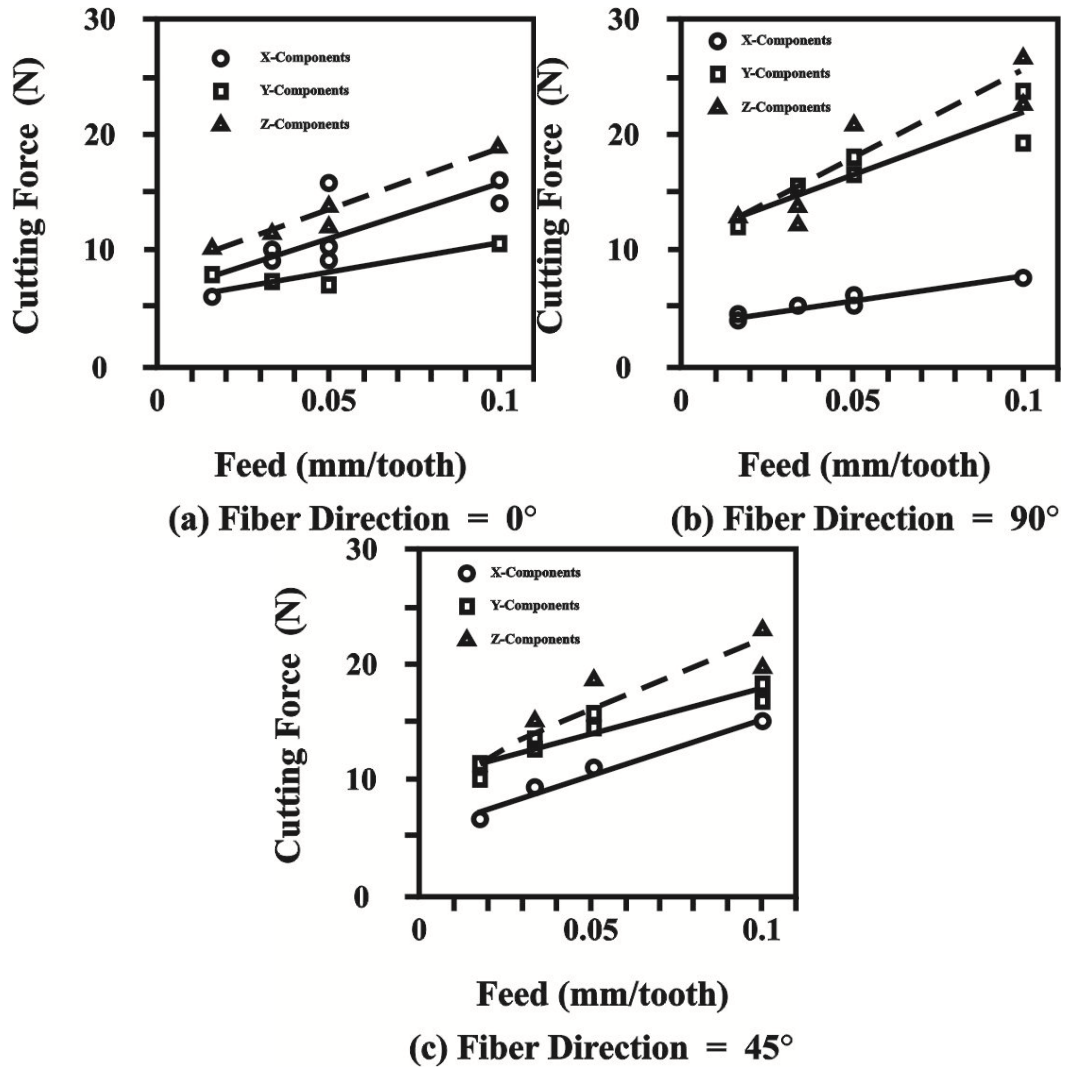


Figure 2.5 Cutting Forces vs. Feed per Tooth for Different Fiber Directions [13]

Cutting forces are heavily influenced by the process parameters like cutting speed, feed rate, and depth of cut. All three components of cutting force mount with increases in the feed rate, and the depth of cut, whereas they decrease with an increase in cutting speed [9], [10], [11], [13], [14], and [15]. Cutting forces also escalate with an increase in tool wear [16].

Mechanistic modeling is a simple, operative and strongly formed semi-empirical technique. In this technique, existing cutting forces are modeled by experimenting to identify constant parameters of tool geometry-workpiece material pairs. As the structure of composites is heterogeneous, it is much more difficult to investigate the machinability analytically, particularly for real-life problems where multi-directional

composites are widely used. In this sense, empirical models might be argued to be much more efficient than the analytical ones with an acceptable error.

A study that was able to predict the cutting forces for helical milling tools was undertaken by Kalla and Sheikh-Ahmad [17]. They adopted a mechanistic modeling methodology by converting specific cutting energies from orthogonal cutting to oblique cutting. The model was able to make congruent cutting force predictions for helical end milling by dividing the cutter into a stack of disk elements of finite thickness with oblique cutting edges along the axis. The related figure is shown in Figure 2.6. Overall cutting force was obtained by estimating and integrating the force contribution of each differential disk over the laminate thickness. The experiments were undertaken with the use of two-fluted, carbide helical end mills. The 9.5 mm diameter of this tool is half of the straight edge tool used to generate the orthogonal cutting database.

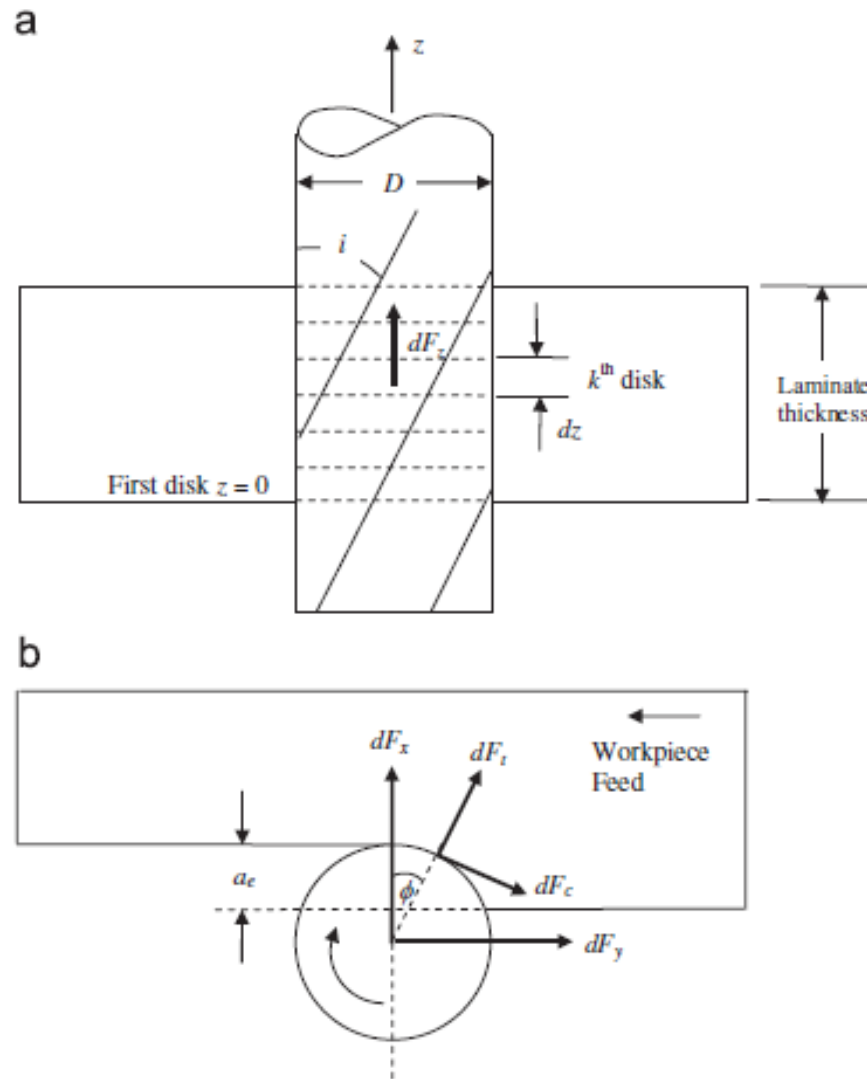


Figure 2.6 Schematic View of Helical End Milling Tool Segmented into Disks and Convention for Cutting Forces (a) Front view and (b) Top view [17]

Besides, Kalla and Sheikh-Ahmad, Karpat also conducted studies on mechanistic force modeling [21], [22]. A mechanistic cutting force model for milling CFRPs was asserted in the study based upon experimental cutting force data collected during slot milling of unidirectional CFRP laminates where two different polycrystalline diamond cutters were used. Cutting force coefficients in radial and tangential directions were calculated as a function of the fiber cutting angle. The relationship is epitomized with simple sine functions. The mechanistic model was shown to be able to predict cutting forces in course of the milling of multidirectional CFRP laminates.

Cutting forces that act on the tool during the milling process is shown in Figure 2.7. The figure clearly depicts that tangential forces ( $F_t$ ) act in the opposite directions of the cutting whereas radial forces ( $F_r$ ) are directed towards the center of the tool. Radial and tangential forces can be calculated via the mechanistic force modeling approach [21], [22] in relation to material and tool properties. This approach can be used to obtain cutting force coefficients in tangential and radial directions as a function of fiber cutting angle using milling tests.

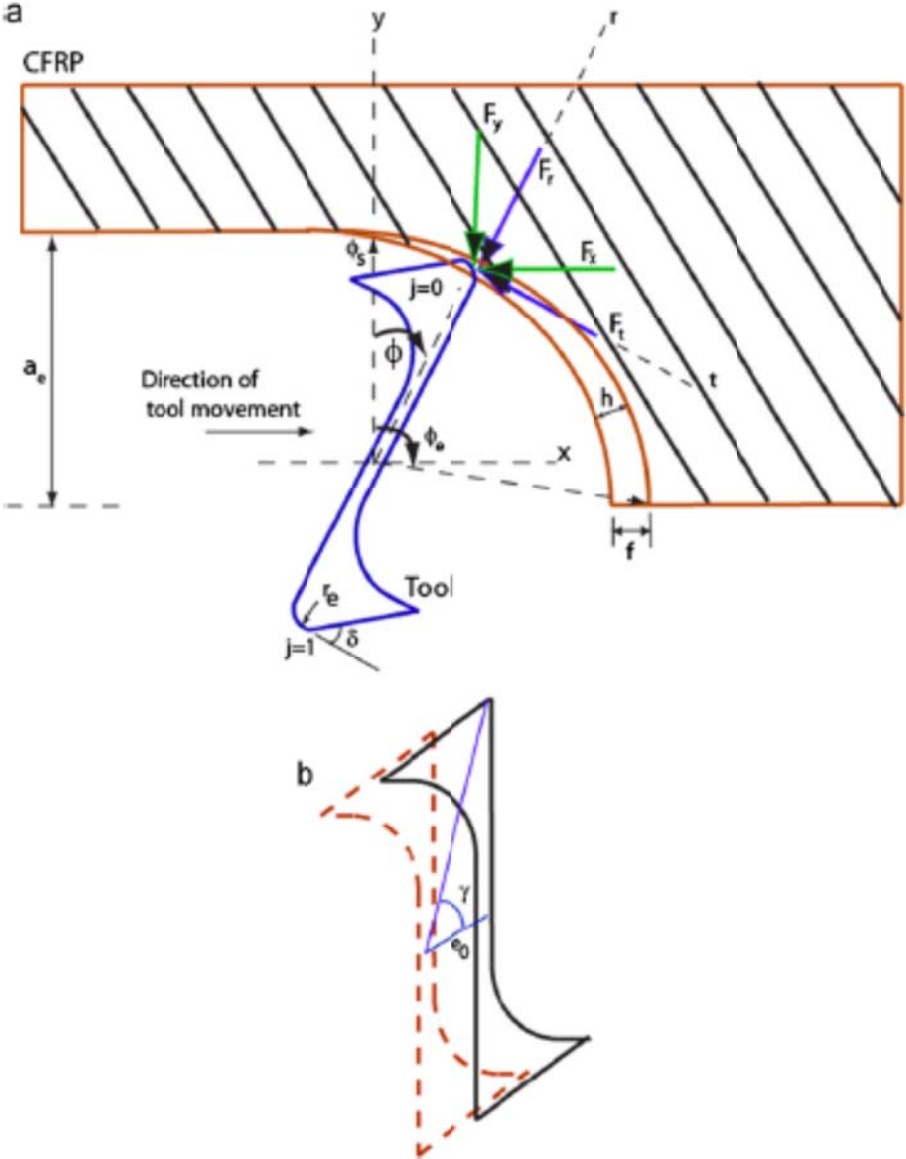


Figure 2.7 Milling of CFRP Laminates: (a) Milling forces acting on the tool; and (b) Tool eccentricity [22]

In order to avoid carbon powders, the experiments were conducted under wet conditions. Milling force measurements in x, y, and z directions pursuant to the reference system of the dynamometer are presented in Figure 2.8. In all milling cases, forces in vertical directions ( $F_z$ ) were quite small due to the zero helix angle of the cutter.

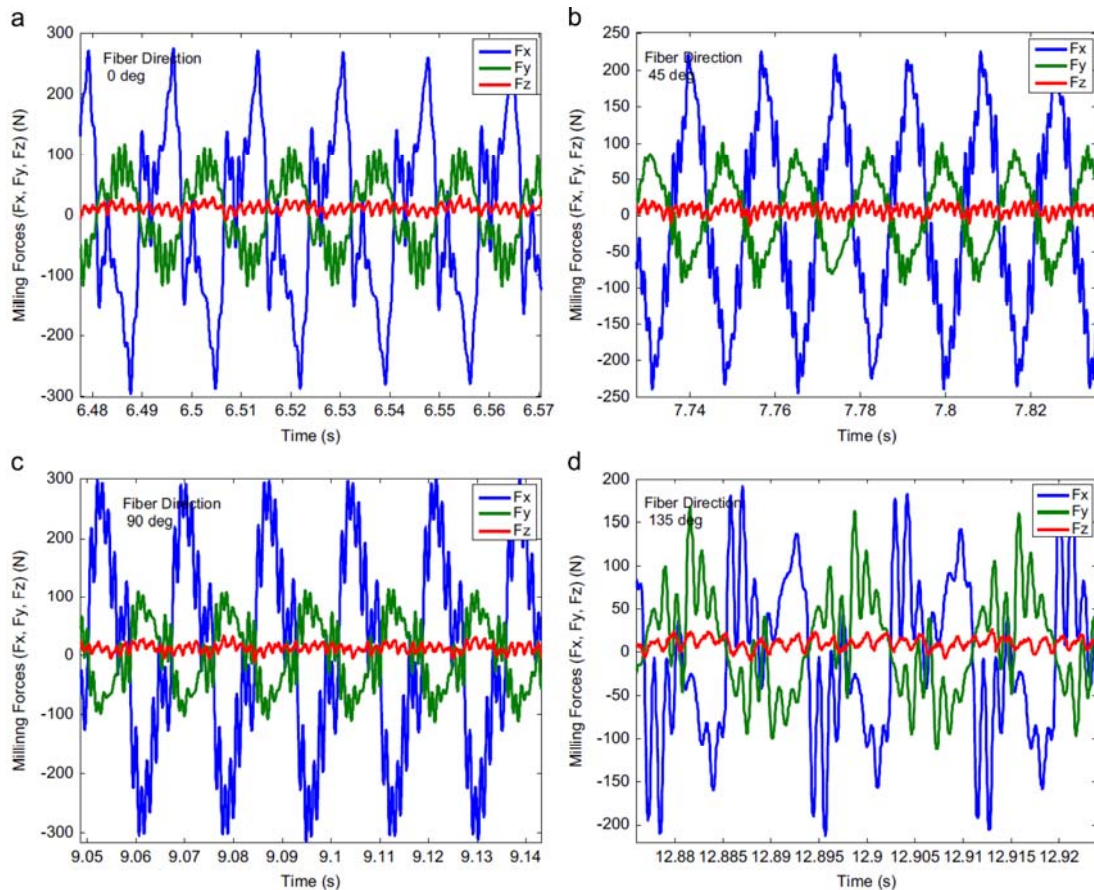


Figure 2.8 Unfiltered Force Data for: (a)  $0^\circ$ ; (b)  $45^\circ$ ; (c)  $90^\circ$ ; and (d)  $135^\circ$  fiber direction CFRP laminates [22]

Milling forces in tangential and radial directions as a function of tool rotation angle is shown in Figure 2.9. As can be seen from the figure, force measurements ( $F_r$ ) in radial direction are significantly greater than that of tangential force measurements ( $F_t$ ).

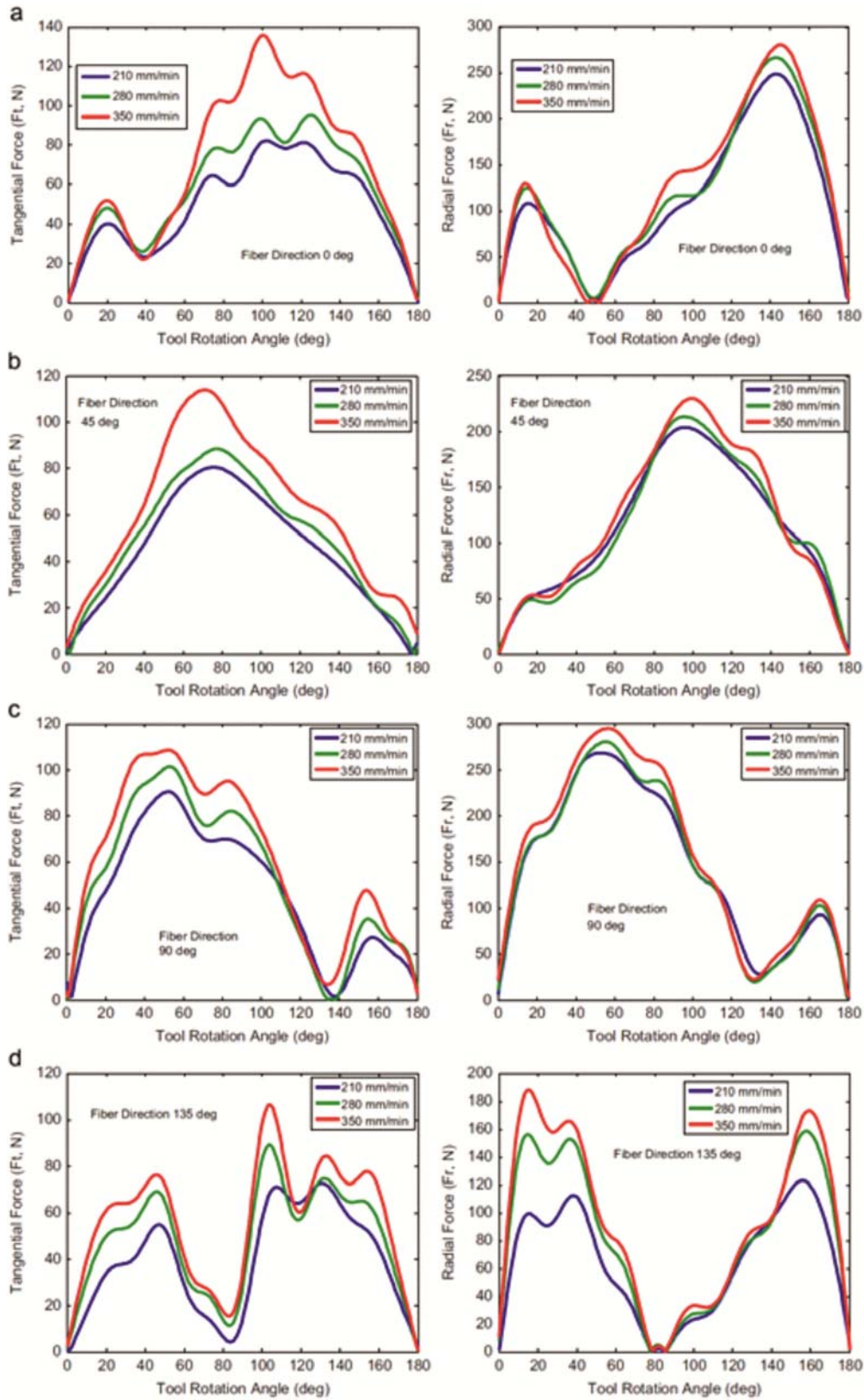


Figure 2.9 Tangential ( $F_t$ ) and Radial ( $F_r$ ) Milling Forces: (a) 0°; (b) 45°; (c) 90°; and (d) 135° fiber direction (after filtering) [22]

## 2.5 Surface Quality in FRP Machining

Different methods are used in the evaluation of machined surfaces which have differing characteristics corresponding to quality requirements. The inspection technique to be adopted is dependent on the equipment that is available, the investigator, and the terms of guidelines related to quality control. Residual stress induced in the material and surface topography is the main determinants of mechanical performance of homogeneous materials [18]. As the residual stresses are not developed by FRP in machining, the quality of machined FRP is utilized in the light of surface profilometry and visual techniques.

Quality in fiber reinforced composite is based on two main aspects that are surface topography and machine damage. The former is characterized by surface roughness whereas the latter is characterized by delamination. The surface of machined FRP is characterized with small holes, fiber cracks, fiber chipping, and blurs of matrix material; and its quality is dependent on fiber type and orientation. When exposed to tensile, bending and shearing stress; glass and carbon fiber undergo brittle fracture. On the other hand, aramid fibers are fractured when they are subjected to simultaneous tensile and shearing stress. A review of related literature showed that as the fiber is cut with both compressive and bending stress at 30° and 45° fiber orientation, the surface is very poor, whereas at a fiber orientation of 90° [16] a better surface is obtained. Besides, tool wear, feed rate, and temperature can be considered among the other factors that influence the surface roughness; and studies show that an increase in these factors leads to greater surface roughness.

Parameters characterizing machined surfaces are roughness parameters and statistical parameters. The former includes the arithmetic average height (Ra), the root-mean square height (Rq), the peak to valley height (Rt), the valley to mean height (Rv) and the ten-point average height (Rz), whereas the latter involves parameters like skewness, kurtosis and frequency height distributions. None the less, studies show that Ra and Rq demonstrate restricted variation in their values with regards to fiber orientation [18]. For that reason, the peak to valley height (Rt) and ten-point average height (Rz) which is the average of five peak points and five valley points are the preferred roughness parameters for representing the surface features of composites

[3]. Their role is to estimate the surface produced by a machining process and to measure how much machining damage is caused by various process parameters such as cutting speed, feed rate and depth of cut. Roughness values also signal alterations in the mechanical properties of machined FRP. Studies have proven that increasing the roughness, the fatigue strength and the impact strength are lowered [19].

Stylus profilometers are used to measure roughness on machined surfaces. Roughness value is given by the vertical displacement of a diamond stylus tip which moves along the machined surface. Since the fiber direction changes based on the layer the roughness measurement results are highly dependent on the stylus path. A more efficient method for measuring roughness is to keep the stylus in one layer and taking readings at different locations of this layer, or at different locations of different layers; and then taking the average of the data collected through these readings. Another important point that needs to be taken into account in taking roughness measures of a composite surface is matrix smearing, fiber protruding, and fiber clinging to the stylus tip since these will distort the reading and will not give an exact description of the surface. Therefore a visual investigation coupled with profilometer readings is necessary to calculate surface topography parameters.

Fiber reinforced composites are damaged by machining in different ways. Among these damages, the most important ones can be noted as delamination, which is the separation of the interplay; debonding which refers to the failure of fiber-matrix adhesion, and fiber pullout which can be described as the removal of fiber from matrix and the bulging out of these fibers from the surface. Machining damage of fiber-oriented composites is highly connected to fiber orientation in relation to the cutting direction. Multidirectional laminates are damaged in forms of during machining which makes the maintenance of surface quality difficult.

Edge trimming studies of FRP showed that there are four types of delamination characterized as Type I, Type II, Type I/II and Type III delamination irrespective of the cutting mode and condition as shown in Figure 2.10 [20].

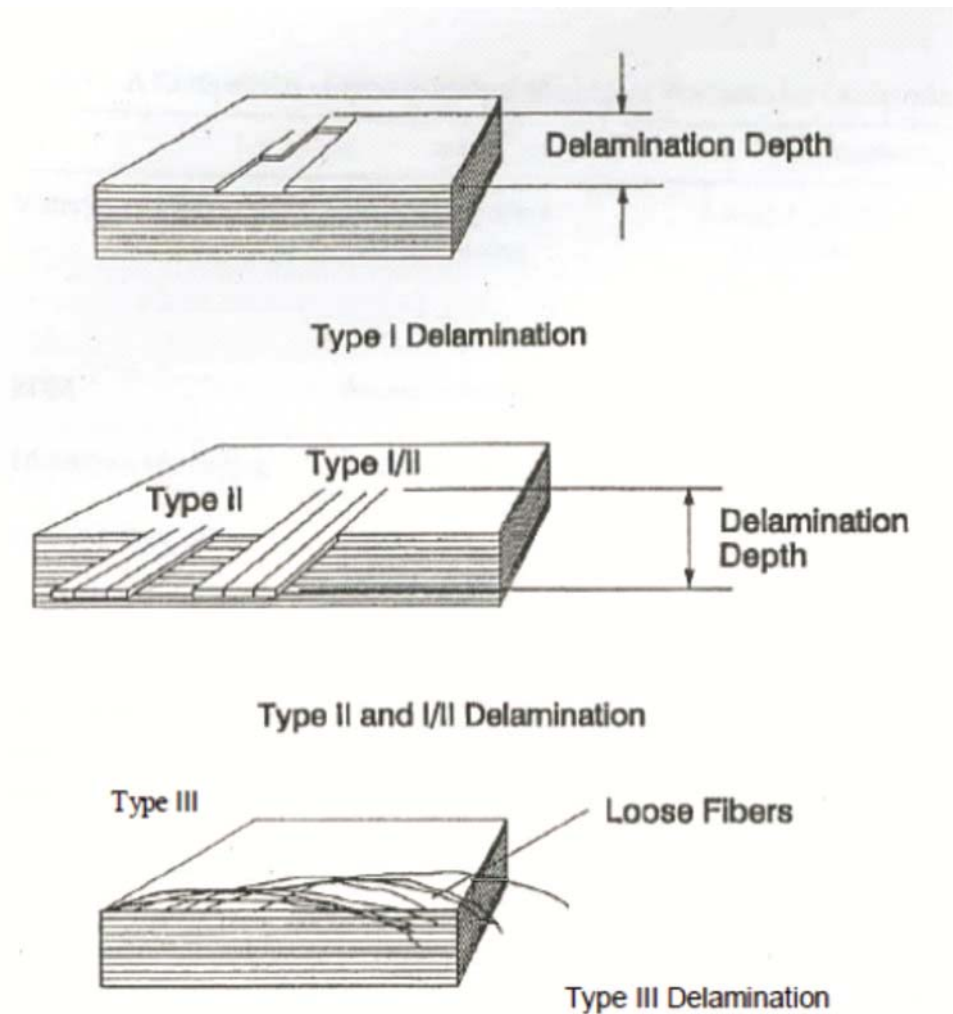


Figure 2.10 Delamination Types [20].

Type I delamination is characterized by the areas with inwardly broken plies and which are seen as the areas where plies are missing from the trimmed edge. Type II delamination involves uncut fibers protruding from the trimmed edge. Type I/II delamination is made up of plies which have broken inwards and which extend outwards from the trimmed surface. Type III delamination on the other hand, consists of fibers protruded from the trimmed surface along the cutting direction. Aforesaid delaminations occur in edge trimming operations because the surface plies are not stabilized by the adjacent plies. Moreover, machining forces act in one direction and tend to lift the layers, resulting in severe delamination.

Studies indicated that cutting parameters have an influence on machine damage with increasing cutting speed and lower feed rate resulting in less damage.

In aerospace applications, a threshold value of 2.5mm is determined for delamination damage depth for the top and bottom plies [20]. Based on this value, process parameters like cutting speed, feed rate, cutting mode (up milling or down milling) and depth of cut are chosen which enable the production of parts with delamination below 2.5mm.

An examination of delamination for particular process parameters was conducted in a study by cutting a number of work pieces at a particular speed and feed rate. After that the parts were analyzed for delamination depth above 1mm (in that study 1mm was set as the threshold value for delamination depth). Delamination depth was represented in terms of percentages, which was calculated by taking the number of delaminated parts above 1mm and dividing the value by the total number of parts machined at that particular cutting speed and feed rate to see the impact of machining parameters on surface quality [20]. The cutting speed was kept constant while the feed rate was altered in that study. The work piece used composed of eight plies and was made of graphite/epoxy composite material. Two types of cutting tools of varying diameters were used one of which was a carbide tool of 10 °helix angle and the other was a polycrystalline diamond tool of 30 °helix angle. Tool condition was also found to influence delamination. Machine damage also increased in line with tool wear. In addition, it was found that polycrystalline diamond tool induced less delamination since it's worn slowly. The study also concluded that slow feed rate had a significant effect in reducing delamination.

This inhomogeneity is what makes FRP unique but creates some problems in machining at the same time which leads to the optimization of the machining process. For the present and future applications of fiber reinforced composites, it is essential to understand the effects of process parameters on the quality of CFRP materials. The number of studies on how process parameters affect the quality of CFRP composite materials is insufficient. Therefore the aim of this study is to find out the effects of process parameters and tool wear on the machined surface quality

of a CFRP composite material. The experiment is conducted by varying spindle speed and feed rate on a CNC router using edge trimming operation and by monitoring delamination depth and surface roughness. The goal here is to develop a machining database to obtain optimal cutting speed and feed rate in routing composite materials. This machining database will help operators to set the optimum cutting parameters to obtain machined parts consistent with the quality criteria.

Hintze pointed out that top layer delamination is not primarily dependent on fiber orientation angle in relation to the feed direction, but rather strongly depends on the instantaneous fiber orientation angle, which is constantly changing in course of edge milling [23]. Moreover, he concluded that delamination occurrence is critical when the fiber orientation angle is in the range of  $90^\circ < \theta < 180^\circ$ . On the other hand, the range  $0^\circ < \theta < 90^\circ$  results no delamination even with the worn tool.

Furthermore, in the aforementioned study, Hintze asserts that the delamination propagation is another important mechanism [23]. Delamination can mount from the critical cutting angle range to the edge of the component on condition that fibers are initially cut at a cutting angle of  $90^\circ < \theta < 180^\circ$  and with a cutting angle of  $0^\circ < \theta < 90^\circ$  at the component edge. The systematic scheme prepared by Hintze to describe the occurrence of delamination in milling is shown in Figure 2.11 [23].

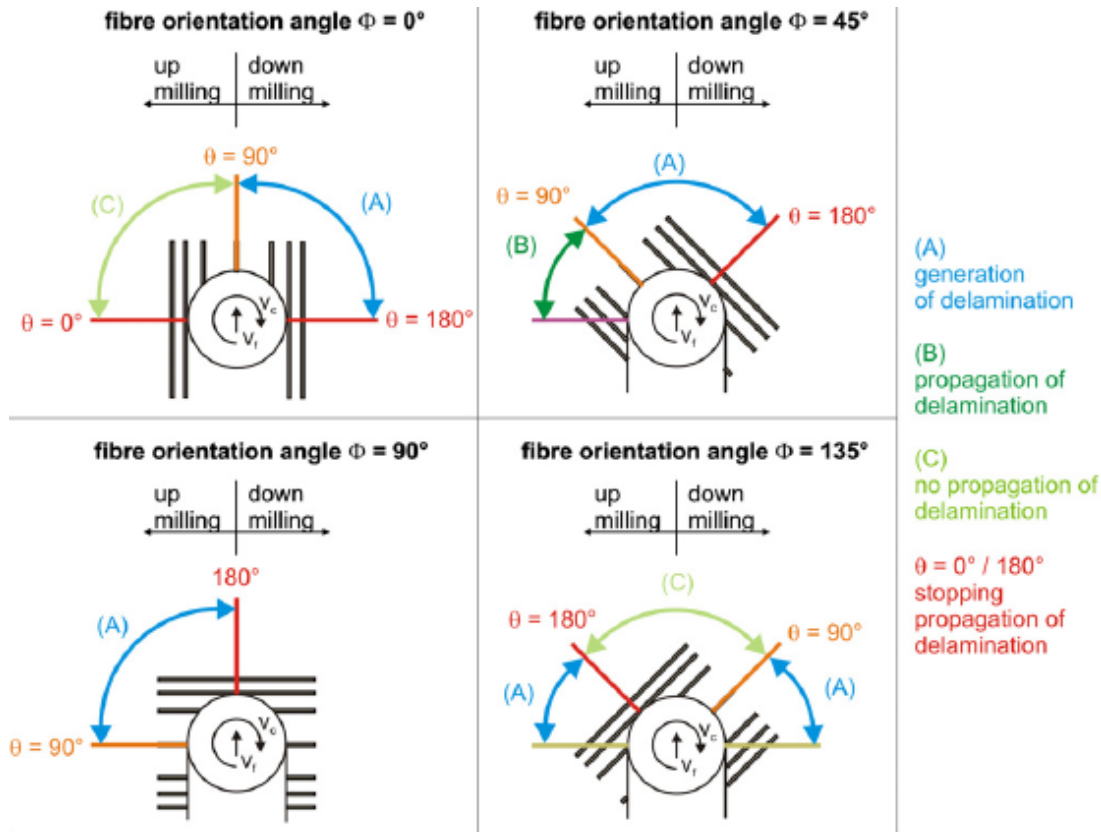


Figure 2.11 Systematic scheme given to describe the occurrence of delamination [23]

## 2.6 Chip Formation in FRP Machining

The chip pattern observed in machining FRPs was an impermanent type in powder and scrap form. Koplev was the first to use the macro chip method to carry out chip formation analysis on unidirectional composite material. Findings suggested that the chip was not plastically deformed and that chip formation in FRP machining primarily took place via brittle fracture. This finding is also true for multi-laminate composite materials [12].

Chips manufactured during the milling process of CFRP materials were triptych: huge brush-like chips, powder-like chips of tens of micrometers in diameter, and ribbon-like chips of just a few millimeters in length [11], [13]. The composition of huge brush-like chips was because of delamination, due to intralaminar shear.

Powder-like chips indicated production via fracture whereas ribbon-like chips were resulting from segments that were not broken due to fiber breakage and fracture.

Disparity in chips produced in the machining of CFRPs is not affected by variations in machining parameters but are mainly because of fiber orientation [8].

Fracture, shear or both can be considered as reasons behind chip formation during FRP machining coupled with tool geometry and fiber orientation [12].

FRP chip formation mechanisms have been investigated by Puw and Hocheng who carried out their milling experiments under orthogonal cutting conditions [24]. They observed three main types of chip formation mechanisms, which are delamination, buckling and bending as shown in Figure 2.12. These chip formations can occur singularly or combined with respect to the fiber direction and rake angle. As fibers cause most of the load during cutting, it can be said that fiber direction and type substantially defines chip formation and the cutting force characteristics [24].

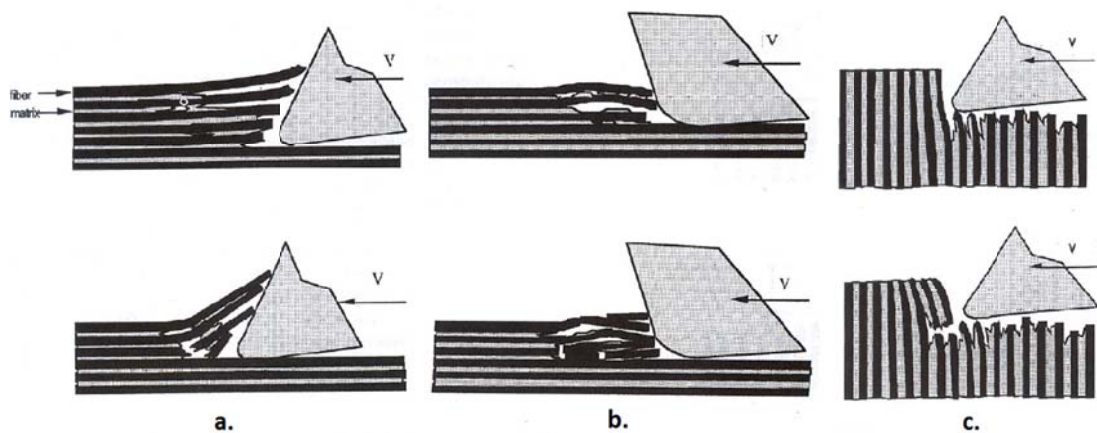


Figure 2.12 Chip Formation Mechanisms a) Delamination, b) Buckling and c) Bending [24]

The delamination chip formation, which can be observed when cutting parallel to fibers with a positive rake angle, needs relatively less cutting force. This is because it's a separation between the fibers of the material, which occurs mainly with a crack growth in the matrix material of the CFRP. Buckling failure of fibers is dominant

when cutting parallel to fibers with negative rake angle and bending can be seen when the fiber orientation is perpendicularly cut. [24]

## **CHAPTER 3**

### **EXPERIMENTAL PROCEDURE**

#### **3.1 Introduction**

The inhomogeneous nature of CFRP makes its machining very difficult, especially in obtaining the required surface quality. The only option in which acceptable machined surfaces can be obtained is by controlling the process parameters. This work presents a study on determining optimum cutting speed, feed speed and tool condition for obtaining quality machined surface based on delamination depth and surface roughness. The machining operation used for this study is edge trimming, which is a type of milling operation and is one of the major finishing operations done for CFRP materials in the aerospace industry. The experiments were performed in Turkish Aerospace Industry. The machine tool used for the experiment is a 3-axis vertical machining center manufactured by OKUMA. The machine has a maximum spindle speed of 7,000 rpm. An experimental matrix for machining was prepared based on three spindle speeds of 3000, 5000 and 7000 rpm and various feed speeds. The cutting tool used for the experiment is a diamond coated interlocked knurled tool of 10 millimeter diameter manufactured by OSG which is the common cutting tool producer in the industry for composite edge trimming process. A constant radial depth of cut of 10 millimeter is maintained throughout the experiment. The type of cutting configuration used for the entire experiment is climb milling. The dimensions of the CFRP board used for the experiment are 400x188x3.5 millimeters. The surface quality was observed using an optical microscope.

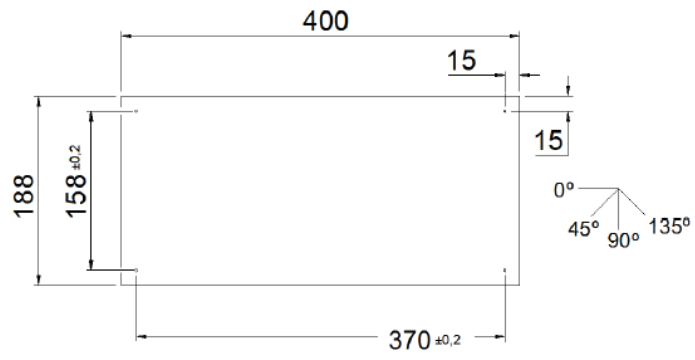
## 3.2 Experimental Set Up For Tool Wear

### 3.2.1 Workpiece Material

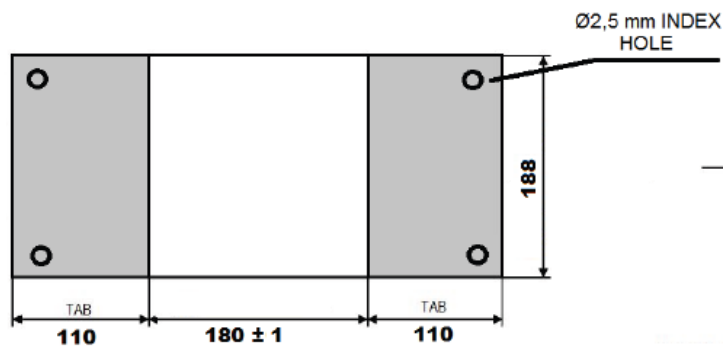
The workpiece material used in the experiment is a unidirectional continuous carbon fiber reinforced composite, with 3.5 millimeter thickness and each layer has 0.127 millimeter thickness. The material code is ABS5377A0000-01 used in the experiments and it is also epoxy prepreg material which contains 194 g/m<sup>2</sup> fiber in it. The tensile strength of material is 2980 MPa and its tensile modulus is 170 GPa. The structure of the unidirectional carbon fiber reinforced composite material is shown in the Figure 3.1. The workpiece was cut into blanks of 400x188 millimeter in an automated cutting machine for the experiment. The material dimension is given in Figure 3.2. The CFRP material used has a 28-ply lay up and the orientation of the fiber used in the composite is given in Table 3.1.



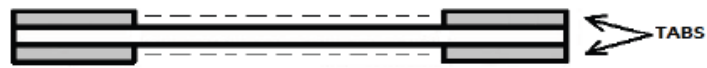
Figure 3.1 The Structure of the Unidirectional (UD) Continuous CFRP Composite Material



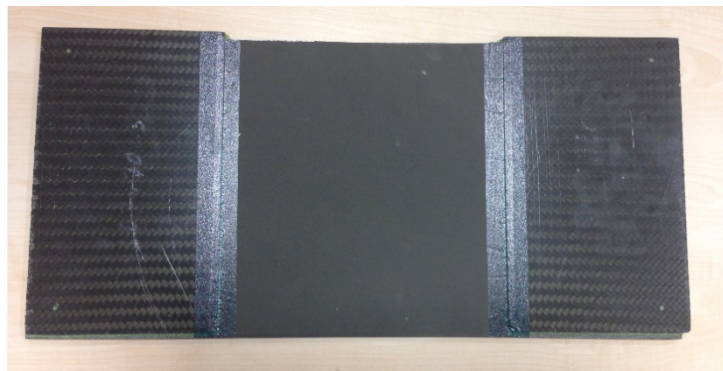
(a)



(b)



(c)



(d)

Figure 3.2 The Dimensions of Test Material

Table 3.1 Fiber Orientation of the CFRP Material

<b>PLY NO</b>	<b>DIRECTION</b>	<b>MATERIAL</b>
1	45	ABS5377A0000-01
2	135	ABS5377A0000-01
3	90	ABS5377A0000-01
4	135	ABS5377A0000-01
5	0	ABS5377A0000-01
6	45	ABS5377A0000-01
7	0	ABS5377A0000-01
8	135	ABS5377A0000-01
9	0	ABS5377A0000-01
10	45	ABS5377A0000-01
11	0	ABS5377A0000-01
12	135	ABS5377A0000-01
13	90	ABS5377A0000-01
14	45	ABS5377A0000-01
15	45	ABS5377A0000-01
16	90	ABS5377A0000-01
17	135	ABS5377A0000-01
18	0	ABS5377A0000-01
19	45	ABS5377A0000-01
20	0	ABS5377A0000-01
21	135	ABS5377A0000-01
22	0	ABS5377A0000-01
23	45	ABS5377A0000-01
24	0	ABS5377A0000-01
25	135	ABS5377A0000-01
26	90	ABS5377A0000-01
27	135	ABS5377A0000-01
28	45	ABS5377A0000-01

### 3.2.2 Cutting Tool

The tool used in the experiment is diamond coated interlocked knurled tool which is named DIA-CR-BNC manufactured by OSG Corporation in USA. The tool is made of sub-micron grade tungsten carbide material. The diameter of the tool is 10 millimeter, the nose radius is 0.5 millimeter, the overall length is 100 millimeter, and the cutter length is 30 millimeter with 12 cutting edges. The diamond interlocked tool used for the experiments and its two-dimensional image are shown in the Figure 3.3. In the Figure 3.4, the technical details about the cutting tool are given.



Figure 3.3 Diamond Interlocked Knurled Tool and Two-dimensional Image

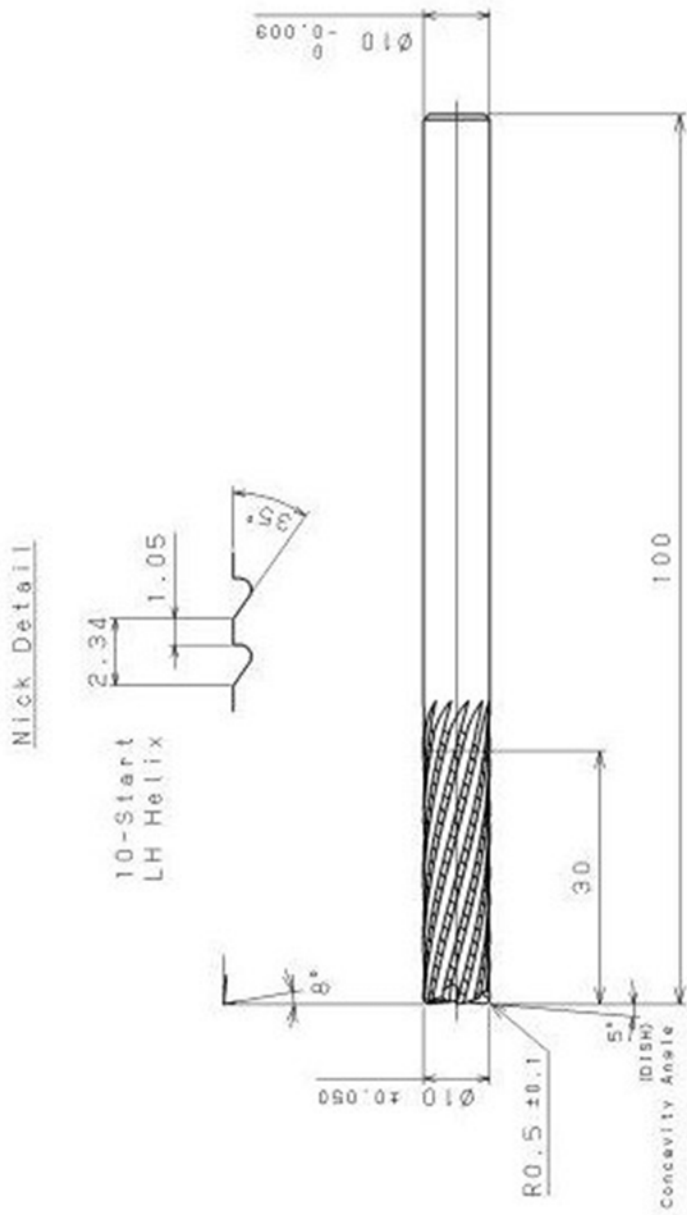
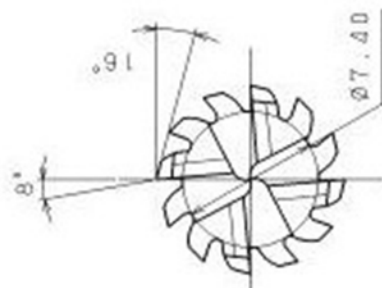


Figure 3.4 Technical Parameters of Cutting



### **3.2.3 Machine Tool Set Up**

The machine used for this experiment is a 3-axis vertical CNC machine of model number MC-45VAE manufactured in 1996 by OKUMA which is a Japanese firm. The vertical machine has a maximum spindle speed of 7,000 rpm and its axis limits are X=560 mm, Y=460 mm, Z=450 mm. It has a 760x460 millimeters work table. The specifications of the machine are given in Table 3.2 and Figure 3.5 shows the CNC machine which is used in the experiments.

Table 3.2 The CNC Machine Tool Specifications

	Unit	MX-45VA[E]
<b>TRAVEL</b>		
X-axis (Table)	mm (in.)	560 (22.05) [762 (30.00)]
Y-axis (Saddle)	mm (in.)	460 (18.11)
Z-axis (Spindle head)	mm (in.)	450 (17.72)
Spindle end to table surface	mm (in.)	160 to 610 (6.30 to 24.02)
<b>TABLE</b>		
Working surface on table	mm (in.)	460 x 760 (18.11 x 29.92) [1000 (39.37)]
Table size	mm (in.)	460 x 760 (18.11 x 29.92) [1000 (39.37)]
Table surface to floor level	mm (in.)	750 (29.53)
Load capacity	kgf (lbf)	350 (770) [500 (19.69)]
<b>SPINDLE</b>		
Speed range	min <sup>-1</sup> (rpm)	50 to 7000
Number of speeds		Infinitely variable
Taper of spindle hole		7/24, Taper No.40
Diameter at front bearing	mm (in.)	Ø70 (2.76)
<b>FEEDRATE</b>		
Rapid feedrate (X-/Y-/Z-axi)	mm/min (pm)	X, Y,: 20 (0.79), Z:15 (0.59)
Cutting feedrate (X-/Y-/Z-axi)	mm/min (pm)	10 (0.39)
<b>ATC</b>		
Tool shank		MAS BT40
Pull-stud		MAS 2
Tool magazine capacity		20 tools [optional: 32 tools]
Max. Tool diameter with adjacent tools	mm (in.)	Ø90 (3.54)
Max. Tool diameter without adjacent tools	mm (in.)	Ø125 (4.92)
Max. Tool length	mm (in.)	250 (9.84)
Max. Tool weight	kg (lb)	8 (17.6)
Tool selection		Memory random
<b>MOTORS</b>		
Main spindle drive motor	kw (hp)	VAC 7.5/5.5/ (10/7.5)
Feed motor	kw (hp)	X, Y, Z: 2.0 (2.75)
<b>OTHER SPECIFICATIONS:</b>		
Machine height	mm (in.)	2650 (104.33)
Floor space	mm (in.)	1800 [2200] x 2380 (80.91 [86.61] x 74.61)
Machine weight (Inc. CNC unit)	kg (lb)	5000 (11000) [5500 (12100)]



Figure 3.5 The CNC Machine

The machine tool maximum spindle torque is 95 Nm and its maximum spindle output is 7.5 kW when it runs 30 minutes and 5.5 kW when it runs continuously. The spindle speed range and the torque diagram are shown in Figure 3.6.

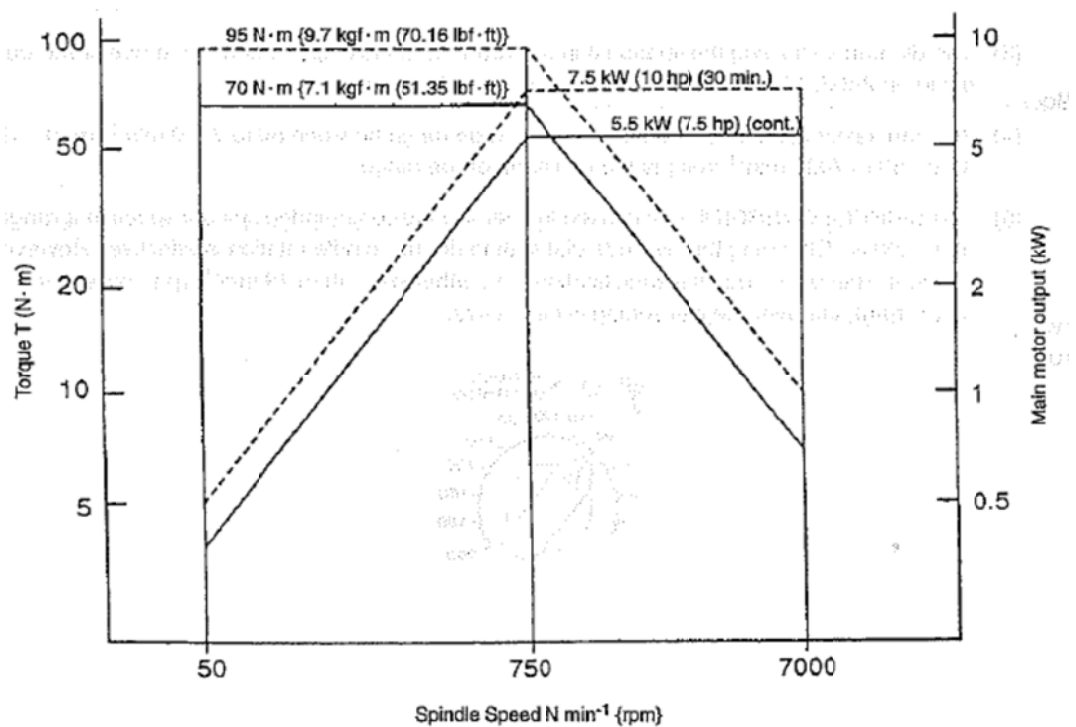


Figure 3.6 Machine Tool Spindle Speed- Torque/Output Diagrams

### 3.2.4 Workpiece Clamping System

The workpiece used for the experiment is mounted on the table using four clamps as shown in Figure 3.7. The workpiece was clamped securely and carefully on the fixture so that eliminating the vibration forces while cutting.

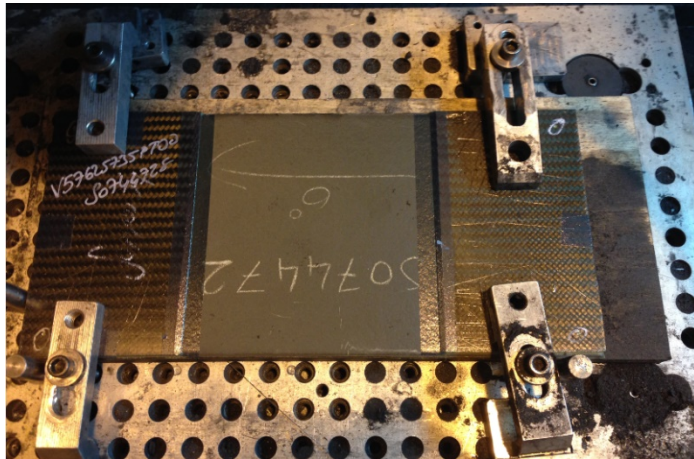


Figure 3.7 A View of the Workpiece Clamping System

### 3.2.5 Machining Configuration

There are two main types of machining configurations; which are up (conventional) and down (climb) milling. In up milling, the cutting speed direction of the edge in contact with the workpiece is in the opposite direction of the feed. Here the chip area is “comma” shaped, and the cutting edge starts to engage the chip at the thin section of the comma. Such machining configuration leads to low engagement force and lifts the workpiece up.

On the other hand, the direction of the cutting speed of the edge in contact with the workpiece in down milling is in the same direction of the feed, which engages the cutting edge with the chip at the thick section of the comma. In this machining configuration, engagement forces are high and lead to the pushing of the workpiece against the work holding surface. The schematic representation of both milling types are shown in Figures 3.8 and 3.9, respectively.

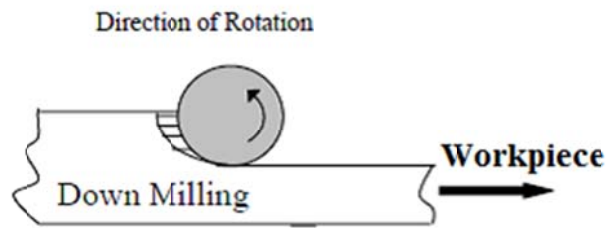


Figure 3.8 Down (climb) Milling

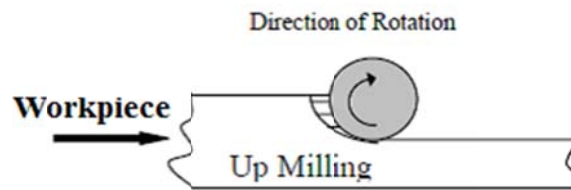


Figure 3.9 Up (conventional) Milling.

In the experiments, down (climb) milling is used because of reducing the load from the cutting edge, less tool wear and surface quality improvement.

### 3.2.6 Machining Parameters

The machining parameters used to quantify tool wear and to specify the optimum cutting condition when the CFRP panels are routed were obtained. The machining parameters used are shown in Table 3.3.

Table 3.3 The Machining Parameters in 5000 rpm

<b>Spindle Speed(rpm)=5000</b>	
<b>Feed per tooth (mm/tooth)</b>	<b>Feed Speed (mm/min)</b>
$f_z1=0.01$	$V_f1=600$
$f_z2=0.015$	$V_f2=900$
$f_z3=0.02$	$V_f3=1200$
$f_z4=0.025$	$V_f4=1500$
$f_z5=0.03$	$V_f5=1800$
$f_z6=0.035$	$V_f6=2100$
$f_z7=0.04$	$V_f7=2400$
$f_z8=0.05$	$V_f8=3000$
$f_z9=0.06$	$V_f9=3600$
$f_z10=0.065$	$V_f10=3900$
$f_z11=0.07$	$V_f11=4200$
$f_z12=0.075$	$V_f12=4500$
$f_z13=0.08$	$V_f13=4800$
$f_z14=0.09$	$V_f14=5400$
$f_z15=0.095$	$V_f15=5700$
$f_z16=0.1$	$V_f16=6000$

By knowing the spindle speed and the feed per tooth, it is possible to determine the feed speed by using the formula below,

$$V_f = n * z * f_z \quad (3.1)$$

Where

$V_f$  : feed speed (mm/min)

$n$  : spindle speed (rpm)

$z$  : number of cutting edges

$f_z$  : feed per tooth (mm/tooth)

For different spindle speed values, the material was tested for the feed speed values given in Table 3.3. Throughout the routing operation, a radial depth of cut of 10 millimeter (100% of tool diameter) was kept constant and dry machining was

applied. A CNC program was written for conducting tool path and cutting conditions. The workpiece is given in Figure 3.10 before and after machining respectively. The machining operation during the experiments and the position of tool are shown in Figure 3.11 step by step.

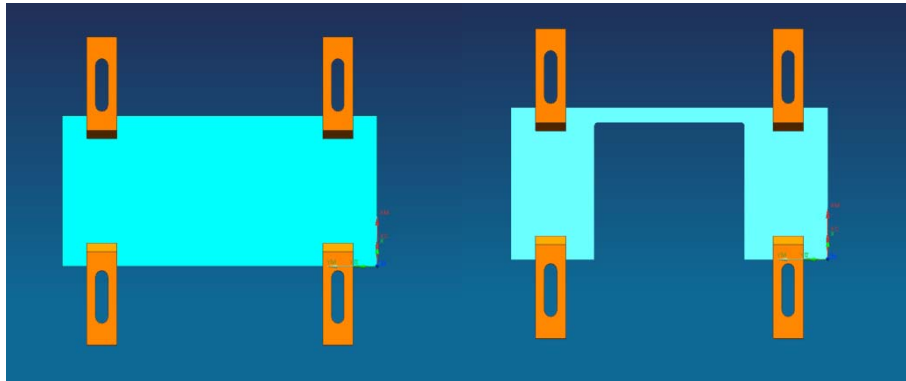


Figure 3.10 The Workpiece Before and After Machining

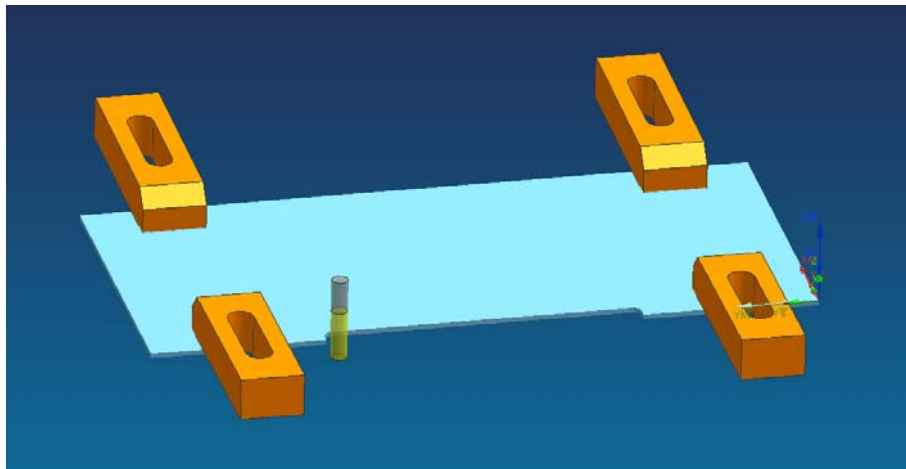


Figure 3.11 The Machining Operation and The Position of Tool During Cutting

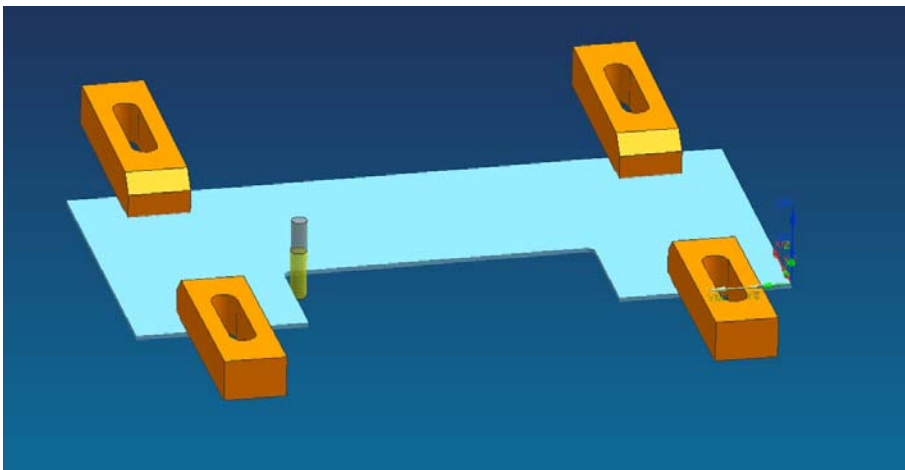
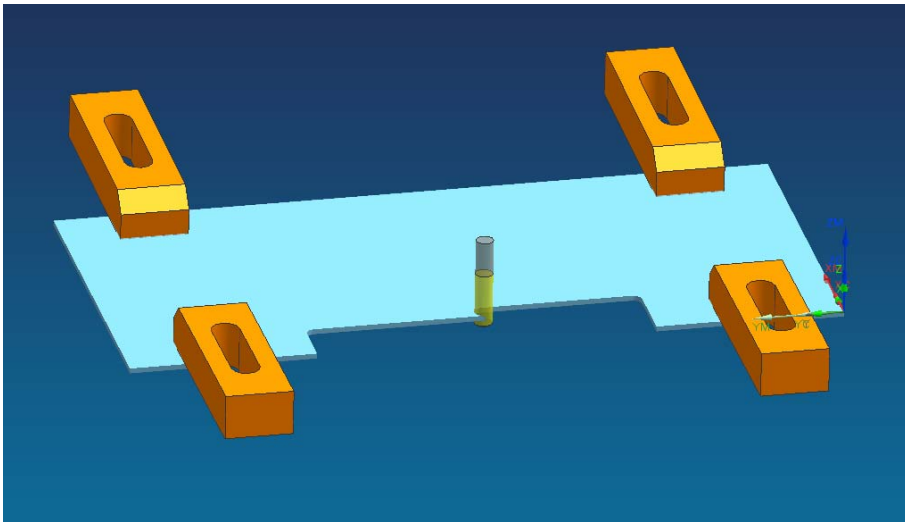
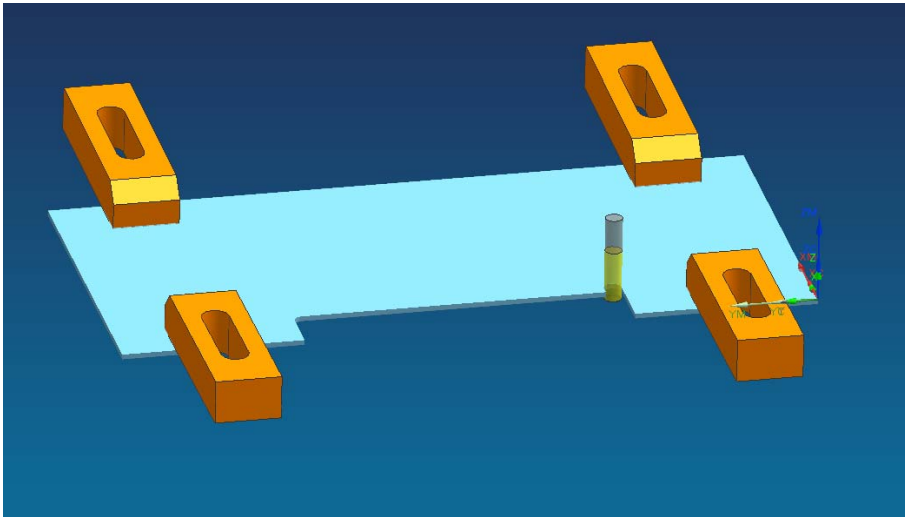


Figure 3.11 (Continued)

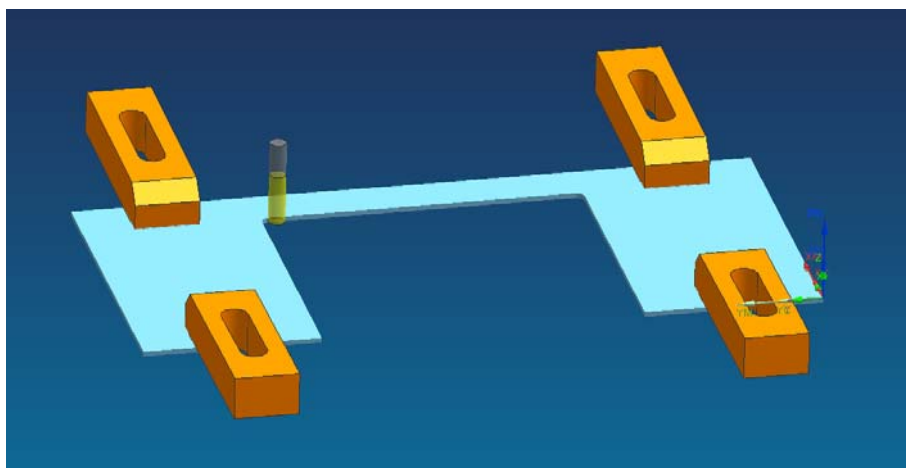
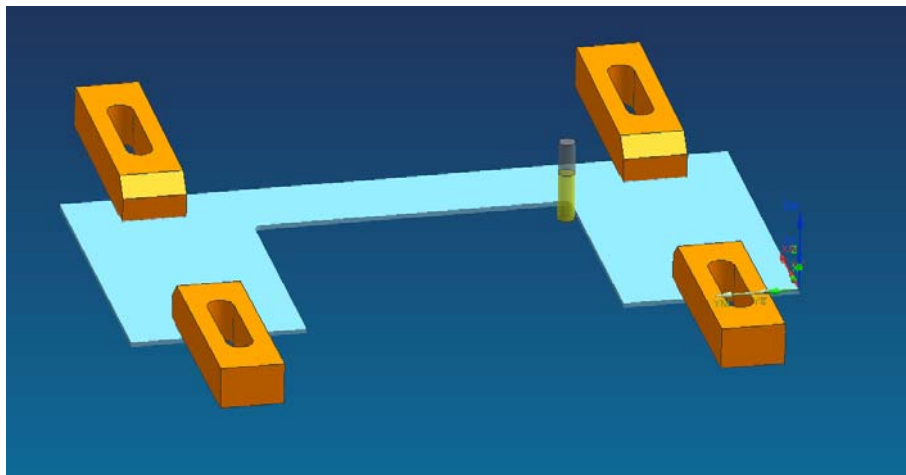
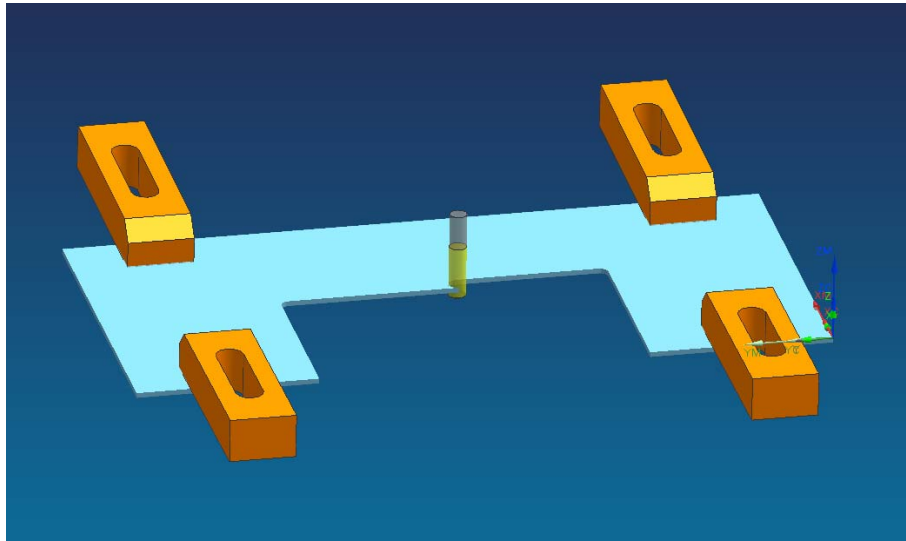


Figure 3.11 (Continued)

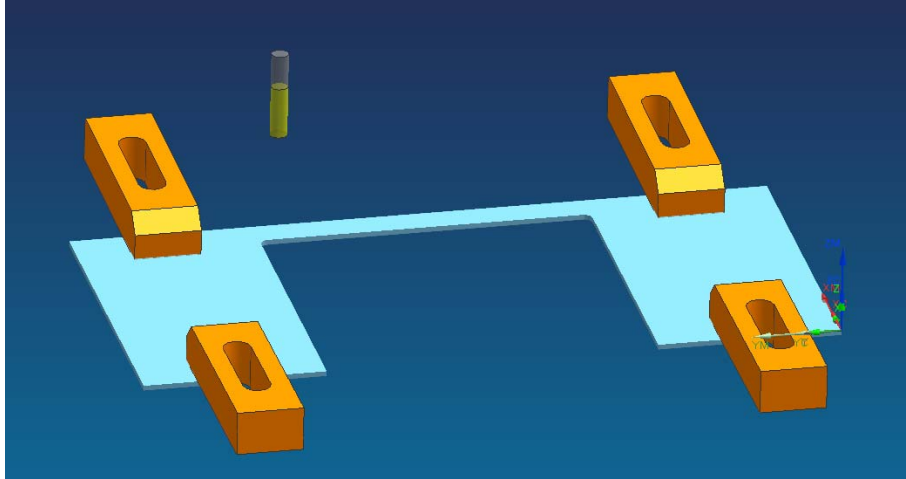


Figure 3.11 (Continued)

The combination of the machining parameters gives sixteen matrix points, and the experiments were carried out for all the sixteen combinations of feed speed at 5000 rpm. During the experiments, 3060 millimeter (about one piece of workpiece) length was machined for each matrix point. And also, for each matrix point a new tool is used, so a total of 16 cutting tools were used for the experiments. During the experiments, the cutting forces are recorded and at the end of each run, the tool wear and the delamination depth were measured.

### **3.3 Cutting Force Measurement**

Measurement of the cutting force during the trimming operation of CFRP materials was done by a rotary type dynamometer (Kistler type). The dynamometer's maximum amplifying load measuring range along the three axes with its sensitivity values are given in Table 3.4.

Table 3.4 Kistler Dynamometer Operating Range

Channel	Label	Measuring Range [M.U.]	Unit	FSO [mV]	Sensitivity [mV/M.U.]
1	F <sub>x</sub>	4743,83,00	N	10000,00,00	2,108,000
2	F <sub>y</sub>	4768,72,00	N	10000,00,00	2,097,000
3	F <sub>z</sub>	20120,72,00	N	10000,00,00	0,497,000
4	M <sub>z</sub>	186,39,00	Nm	10000,00,00	53,650,000

The dynamometer was located on to the spindle with a special device. Dimensions of the CFRP panels used in the measurement of force were the same as test panel. Care was taken to clamp the workpiece rigidly to the fixture to arrest any vibration during trimming. Every machining parameters were measured carefully under the same conditions. Only one pass of the trimming operation performed on the dynamometer. The schematic set up of workforce representation and dynamometer set up are shown in Figures 3.12 and 3.13, respectively.

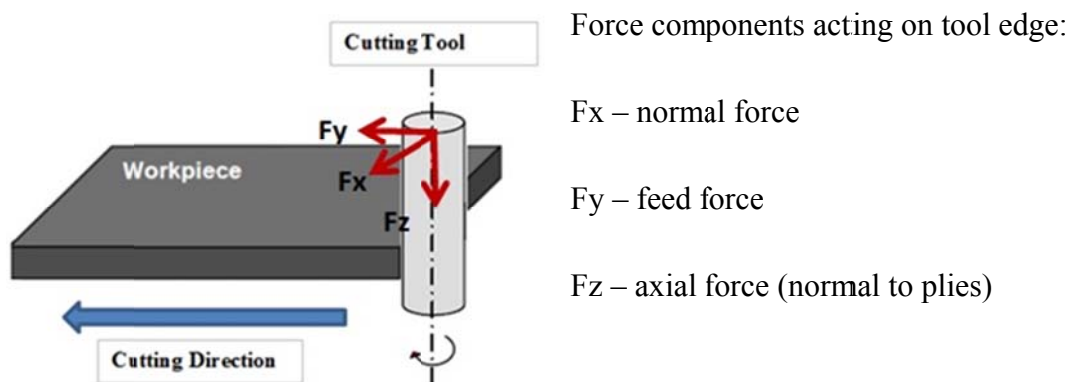


Figure 3.12 Cutting Force Directions

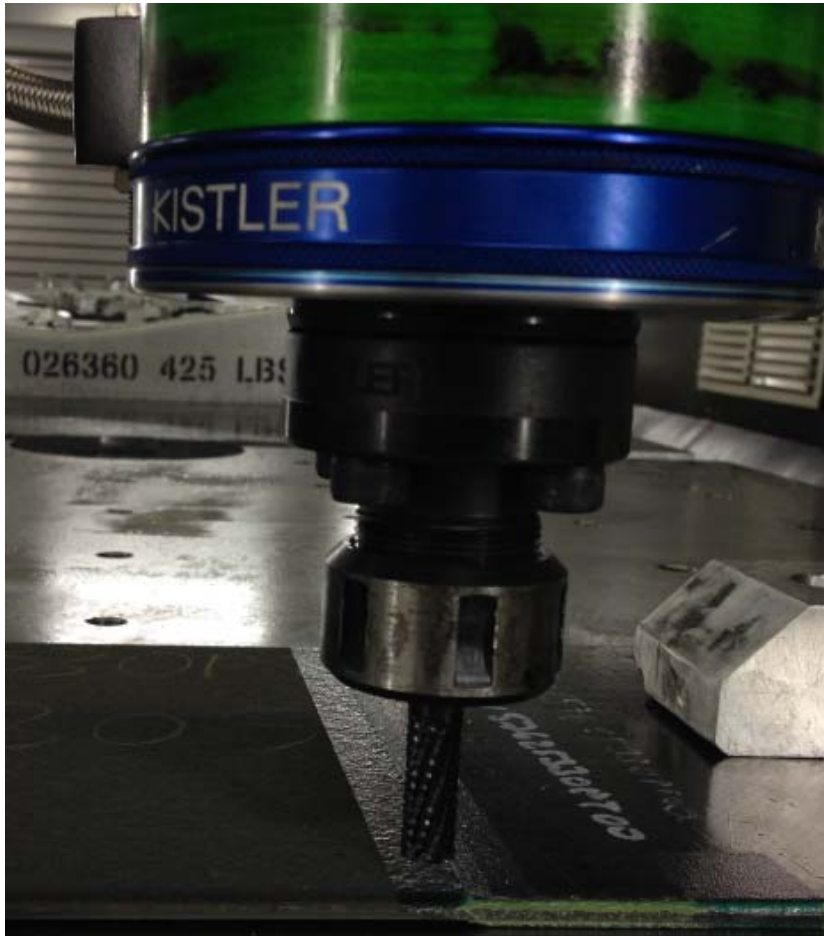


Figure 3.13 Dynamometer Set up

The rotating dynamometer is inserted directly into the machine spindle while the tool is connected with the dynamometer via the respective tool holder. The dynamometer rotates as well during operation due to the connection with the machine spindle. A rotating dynamometer has two advantages over stationary dynamometers. The dynamics of the measurement instrument is not influenced by changing masses, as the tool mass remains constant. On the other hand, it is possible with the aid of the built-in multi component sensor to measure the torque  $M_z$  directly during the entire measurement, thus making it possible to have, for example, precise statements regarding the wear on the tools.

During trimming operations, the cutting force data are collected with respect to every machining parameter via DynoWare. DynoWare is the data acquisition software of

choice for cutting force measurement. It supports Kistler's both measuring systems, which are stationary and rotary. Therewithal, the data measured from the signal amplifiers of other manufacturers can also be calculated and evaluated. The measured cutting force data is given in the Figure 3.14 during experiments.

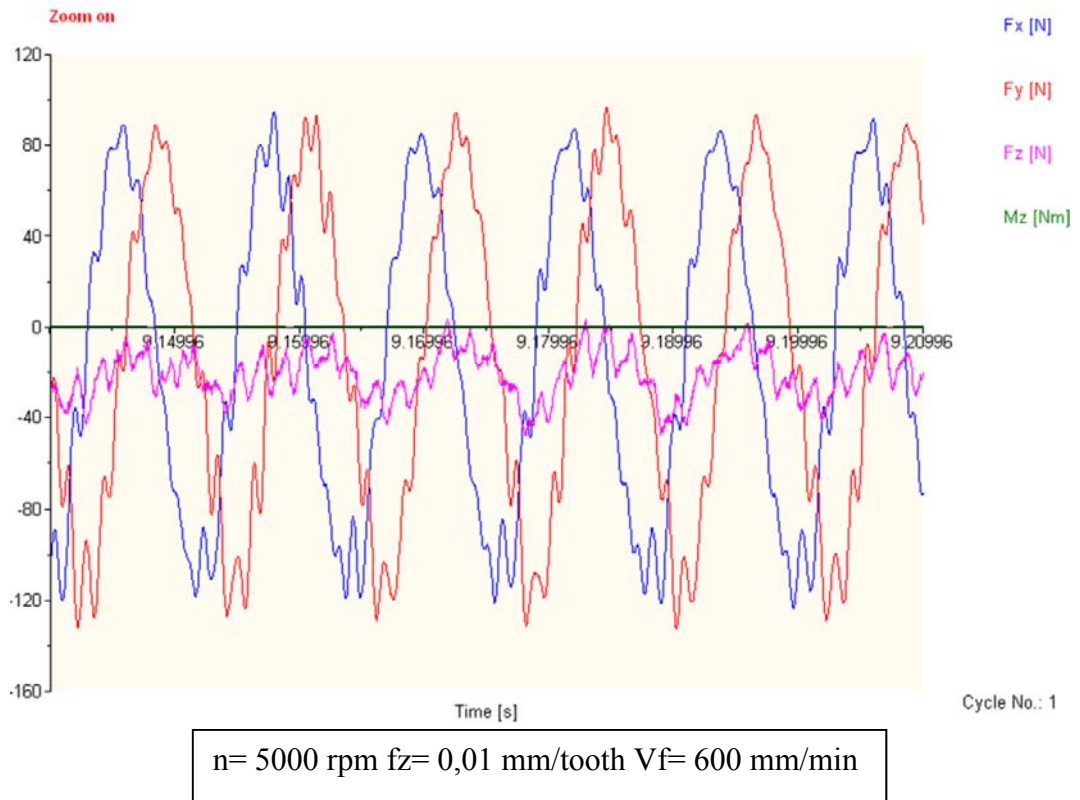
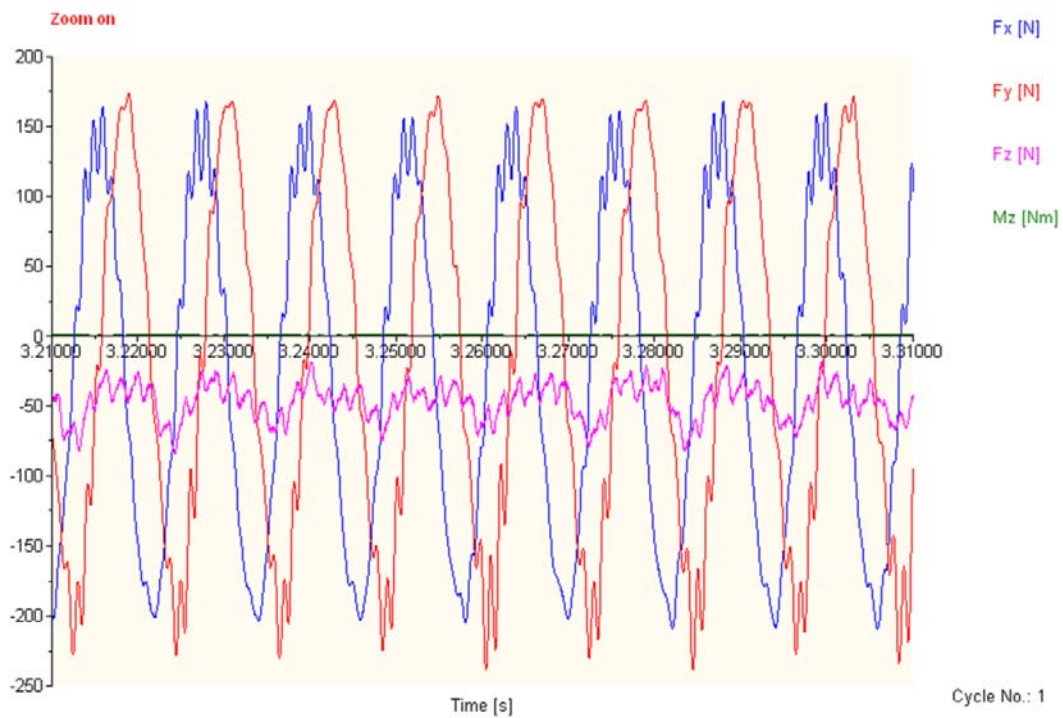
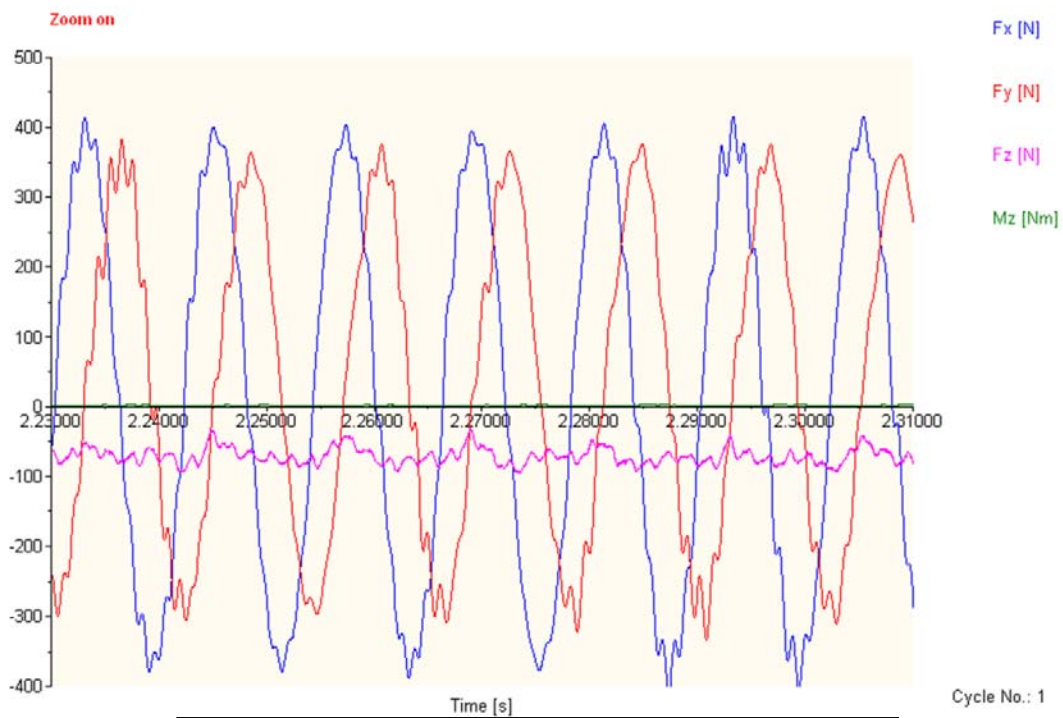


Figure 3.14 Cutting Force Data

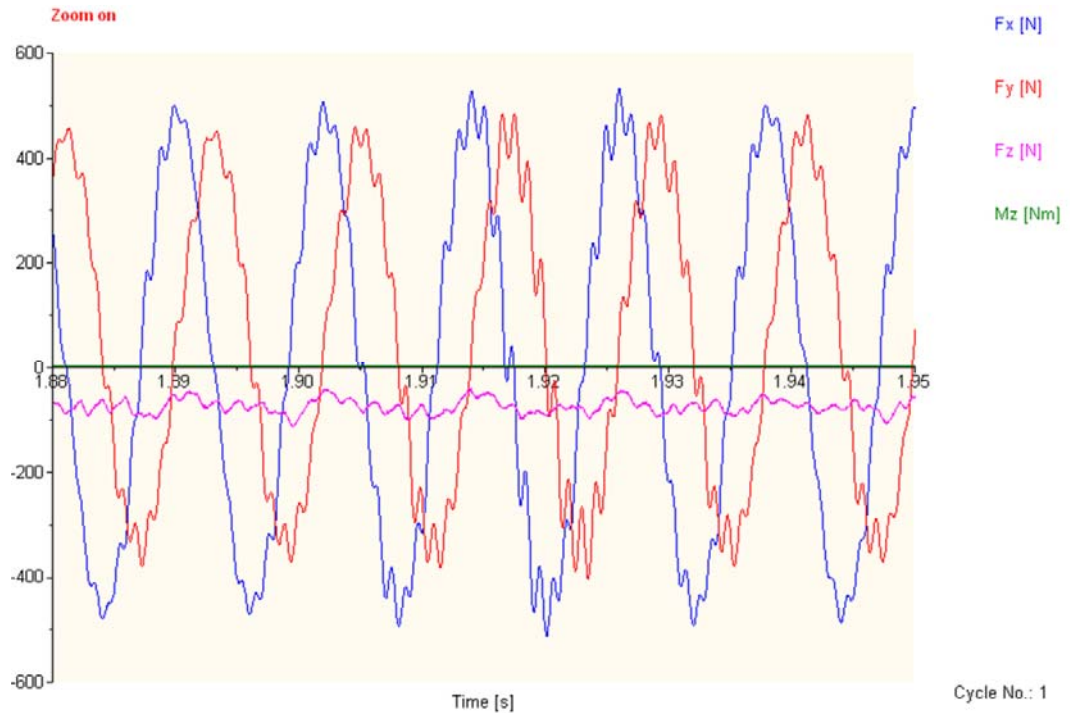


$n= 5000 \text{ rpm}$   $fz= 0,025 \text{ mm/tooth}$   $Vf= 1500 \text{ mm/min}$

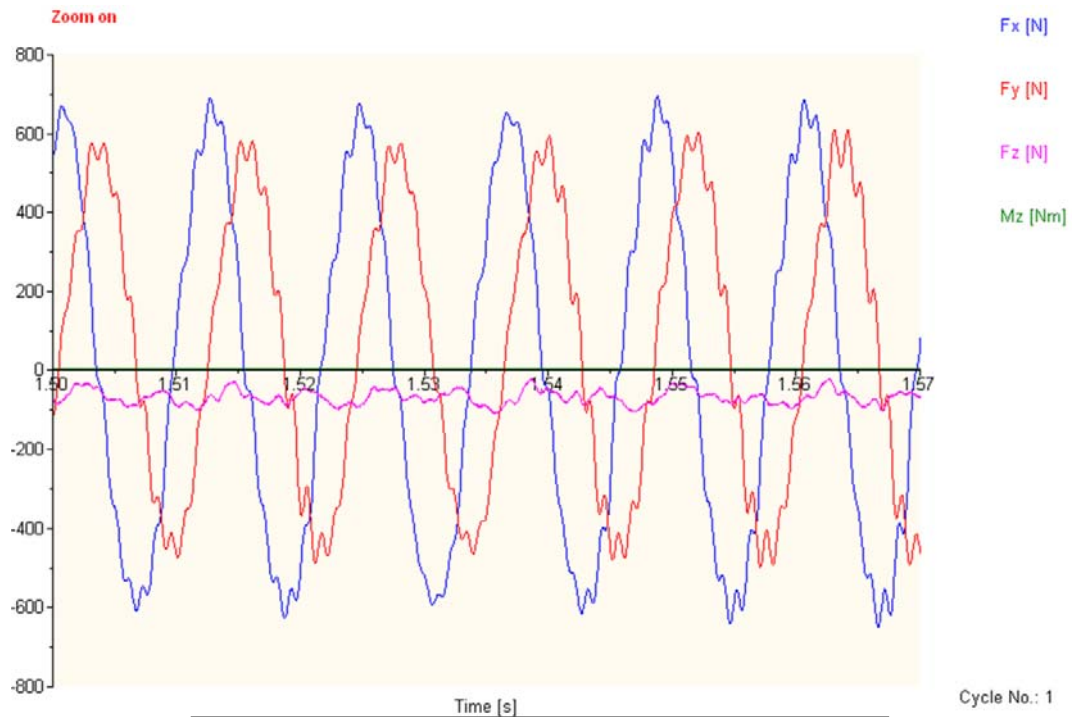


$n= 5000 \text{ rpm}$   $fz= 0,06 \text{ mm/tooth}$   $Vf= 3600 \text{ mm/min}$

Figure 3.14 (Continued)



$n= 5000 \text{ rpm}$   $fz= 0,075 \text{ mm/tooth}$   $Vf= 4500 \text{ mm/min}$



$n= 5000 \text{ rpm}$   $fz= 0,1 \text{ mm/tooth}$   $Vf= 6000 \text{ mm/min}$

Figure 3.14 (Continued)

### 3.4 Tool Wear Measurement

The tool was cleaned with dry air to allow for a clear description of wear land on the router knurled tool before the measurement. The tool wear was analyzed using an optical microscope called Keyence in Mechanical Engineering Laboratory at the Bilkent University. It has 0.1X-5000X magnification range and 360 degree observation. Moreover, it has 2D and 3D imaging and measurement capacity in its optical microscope. The tool wear measurements were carried out with a 20X zoom lens and a 2D measuring system.

The optical microscope set up comprised of the holding system and monitor are shown in Figure 3.15.

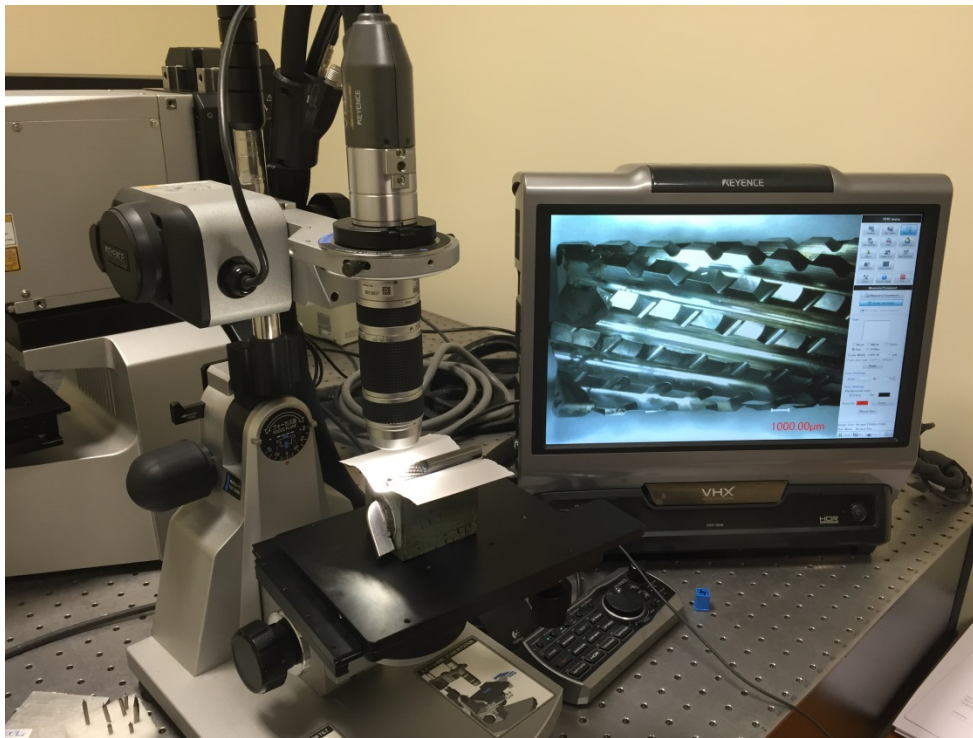


Figure 3.15 A View of the Optical Microscope Set up

Each of the tools used in the experiments were measured in Keyence, optical microscope with the help of special tool device and the monitored results were taken from the software. Some of the results are given in the Figure 3.16 for different feed per tooth at 5000 rpm spindle speed.



n=5000 rpm  
fz=0,025 mm/tooth  
Vf=1500 mm/min



n=5000 rpm  
fz=0,06 mm/tooth  
Vf=3600 mm/min



n=5000 rpm  
fz=0,07 mm/tooth  
Vf=4200 mm/min

Figure 3.16 Some of Cutting Tool Images Under the Microscope for 5000 rpm Spindle Speed

For some of the cutting parameter, the different size of edge chippings occurred on the cutting tool. The observed edge chippings are shown in Figure 3.18. And also the non-damaged cutting tool image is given in Figure 3.17.



Figure 3.17 Non-damaged Cutting Tool Image Under the Microscope

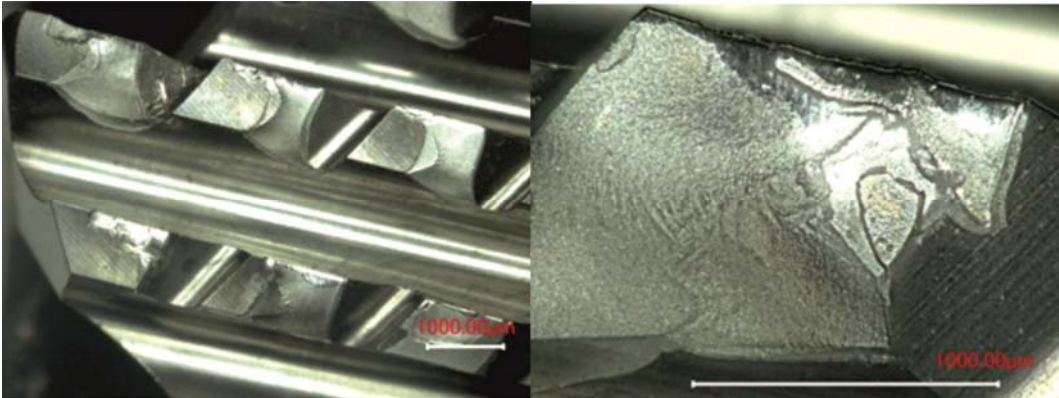


Figure 3.18 Views of Edge Chipping on Cutting Tool Under the Microscope

The damaged cutting tools which occur edge chipping eliminated for the second step tests.

### 3.5 Delamination Measurement

Delamination is measured with an optical microscope the setup of which is presented in Figure 3.15. The measurement is carried out with the placement of the workpiece on the moving table, the process of which is carried out with the help of a special tool device so as to view the machined edge of the workpiece. A 20X zoom lens was used and illumination was adjusted to get a clear image of the machined edge.

Once the software displayed the image, the edge was scanned for delamination. After that, the delamination was classified as Type I, Type II, Type I/II and Type III as discussed in the related literature review. For each type of delamination, the depth of delamination is calculated by measuring the length of the uncut fiber with the help of a micrometer dial attached to the moving table. Delamination depth for all types of delamination on both the top and bottom surfaces of the entire workpiece is noted, and the maximum delamination was taken. Figure 3.19 shows the type II delamination.

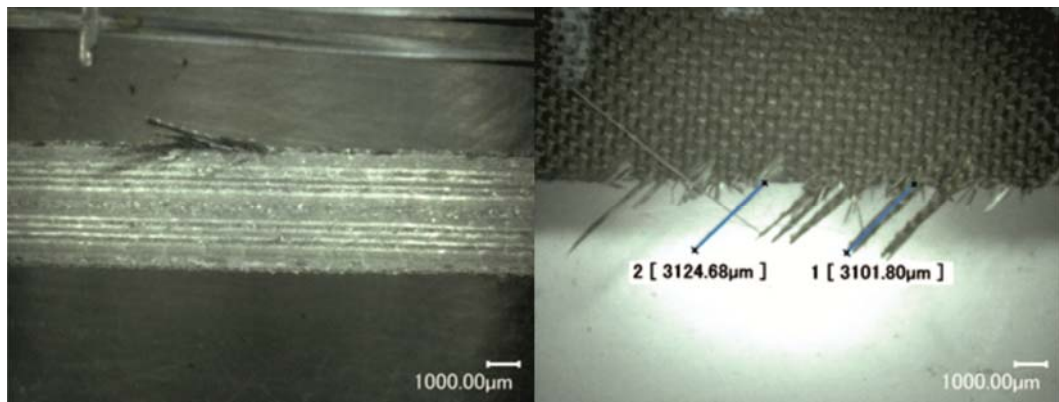


Figure 3.19 Type II Delamination on the Workpiece



## **CHAPTER 4**

### **ANALYSIS OF RESULTS AND DISCUSSIONS**

#### **4.1 Introduction**

Composites require some secondary machining processes to put them into their final dimensional requirement for assembly purposes even though they are largely produced as a near net shape. Conformity of CFRP materials to dimensional requirements during the secondary machining processes are largely affected by the type of tools being used and the process parameters like spindle and feed speed, and the depth of cut. The aim of this study was to gauge tool wear during the edge trimming operation of CFRP composite materials with appropriate cutting parameters so as to provide an indication of the tool replacement time based on delamination depth as a limiting criterion. As the extent of delamination is closely in relation to the extent of tool wear, quantification of tool wear becomes increasingly important in the routing of CFRP materials. Thus, it is necessary to know the point at which a tool must be replaced so that components with severe delamination damages are not passed on to the next stage of the production line.

#### **4.2 Machining Configuration**

Climb milling (down milling) was applied in all experiments to specify the appropriate machining condition for lesser tool wear and to prevent delamination. Nowadays, climb milling is considered to be the optimal way to machine parts. This is because it decreases the load from the cutting edge, leaving a much better surface finish and improved tool life.

Experiments were undertaken for a 5000 rpm spindle speed of with sixteen levels of variation in feed speeds given in Chapter 3. The reason for selecting these machining parameters was to decrease the necessary number of experiments to specify the proper machining configuration to be adopted for the remainder of the experimental matrix.

First of all, 16 different feed per tooth values at 5000 rpm were tested using 16 different cutting tools on workpiece material. A distance of 3060 millimeters was machined from the workpiece at the beginning. After all tests were carried out, all cutting tools were examined with the help of an optical microscope. After examining the results, 6 feed per tooth values were eliminated due to edge chipping on the cutting tools. For the second step tests, 3060 millimeter of distance was machined again from the workpiece with the same methods using the rest of 10 cutting tools. Among these 10 cutting tools, there were edge chippings and tool wear in 4 of them. The cutting parameters in 5000 rpm in the experiments and the results are presented in Table 4.1 below.

Table 4.1 The Results of the Experiments at 5000 rpm

Tool number	Feed per tooth (mm/tooth)	Cutting distance (mm) (1)	Tool wear ( $\mu\text{m}$ ) (1)	Cutting distance (mm) (2)	Tool wear ( $\mu\text{m}$ ) (2)
1	0,01	3060	No	6120	125,87
2	0,015	3060	No	6120	No
3	0,02	3060	No	6120	No
4	0,025	3060	No	6120	No
5	0,03	3060	No	6120	No
6	0,035	3060	No	6120	No
7	0,04	3060	No	6120	No
8	0,05	3060	321,13	6120	Edge chipping
9	0,06	3060	332,54	6120	Edge chipping
10	0,065	3060	344,92	6120	Edge chipping
11	0,07	3060	Edge chipping	-	-
12	0,075	3060	Edge chipping	-	-
13	0,08	3060	Edge chipping	-	-
14	0,09	3060	Edge chipping	-	-
15	0,095	3060	Edge chipping	-	-
16	0,1	3060	Edge chipping	-	-

After the second step tests, three feed per tooth values (0.02-0.03-0.04 mm/tooth) were chosen. This was done with the comparison of cutting time of each feed per tooth values as the suitable cutting parameters in 5000 rpm spindle speed due to the absence of tool wear and edge chipping as shown in the Table 4.1 above. Determined feed per tooth values in 5000 rpm were compared with rates in 3000 rpm and 7000 rpm to see the effect of the spindle speed. The new experiment matrix table is given below in Table 4.2.

Table 4.2 The Experiment Matrix Table

Feed per tooth (mm/ tooth)	Spindle Speeds (rpm)		
0,02	3000	5000	7000
0,03	3000	5000	7000
0,04	3000	5000	7000

#### 4.2.1 Cutting Force Measurement

Cutting forces were monitored and recorded by using a Kistler rotary type dynamometer. The cutting forces that were measured are  $F_x$ , normal force along x-direction,  $F_y$ , feed force along y-direction and  $F_z$ , axial force along z-direction.

The output from dynamometer was collected at a sample rate of 25000 Hz with the help of a special software called Dynoware which is mentioned Chapter 3. Figure 4.1, 4.2 and 4.3 present the cutting force data for 3000 rpm, 5000 rpm and 7000 rpm respectively for the same feed speeds.

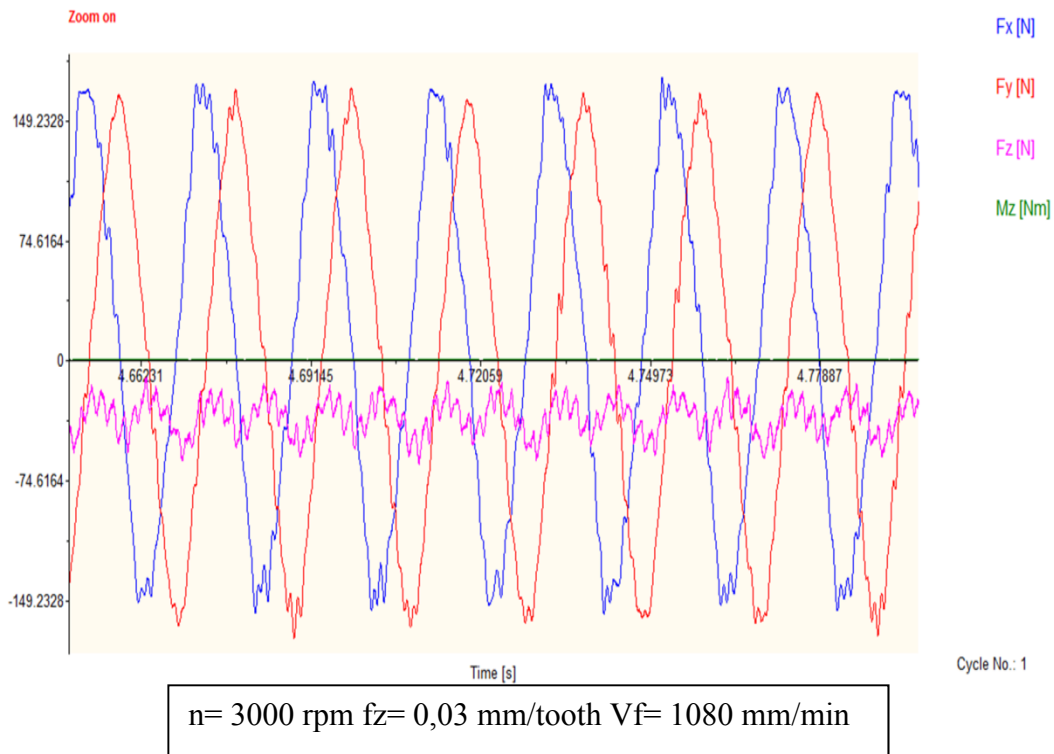
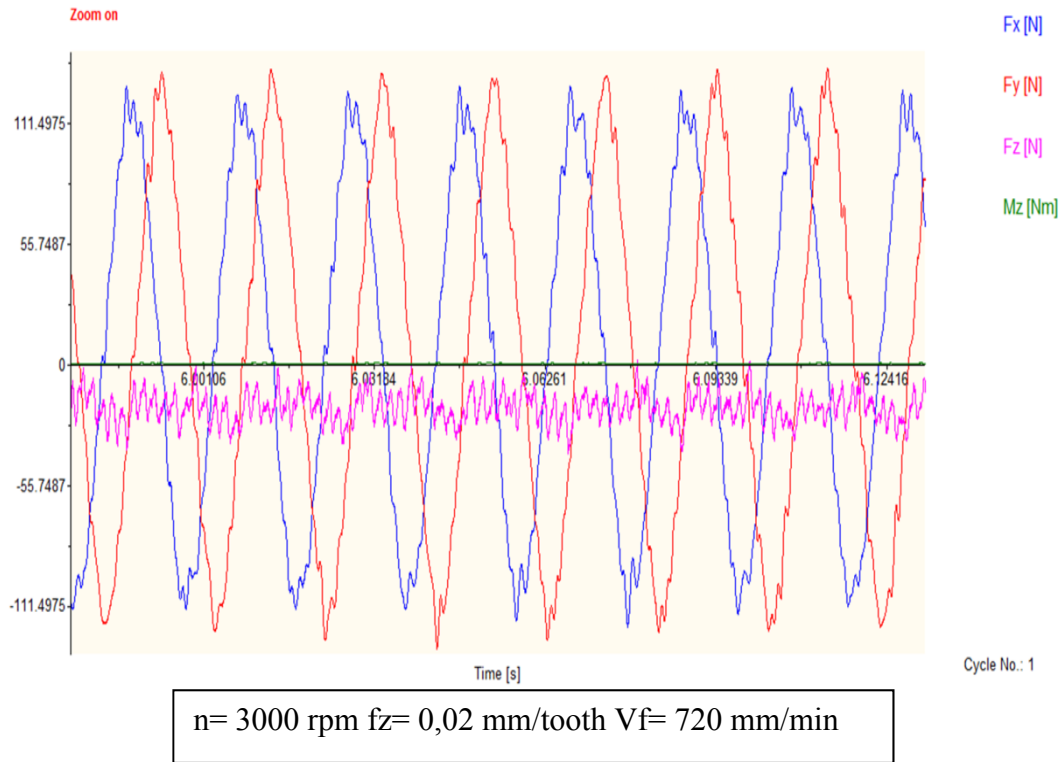


Figure 4.1 The Cutting Forces for 3000 rpm

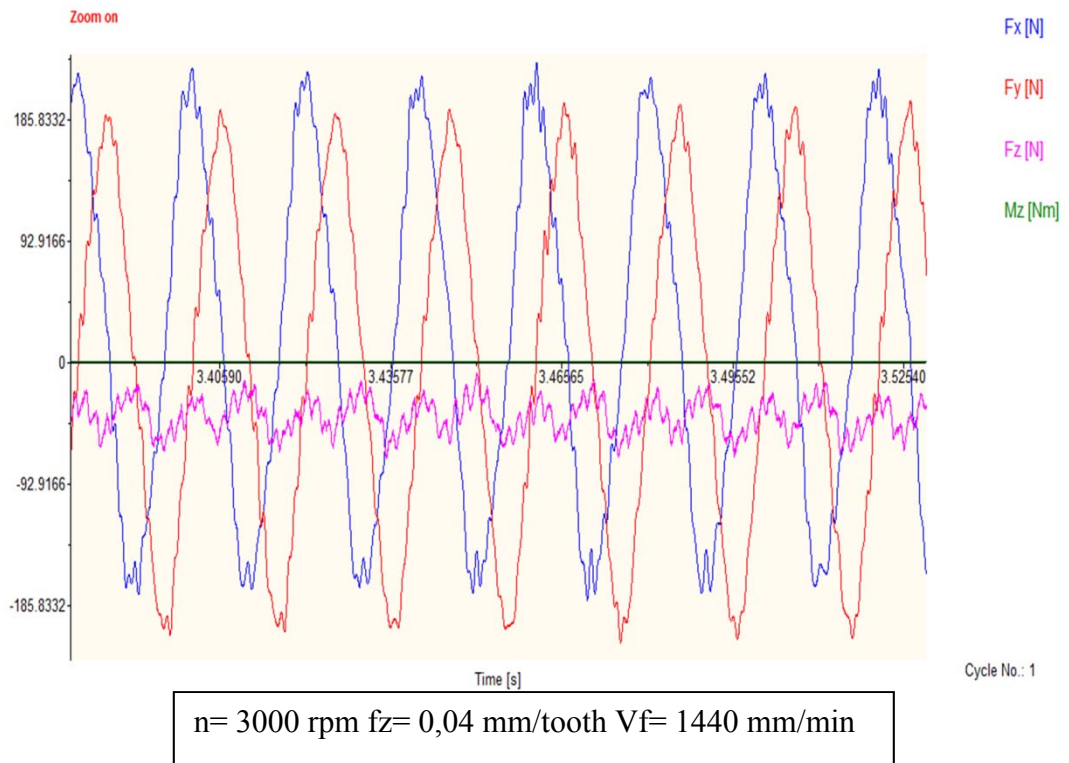


Figure 4.1 (Continued)

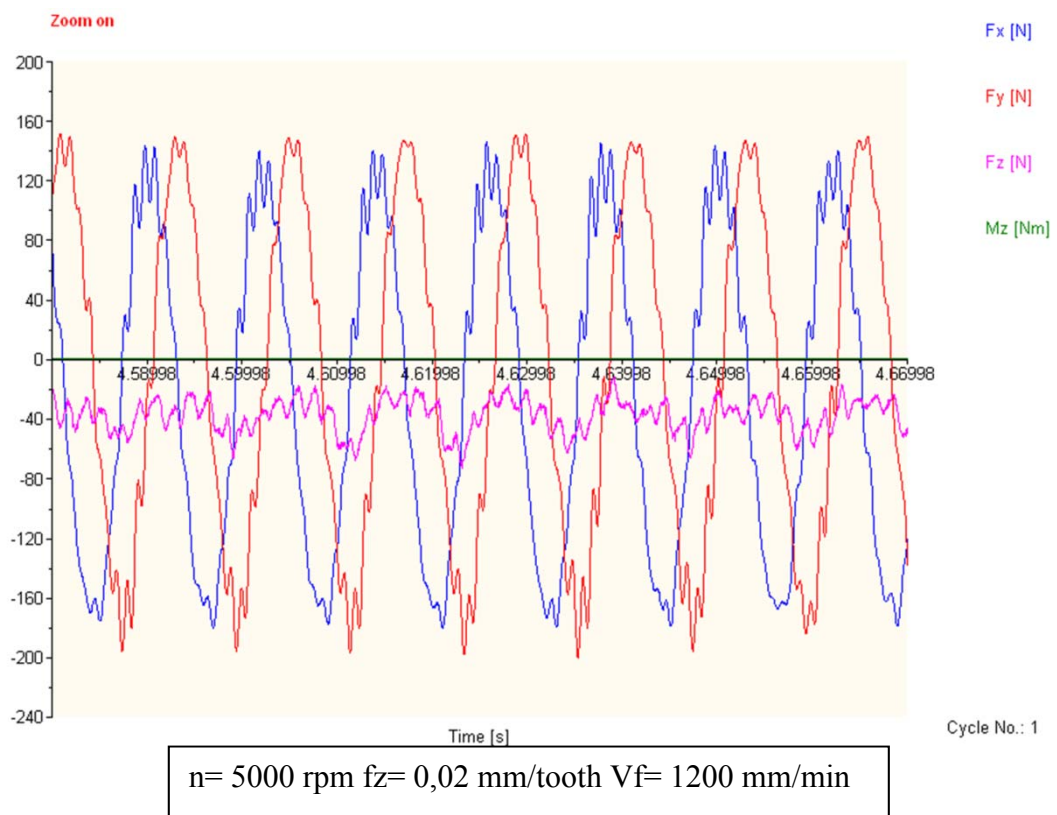
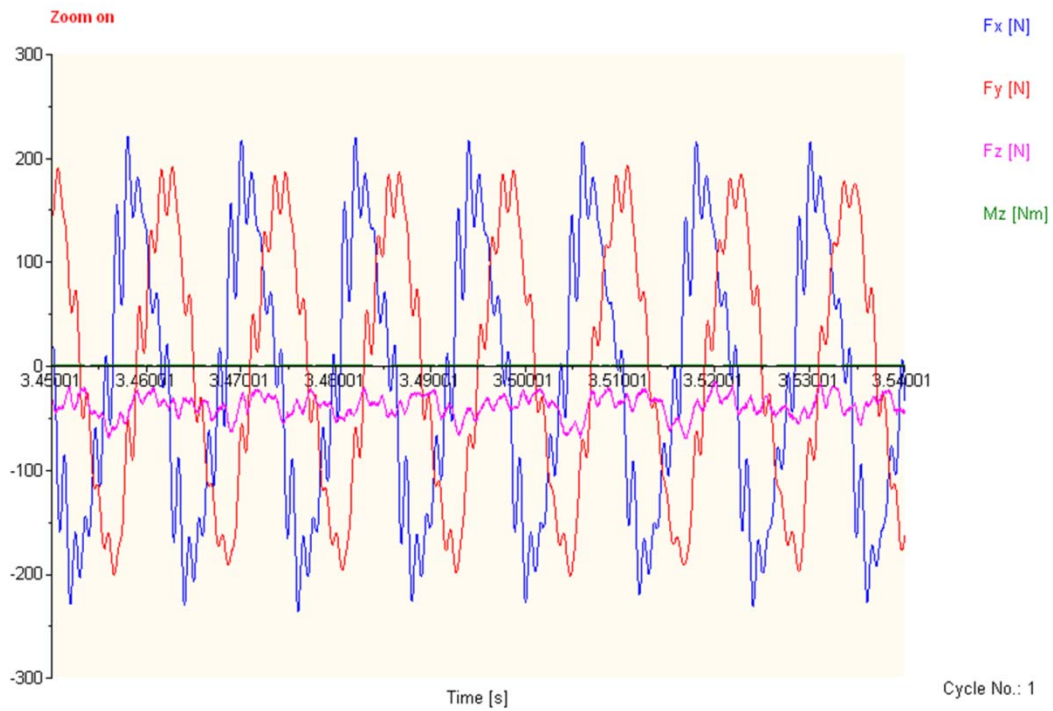
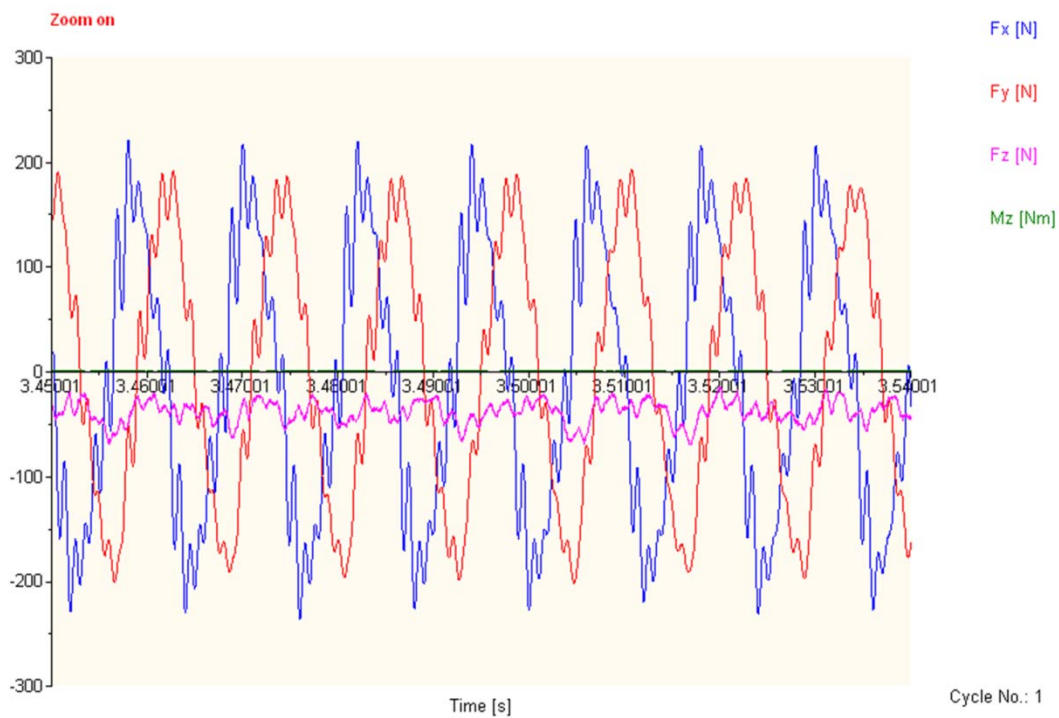


Figure 4.2 The Cutting Forces for 5000 rpm



$n = 5000 \text{ rpm}$   $f_z = 0,03 \text{ mm/tooth}$   $V_f = 1800 \text{ mm/min}$



$n = 5000 \text{ rpm}$   $f_z = 0,04 \text{ mm/tooth}$   $V_f = 2400 \text{ mm/min}$

Figure 4.2 (Continued)

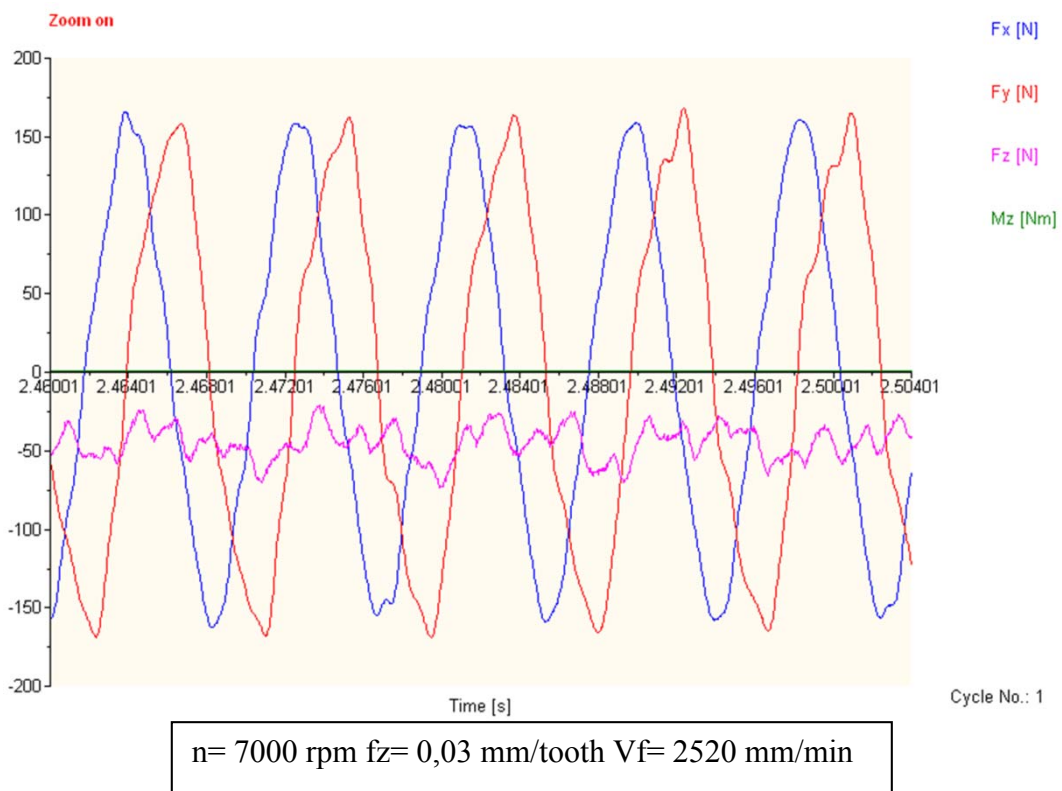
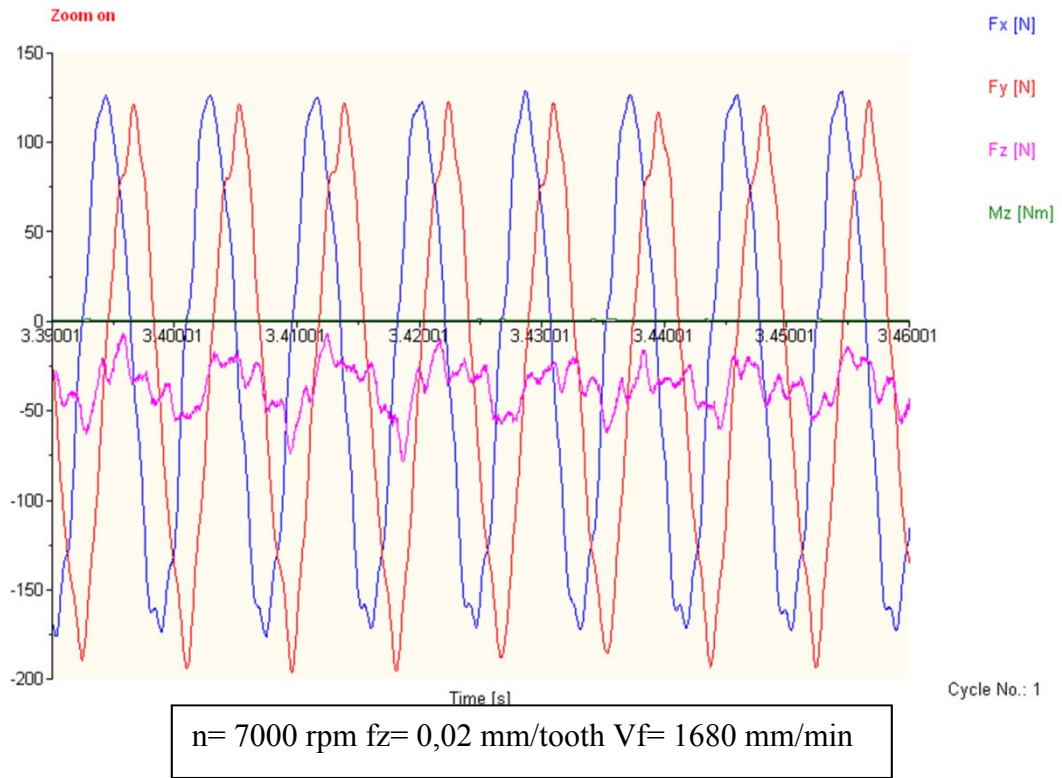


Figure 4.3 The Cutting Forces for 7000 rpm

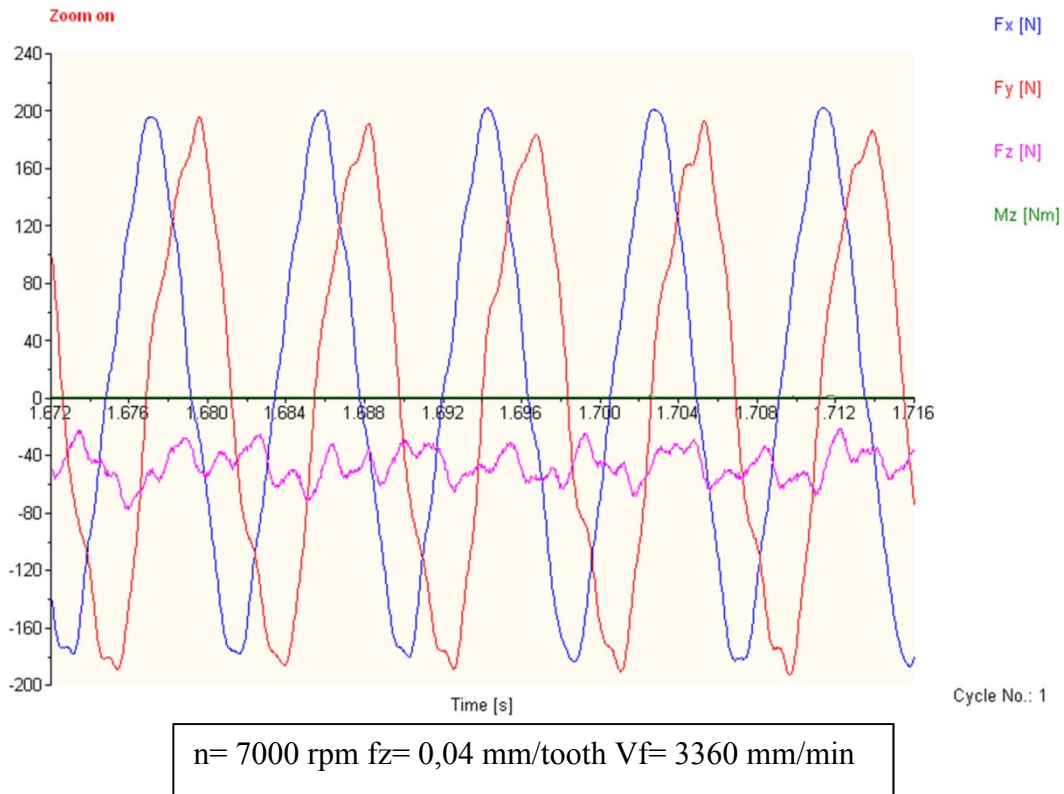


Figure 4.3 (Continued)

After measuring  $F_x$  and  $F_y$  cutting forces radial,  $F_r$  and tangential,  $F_t$  forces were calculated using matlab software for one revolution for each spindle speed. Figure 4.4 shows a schematic view of the cutting forces directions in climb milling. The radial and tangential cutting force components are identified from the orthogonal machining database.

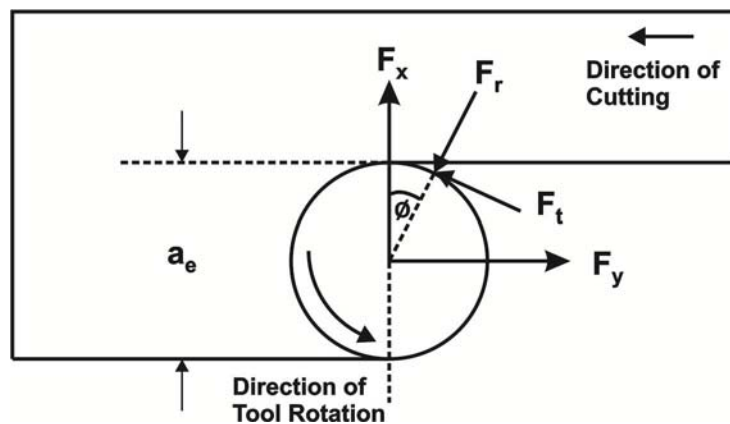


Figure 4.4 A Schematic View of the Cutting Forces Directions in Climb Milling

The radial ( $F_r$ ) and tangential ( $F_t$ ) forces are resolved into feed ( $F_y$ ) and normal to feed ( $F_x$ ) directions, using the below relationships.

$$F_x = F_r \cos(\theta) - F_t \sin(\theta)$$

$$F_y = F_r \sin(\theta) + F_t \cos(\theta) \quad (4.1)$$

Figure 4.5, Figure 4.6 and Figure 4.7 are gives that the mean radial and tangential forces for 3000, 5000, and 7000 rpm at the same feed speeds.

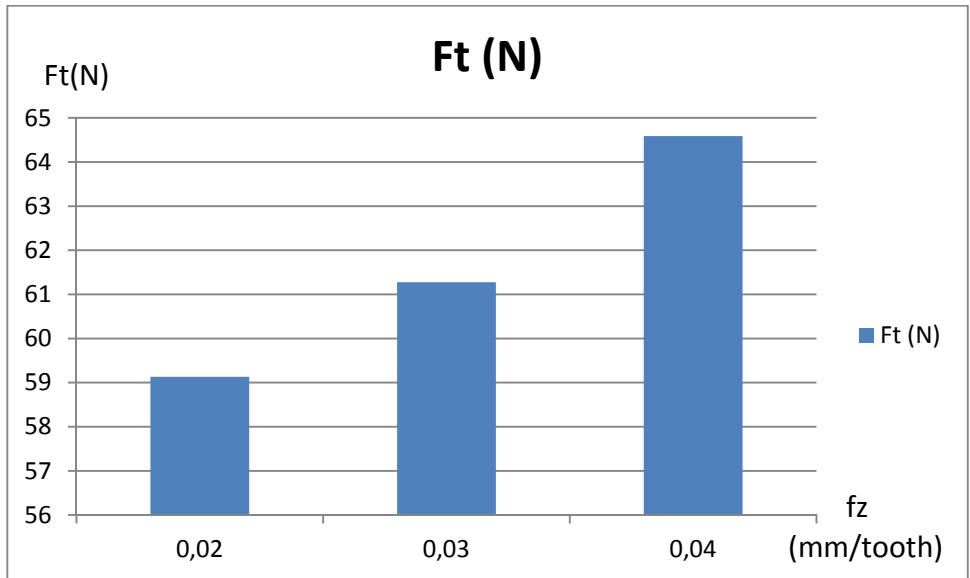
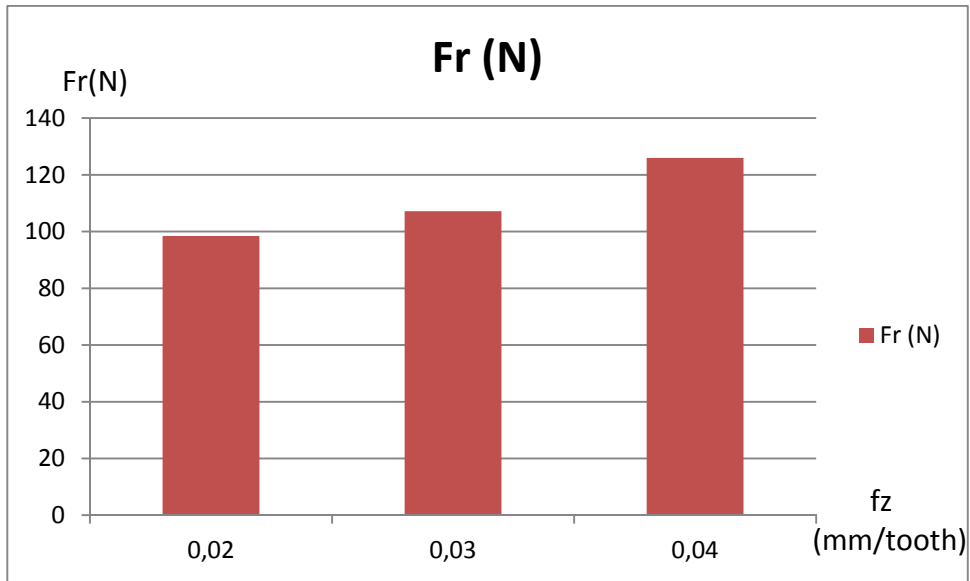


Figure 4.5 The Radial ( $F_r$ ) and Tangential ( $F_t$ ) Forces for 3000 rpm

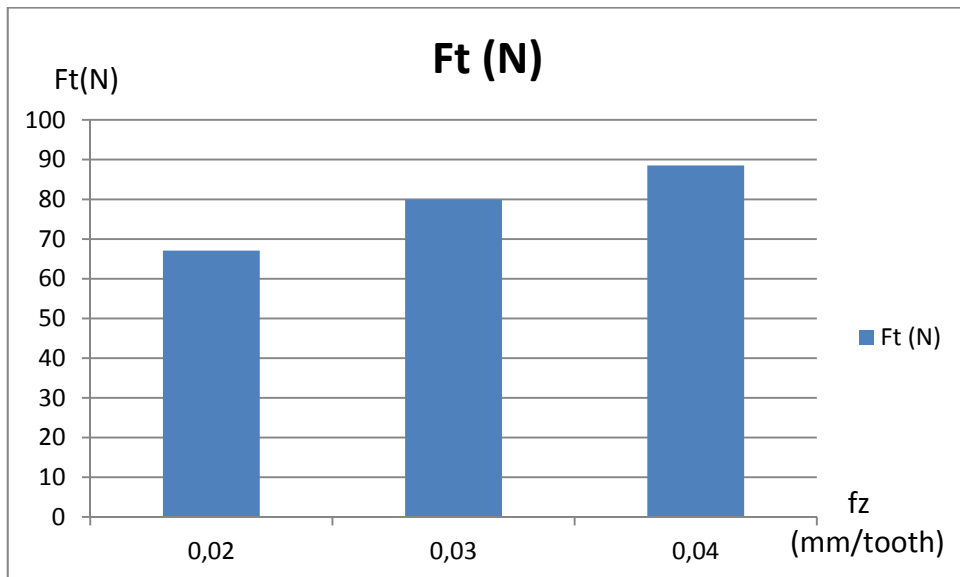
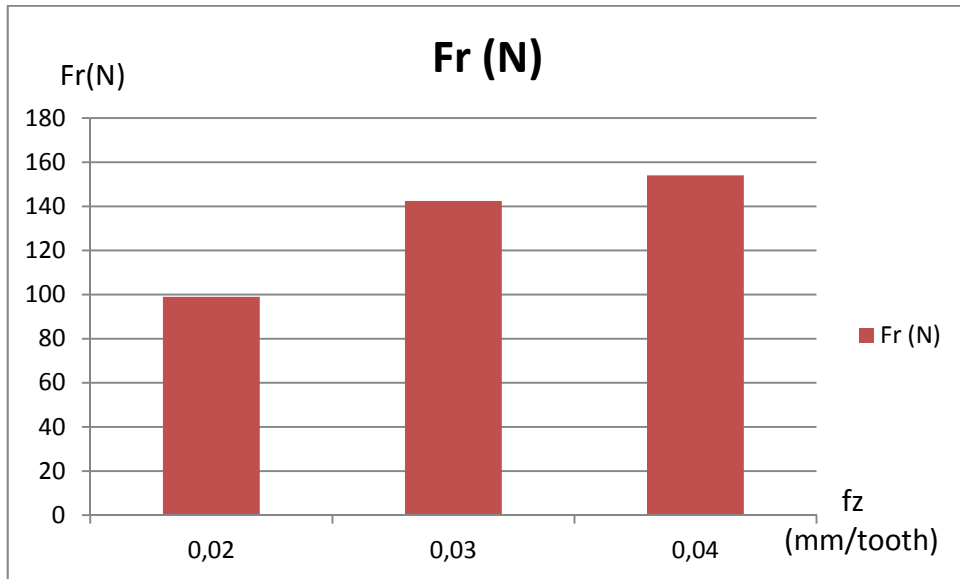


Figure 4.6 The Radial ( $F_r$ ) and Tangential ( $F_t$ ) Forces for 5000 rpm

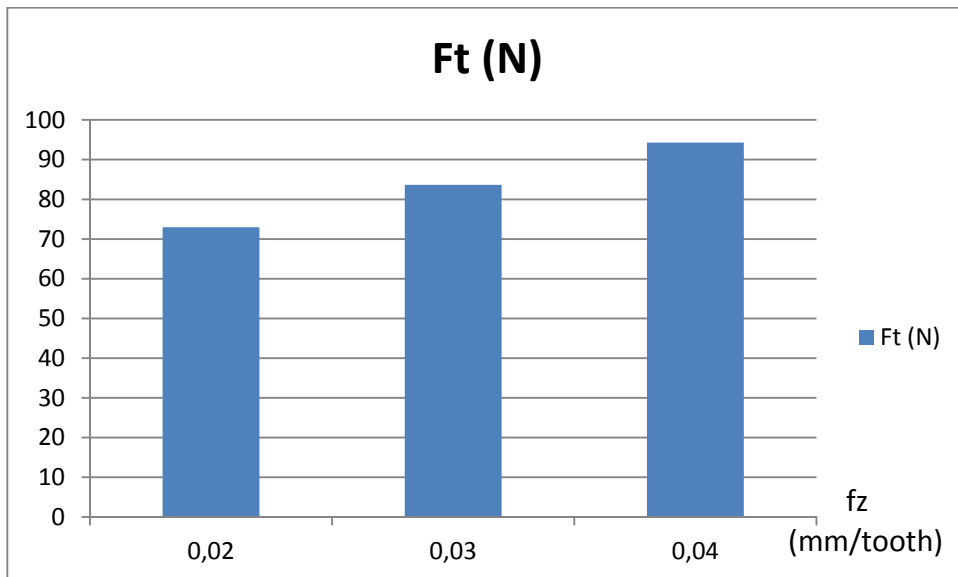
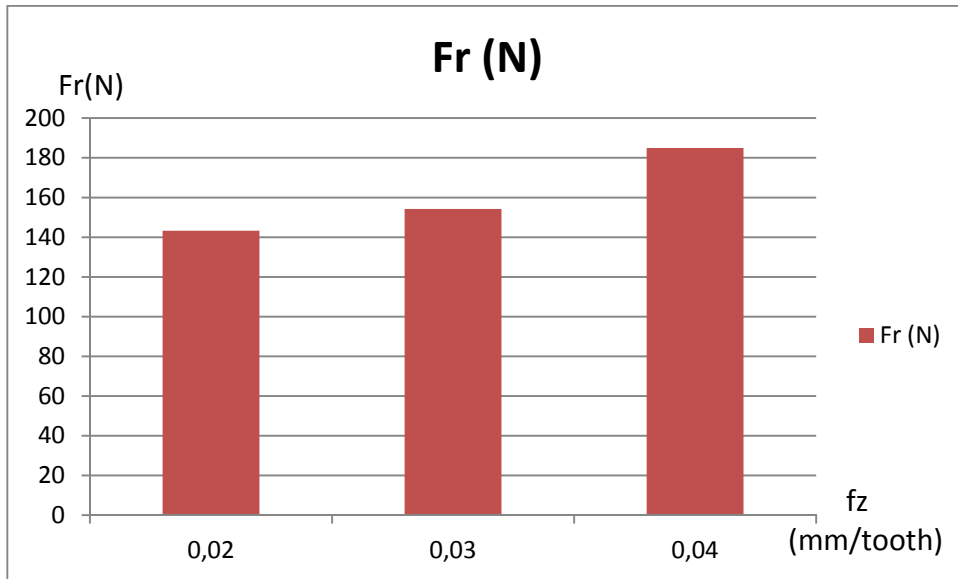


Figure 4.7 The Radial ( $F_r$ ) and Tangential ( $F_t$ ) Forces for 7000 rpm

#### 4.2.2 Tool Wear Measurement

Wear observed in the knurled tool in course of the trimming operation of CFRP composite material can be assorted into two broad categories that are fracture of the tips of the pyramid tooth and flank wear.

The influence of spindle speed or feed speed in wear measurements is not explicit to excessive scatter in the wear data. This may be on account of the inaccuracies in the measurement methods used. Moreover, the self-sharpening of the teeth at higher spindle speeds may cause paradoxes in wear measurement methods. On the other hand, chip formation in the machining of CFRP composite materials is chiefly caused by brittle fracture, not plastic deformation, which normally occurs in homogenous materials. Because of this variation in the wear data with regard to spindle speed and feed speed, quantifying tool wear and deciding on the best time for tool replacement is troublesome. Therefore, the identification of an indirect method is necessary to determine tool replacement time, based on the delamination depth as a limiting criterion.

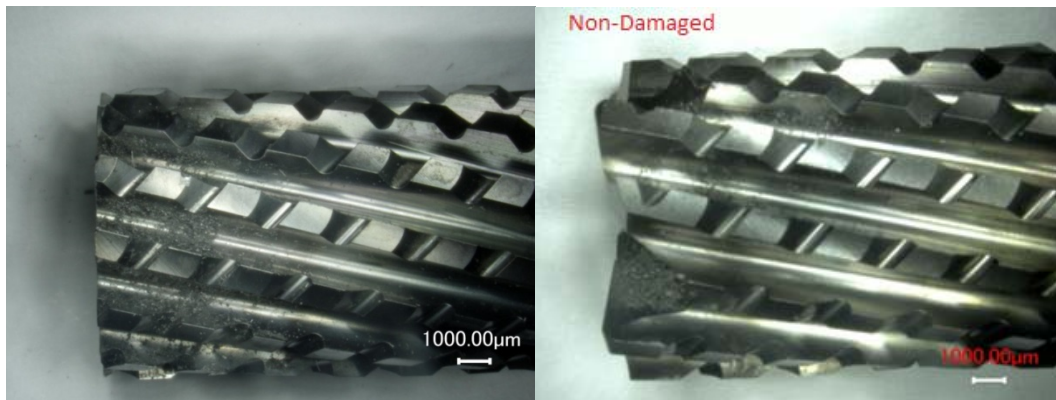
Each spindle speed for the same feed speeds was tested in the same conditions on the same workpiece material with the new 9 cutting tools. The amount of cutting distance machined from the workpiece is 6120 millimeter for each cutting tool. Tool replacement was done for every 6120 millimeter cutting distance. The cutting tools were measured using an optical microscope with 20X zoom lens. The results for each spindle speed are shown in the Figures 4.8, 4.9 and 4.10.



n=3000 rpm fz=0,02 mm/tooth Vf=720 mm/min

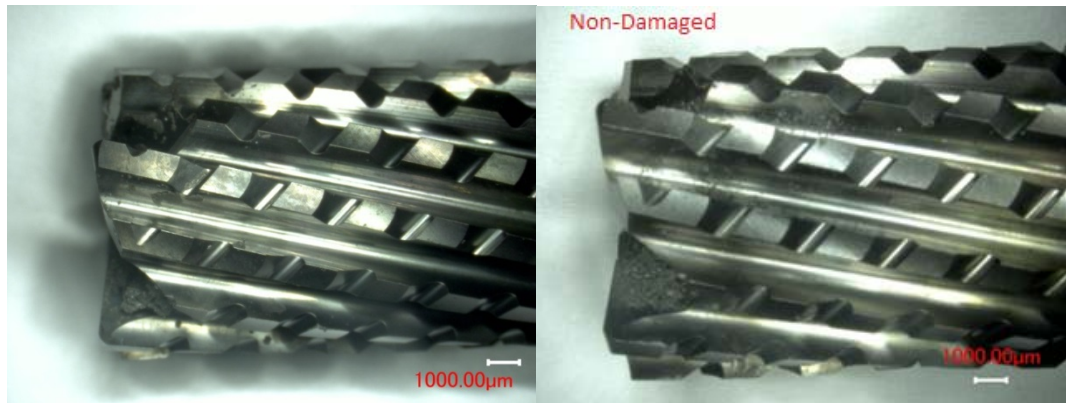


n=3000 rpm fz=0,03 mm/tooth Vf=1080 mm/min



n=3000 rpm fz=0,04 mm/tooth Vf=1440 mm/min

Figure 4.8 The Images of Tool Wear at 3000 rpm



n=5000 rpm fz=0,02 mm/tooth Vf=1200 mm/min

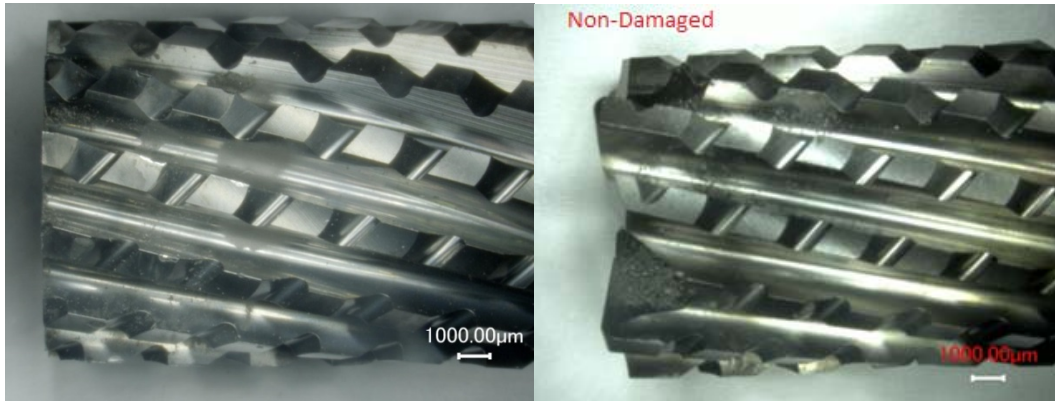


n=5000 rpm fz=0,03 mm/tooth Vf=1800 mm/min

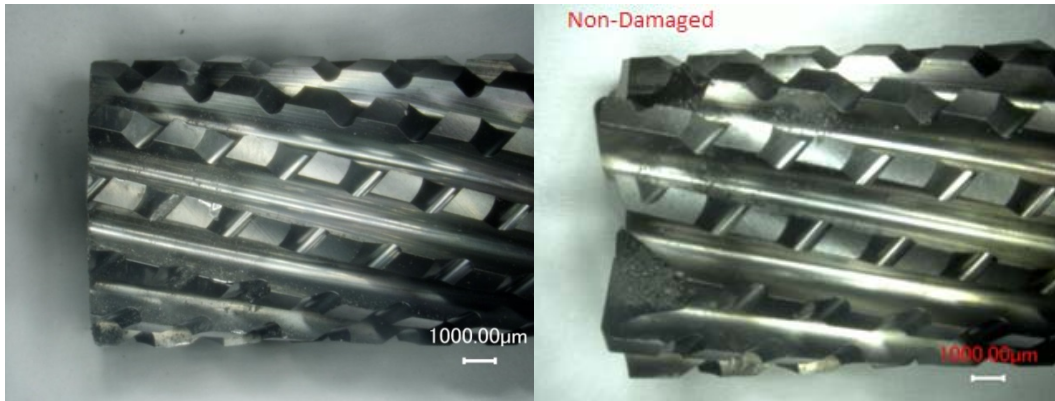


n=5000 rpm fz=0,04 mm/tooth Vf=2400 mm/min

Figure 4.9 The Images of Tool Wear at 5000 rpm



n=7000 rpm fz=0,02 mm/tooth Vf=1680 mm/min



n=7000 rpm fz=0,03 mm/tooth Vf=2520 mm/min



n=7000 rpm fz=0,04 mm/tooth Vf=3360 mm/min

Figure 4.10 The Images of Tool Wear at 7000 rpm

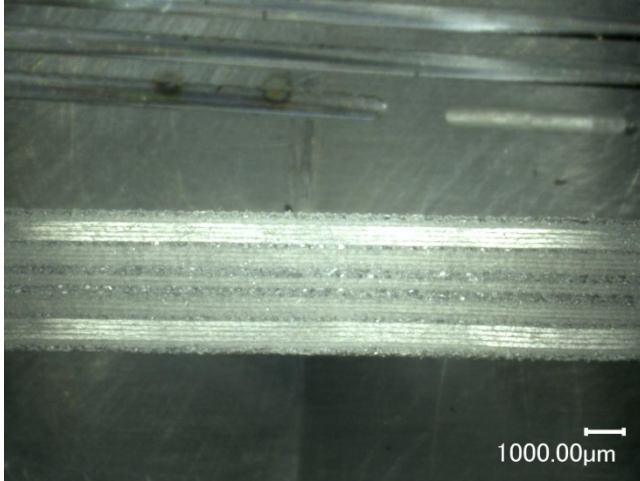
### **4.2.3 Delamination Measurement**

As the quality of the machined surface is crucial for the service life of a component, delamination was considered as a critical contributing cause in this study.

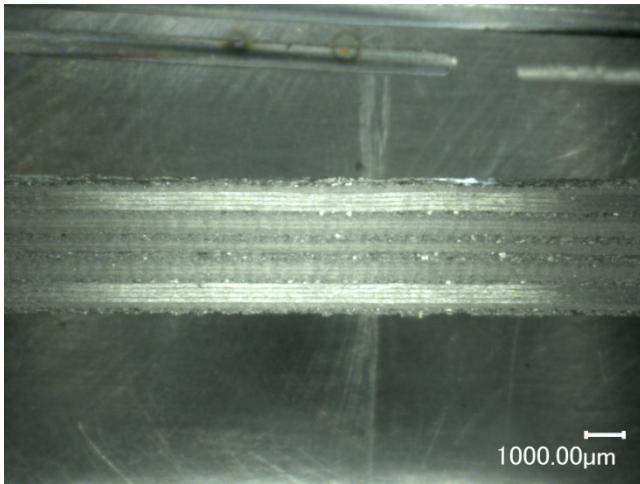
A 2.5 mm threshold was selected for delamination depth, in line with the acceptance range existent in the aerospace industries. Delamination can be categorized into three types as mentioned Chapter 2, which are;

1. Type I
2. Type II
3. Type III

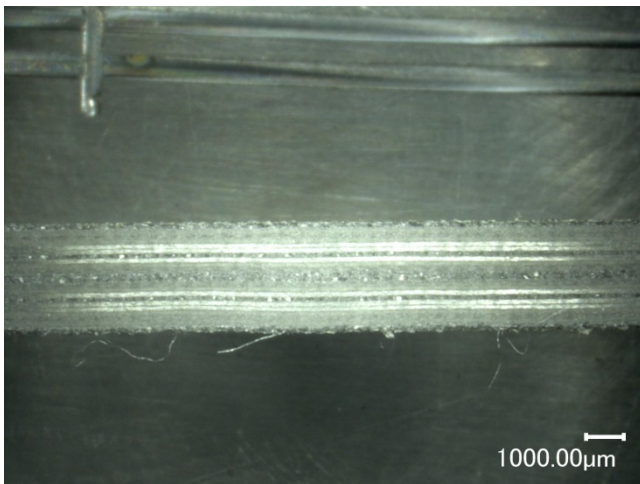
In addition to these delamination categories, a combined category of type I, and type II delamination has also been noted in this study. After testing three different spindle speeds for the same feed speed, 9 workpiece materials were examined with the help of an optical microscope. Figures 4.11, 4.12 and 4.13 show the microscope images for each cutting parameter.



n=3000 rpm  
fz=0,02 mm/tooth  
Vf=720 mm/min

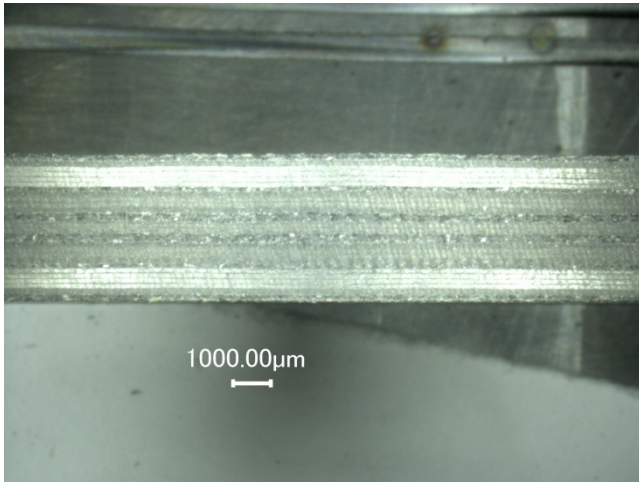


n=3000 rpm  
fz=0,03 mm/tooth  
Vf=1080 mm/min

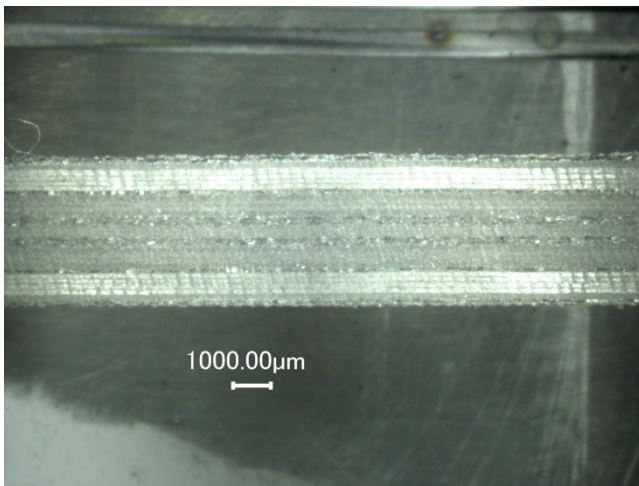


n=3000 rpm  
fz=0,04 mm/tooth  
Vf=1440 mm/min

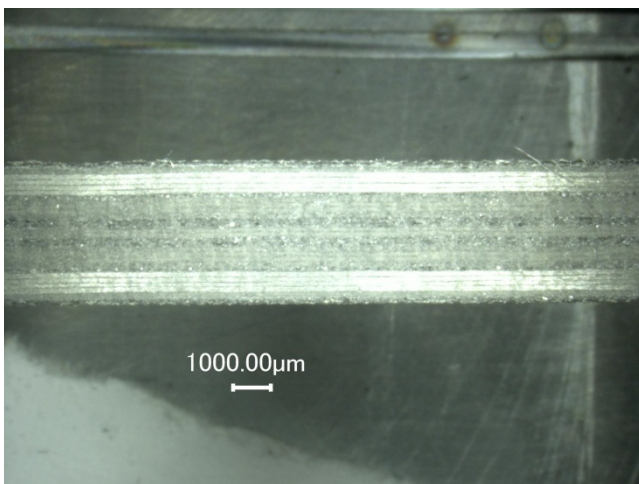
Figure 4.11 The Images of Delamination at 3000 rpm



n=5000 rpm  
fz=0,02 mm/tooth  
Vf=1200 mm/min

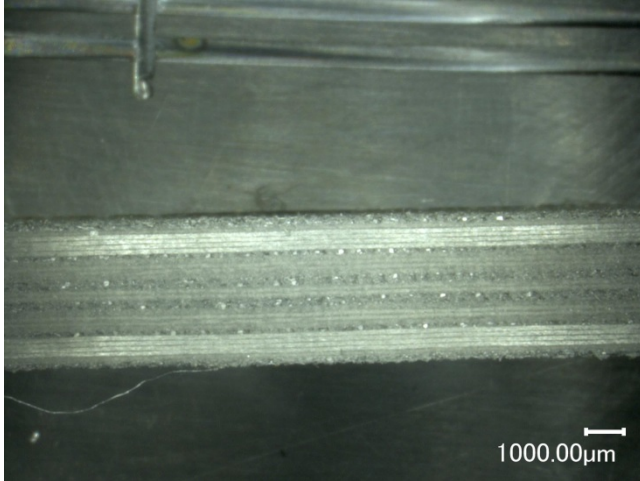


n=5000 rpm  
fz=0,03 mm/tooth  
Vf=1800 mm/min

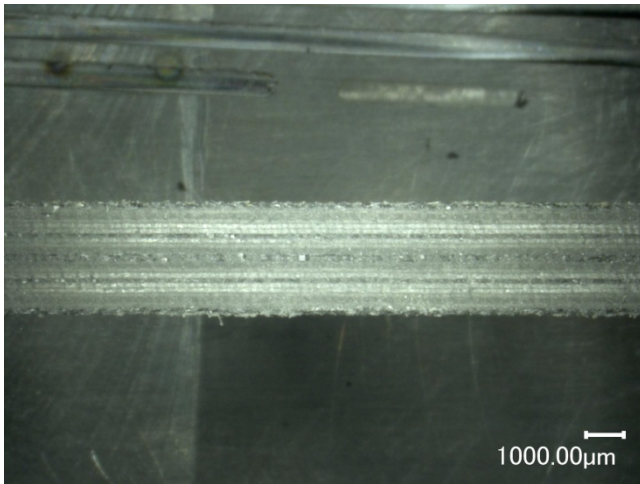


n=5000 rpm  
fz=0,04 mm/tooth  
Vf=2400 mm/min

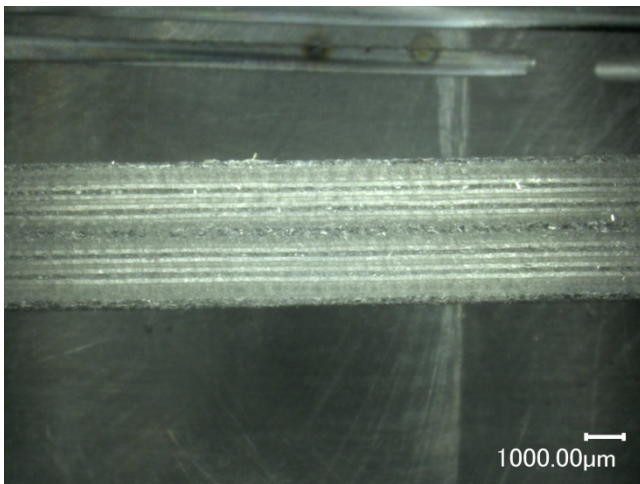
Figure 4.12 The Images of Delamination at 5000 rpm



n=7000 rpm  
fz=0,02 mm/tooth  
Vf=1680 mm/min



n=7000 rpm  
fz=0,03 mm/tooth  
Vf=2520 mm/min



n=7000 rpm  
fz=0,04 mm/tooth  
Vf=3360 mm/min

Figure 4.13 The Images of Delamination at 7000 rpm

### **4.3 The Thickness of Workpiece Material**

There are lots of CFRP materials used in the aerospace industry. CFRP materials are differ in terms of mechanical properties, curing temperature, ply thickness and type of fibers.

All of the experiments were done with the same CFRP material in this study. However, the effects of the cutting parameters on different types of CFRP materials are not known. For this purpose, 5000 rpm with selected feed per tooth values (0.02-0.03-0.04 mm/tooth) were tested on different CFRP workpiece material beforehand to observe the influence of cutting forces, tool wear and delamination.

For new experiments, a new workpiece material (LMAMA002FR49GRBCL1), which is unidirectional continuous carbon fiber reinforced composite was prepared and three new cutting tools were gained. The new workpiece material is epoxy prepreg that contains 228 g/m<sup>2</sup> fiber and the tensile strength of material is 1172 MPa and its tensile modulus is 90 GPa. The new test material has approximately 6 millimeter in thickness with 0.211 millimeter layer thickness and with 28- ply lay-up orientation was used in the workpiece material. The orientation of lay up has the same orientation with the previous workpiece material which is shown in the Table 4.3.

Table 4.3 The Fiber Orientation of the Second CFRP Material

<b>PLY NO</b>	<b>DIRECTION</b>	<b>MATERIAL</b>
1	45	LMAMA002FR49GRBCL1
2	135	LMAMA002FR49GRBCL1
3	90	LMAMA002FR49GRBCL1
4	135	LMAMA002FR49GRBCL1
5	0	LMAMA002FR49GRBCL1
6	45	LMAMA002FR49GRBCL1
7	0	LMAMA002FR49GRBCL1
8	135	LMAMA002FR49GRBCL1
9	0	LMAMA002FR49GRBCL1
10	45	LMAMA002FR49GRBCL1
11	0	LMAMA002FR49GRBCL1
12	135	LMAMA002FR49GRBCL1
13	90	LMAMA002FR49GRBCL1
14	45	LMAMA002FR49GRBCL1
15	45	LMAMA002FR49GRBCL1
16	90	LMAMA002FR49GRBCL1
17	135	LMAMA002FR49GRBCL1
18	0	LMAMA002FR49GRBCL1
19	45	LMAMA002FR49GRBCL1
20	0	LMAMA002FR49GRBCL1
21	135	LMAMA002FR49GRBCL1
22	0	LMAMA002FR49GRBCL1
23	45	LMAMA002FR49GRBCL1
24	0	LMAMA002FR49GRBCL1
25	135	LMAMA002FR49GRBCL1
26	90	LMAMA002FR49GRBCL1
27	135	LMAMA002FR49GRBCL1
28	45	LMAMA002FR49GRBCL1

The workpiece material the size of which was 300x300 millimeter was clamped with the same method in the same machining center, which is shown in Figure 4.14. The workpiece was tested in 5000 rpm with three different feed per tooth values in the same conditions. 6120 millimeter cutting distance were machined with each cutting tool.

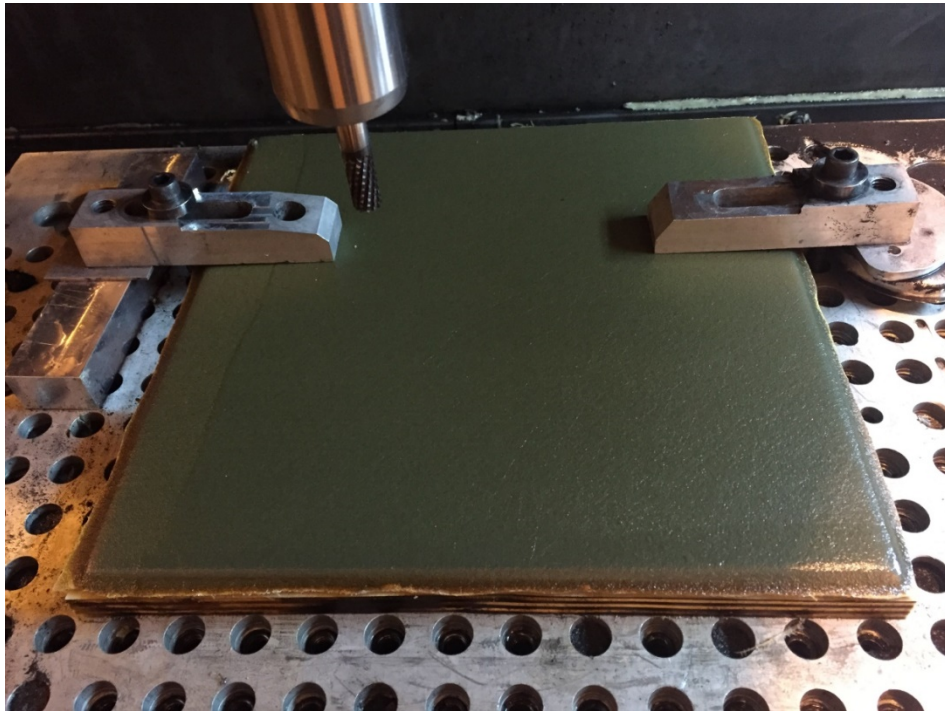


Figure 4.14 The Workpiece Material Clamping System

The cutting forces were measured with the same rotary type dynamometer during the experiments. The cutting force results are shown in figure 4.15.

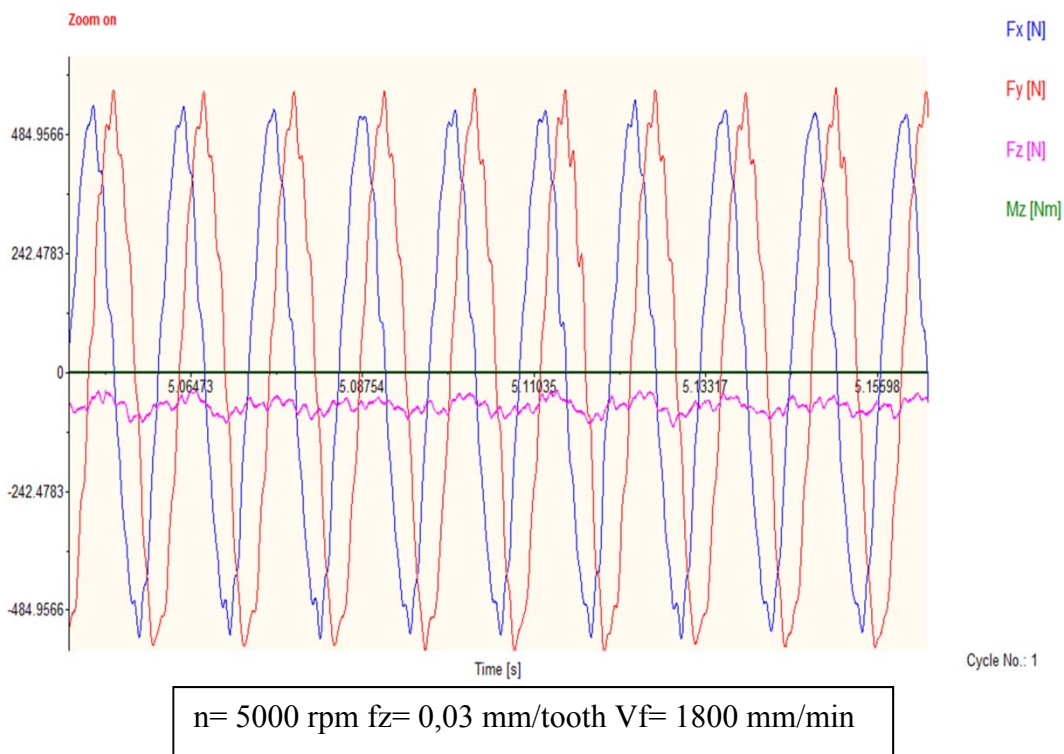
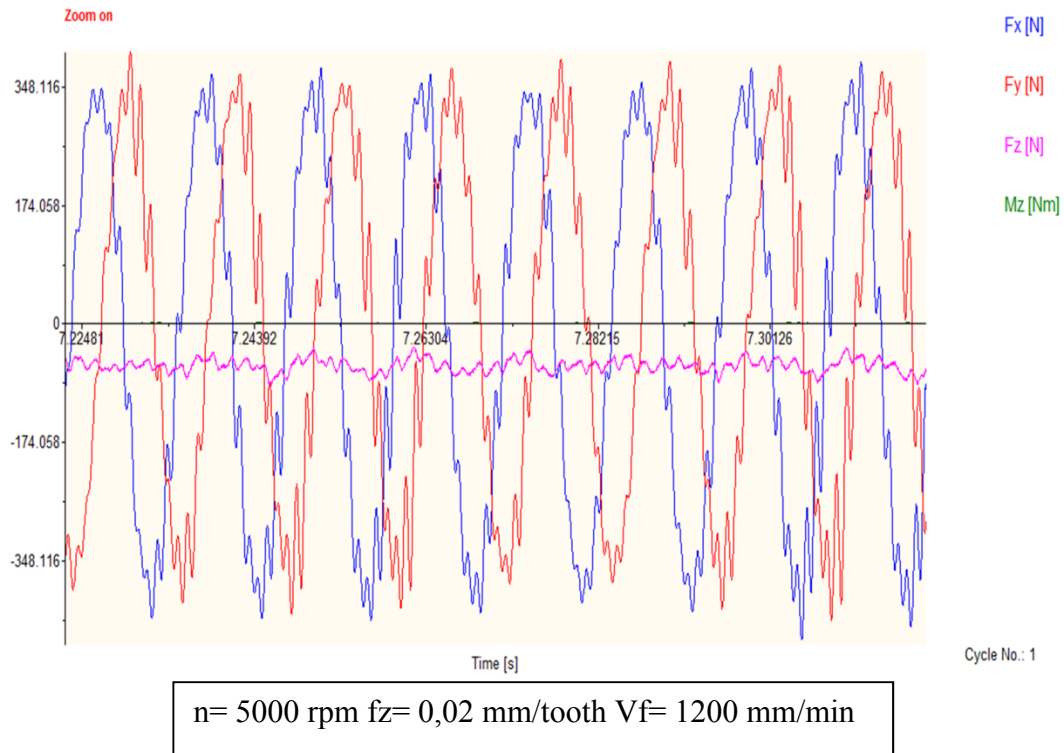


Figure 4.15 The Cutting Forces Results for Second Test Material

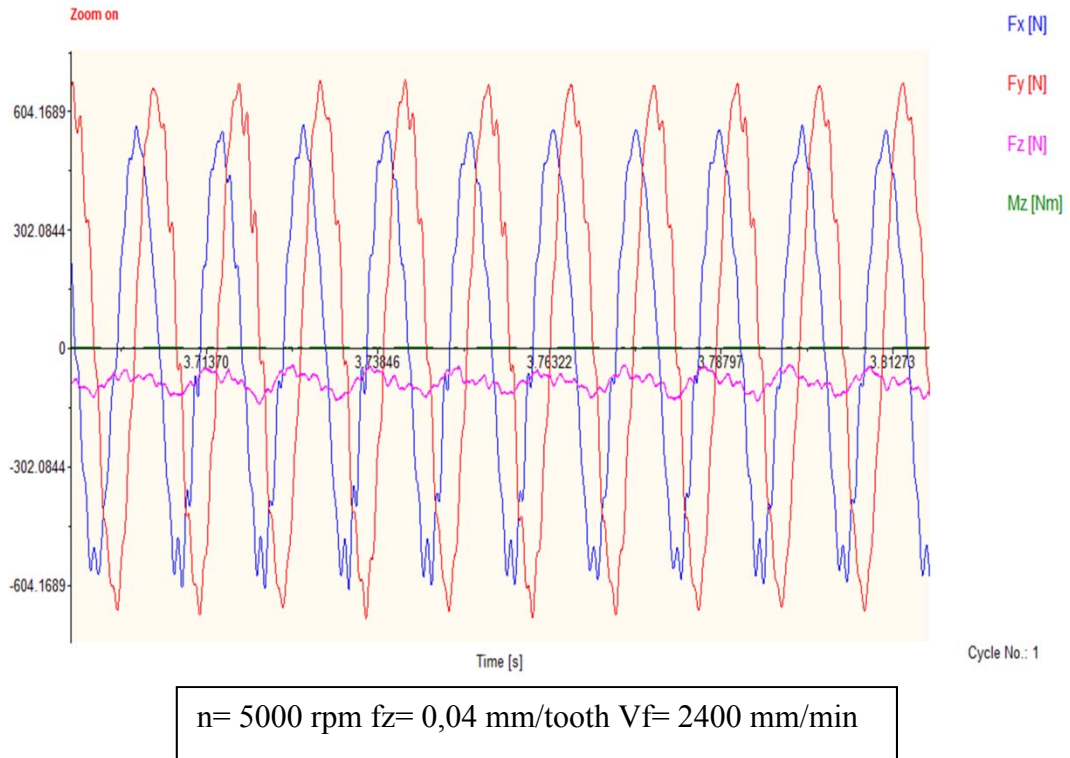


Figure 4.15 (Continued)

As can be seen from a comparison of figures 4.2 and 4.15 in relation to the cutting forces between the two test materials in same spindle speed and feed speeds, it is evident that the cutting forces increase in thicker material.

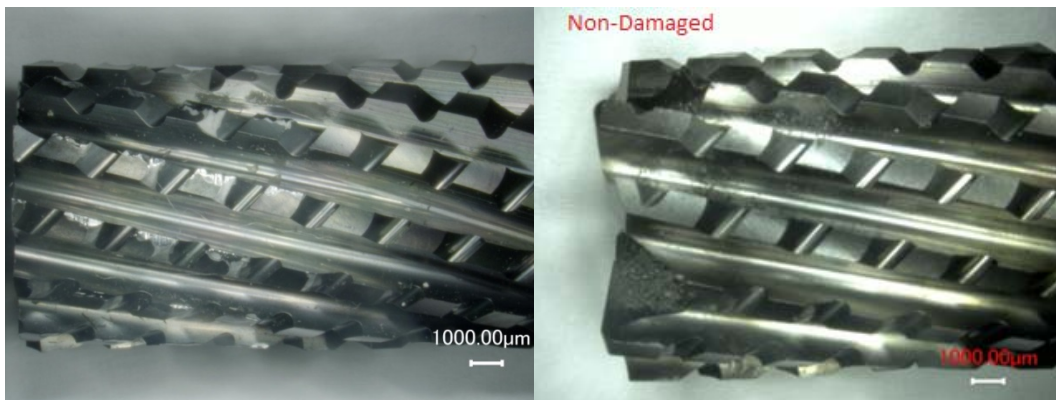
After the cutting tests, the cutting tools were examined by using the optical microscope again. The cutting tool wear images are given in figure 4.16.



n=5000 rpm fz=0,02 mm/tooth Vf=1200 mm/min



n=5000 rpm fz=0,03 mm/tooth Vf=1800 mm/min

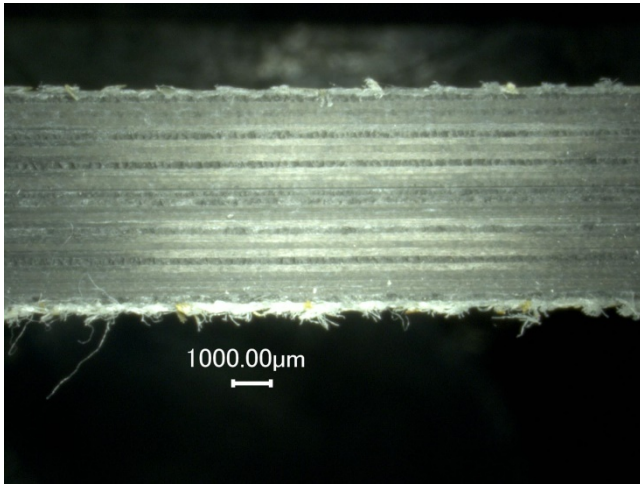


n=5000 rpm fz=0,04 mm/tooth Vf=2400 mm/min

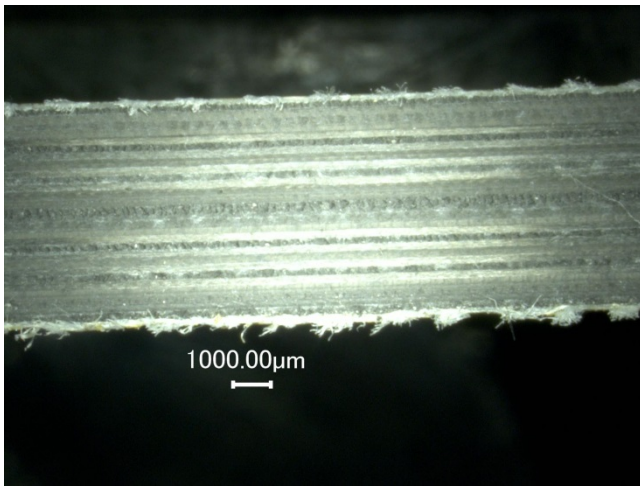
Figure 4.16 The Cutting Tool Images for Second Test Material

The results of wear images between the two materials are shown in Figures 4.9 and 4.16. While high edge chipping on cutting tool edges occurred in thicker test material, there was no wear or edge chipping in the thin one.

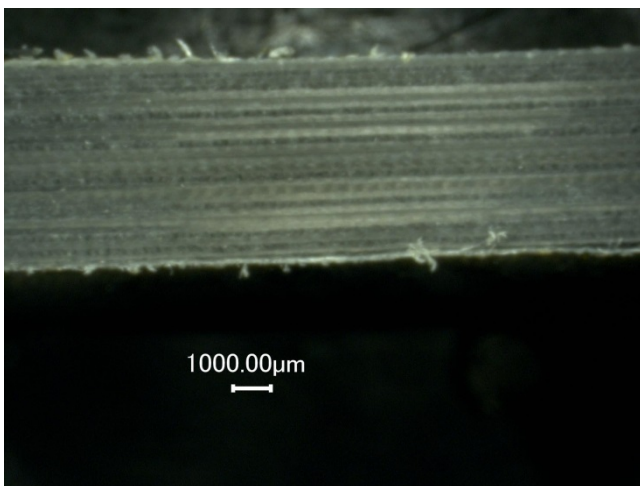
The machined workpiece material surfaces were analyzed under the optical microscope for delamination. The images from microscope are shown in figure 4.17.



n=5000 rpm  
fz=0,02 mm/tooth  
Vf=1200 mm/min



n=5000 rpm  
fz=0,03 mm/tooth  
Vf=1800 mm/min



n=5000 rpm  
fz=0,04 mm/tooth  
Vf=2400 mm/min

Figure 4.17 The Images from Optical Microscope for Second Test Material

According to the figures 4.12 and 4.17 images, there is no difference between the two test material considering surface quality. Delamination does not occur in both of workpiece material.

#### 4.4 The Relation of Cutting Forces Between Non-damaged and Damaged Cutting Tool

After the experiments, the cutting forces on the damaged cutting tool were measured using the rotary dynamometer to determine the cutting force difference between the damaged cutting tool and non-damaged one. Figure 4.18 gives the cutting forces on the damaged cutting tool at 7000 rpm.

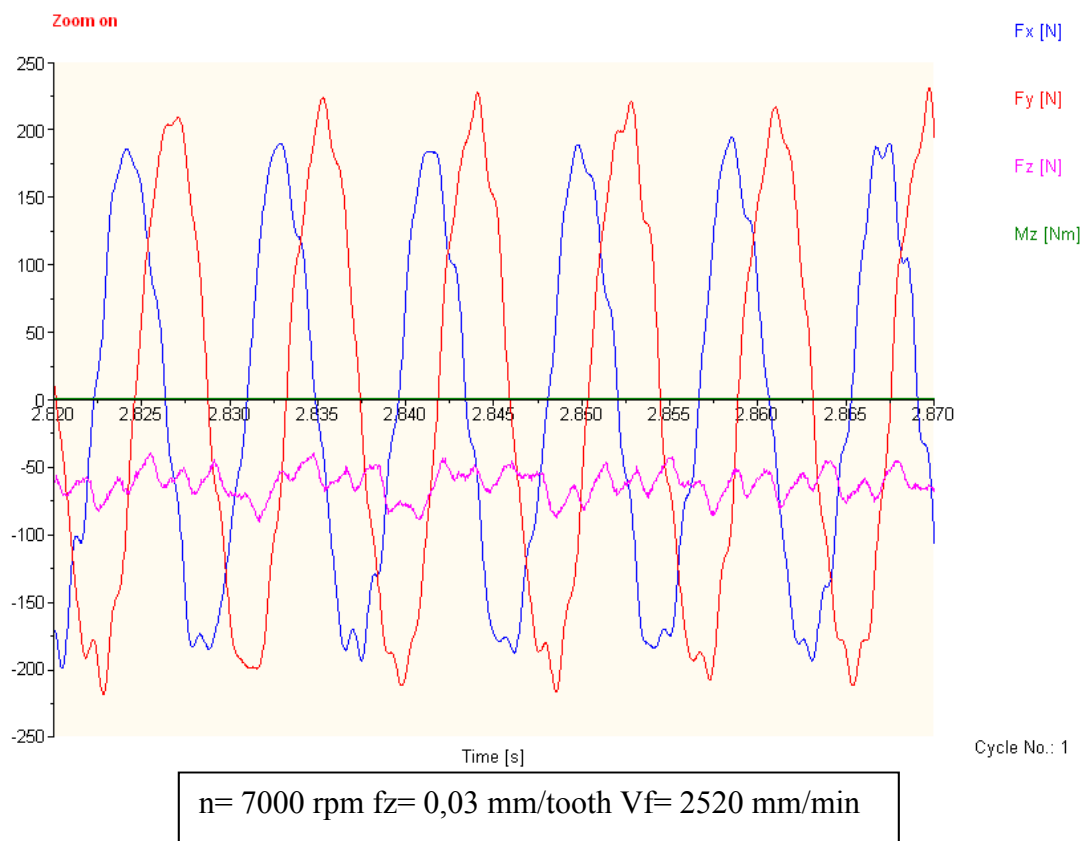


Figure 4.18 The Cutting Force Result on the Damaged Cutting Tool at 7000 rpm

As seen in the Figure 4.18 the cutting forces along x and y directions rises up when compared with the Figure 4.3 which has the same feed speed and spindle speed. In order to prospect the cutting forces which act the cutting tool used on the second workpiece material, again the cutting forces were observed. In the Figure 4.19 the cutting forces on the damaged cutting tool at 5000 rpm while machining the second workpiece material is shown below.

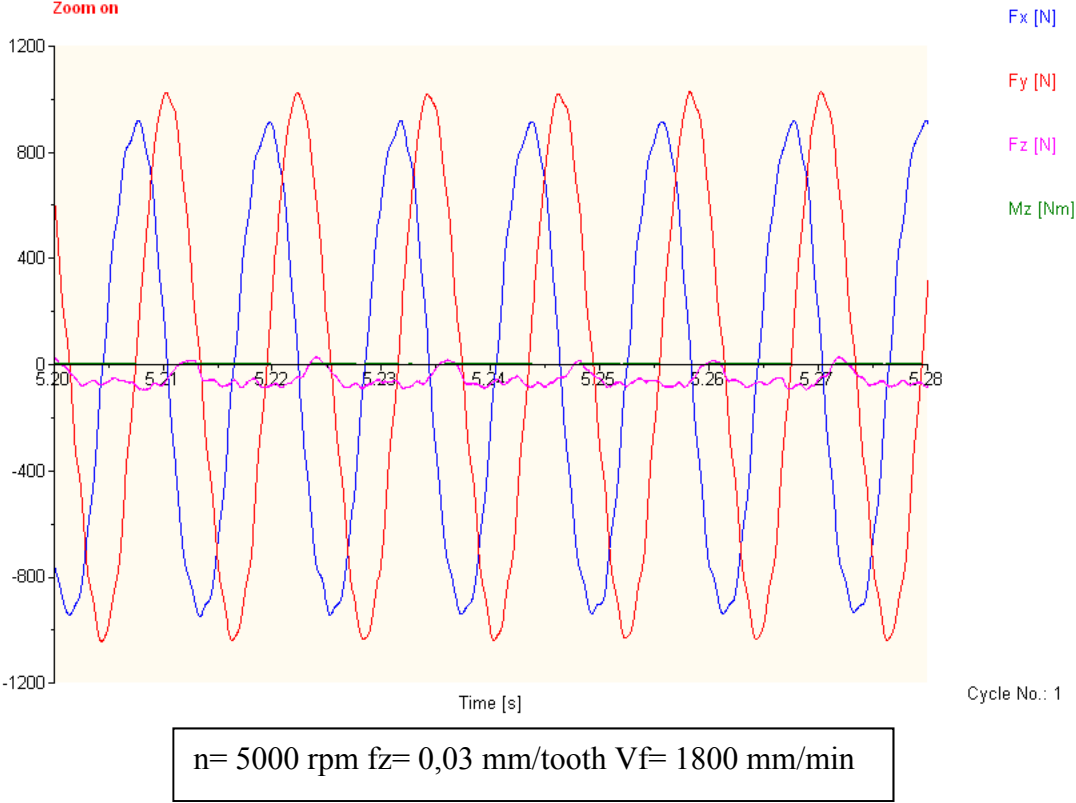


Figure 4.19 The Cutting Force Result on the Damaged Cutting Tool at 5000 rpm for the Second Workpiece Material

Figure 4.19 gives the cutting forces along x and y directions approximately increases twice when comprised with the Figure 4.15 which has the same feed speed and spindle speed. In conclusion, the workpiece material thickness plays an important role on the cutting forces.

## **4.5 Statistical Analysis of Experimental Data**

In order to affirm the experimental results, statistical analysis needs to be carried out in order to draw meaningful conclusions in this respect. Statistical analysis assists in removing experimental errors gathered from the data, provides validity to experimental results and attaches a level of confidence to the results. This in turn, adds to the soundness and validity of the experimental methods, results and conclusions.

The statistical analysis was undertaken using Design-Expert Software Version 9, Stat-Ease, Inc. The factors considered were spindle speed, feed per tooth and cutting distance whereas the response was delamination depth. For the study independent variables were selected as spindle speed, feed per tooth and cutting distance, dependent variable was determined as delamination. The statistical analysis to find out the relationship between variables was analysis of variance (ANOVA) by utilizing the Box-Behnken design. In the following sections, discuss on the statistical results are given.

### **4.5.1 Statistical Design Matrix**

Based on designed matrix, the Stat-Ease software was used to generate experimental matrix. The experimental data was given in the Table 4.4.

Table 4.4 Design Setup of ANOVA Table for the Potential Factors and Response

Exp. Run	A: Spindle Speed (Rpm)	B: Feed per Tooth (mm/tooth)	C: Cutting Distance (mm)	Response: Delamination (mm)
1	5000	0.030	6120	0
2	5000	0.090	6120	0
3	5000	0.010	6120	0
4	5000	0.040	6120	0.198
5	5000	0.100	6120	0
6	5000	0.060	6120	0
7	5000	0.035	6120	0.376
8	5000	0.040	6120	0
9	5000	0.030	6120	2.034
10	5000	0.040	3060	2.447
11	5000	0.020	3060	2.989
12	5000	0.025	3060	3.103
13	5000	0.070	3060	3.125
14	3000	0.050	6120	0
15	3000	0.015	6120	0
16	3000	0.020	6120	0
17	7000	0.030	6120	0
18	7000	0.020	6120	0
19	7000	0.080	6120	0

#### 4.5.2 Normality Analysis of Factors

In order to assess the assumption of ANOVA, residual plots were scanned. In addition, to provide more evidence to collinearity assumption VIF results were checked. In order not to violate normality assumptions the VIF results are not more than 4 to 5. Thus, it can be said that all variables are in accepted which means the assumption of multi-collinearity were met.

To test the normality assumption, the normality residuals were controlled. The normal probability plot demonstrates deviations from normality and the straight line in this figure represents a normal distribution. The observed residuals do lie on the line very well which indicates the normality. So, again it is observed that there is not any problem in the name of normality.

### 4.5.3 Statistical Output Analysis

In order to understand the effect of spindle speed, feed per tooth and cutting distance on delamination, ANOVA analysis was conducted. The confidence interval for variance was selected as %95 which indicates 0.05 alpha. The ANOVA results of first order model showed that value of probability of linear model is less than 0.05 that means the terms in the model could fit and adequate, results are presented in Table 4.5.

Table 4.5 Analysis of Variance Table of Delamination for Linear Model

Source	Sum of Squares	df	Mean Square	F Value	p-value Prob>F	
Model	22.21	3	7.40	140.02	<0.0001	significant
A-Spindle Speed	0.000	1	0.000	0.000	1.0000	
B-Feed per Tooth	0.21	1	0.21	4.05	0.0624	
C-Cutting Distance	3.77	1	3.77	71.28	<0.0001	
Residual	0.79	15	0.053			
Cor Total	23.00	18				

The delamination equation of first order model is;

Final Equation in Terms of Coded Factors:

$$\text{Delamination} = +1.14 + 0.000 * A + 3.38 * B - 0.90 * C \quad (4.2)$$

Final Equation in Terms of Actual Factors:

$$\text{Delamination} = +4.15331 + 0.000000 * \text{Spindle Speed} + 8.36634 \text{ Feed per Tooth} - 7.14772\text{E-}004 * \text{Cutting Distance} \quad (4.3)$$

The table 4.5 shows the 95% confidence interval for the experiments. The analysis of variance of first order- model is shown in table 4.5. For the linear model, the p-value for model of fit is 140.02 ( $p < 0.05$ ) is significant. This implies that the model could fit

and it is adequate. Moreover, from the coefficient estimates presented in Table 4.6, feed per tooth has the most significant effect on delamination. The equation shows that feed per tooth increases when spindle speed increase and decrease cutting distance.

Table 4.6 Coefficient Table of Delamination for Linear Model

Factor	Coefficient Estimate	df	Standard Error	95% CI Low	95% CI High	VIF
Intercept	1.14	1	0.059	1.01	1.27	
A-Spindle Speed	0.000	1	0.094	-0.20	0.20	1.00
B-Feed Speed	0.38	1	0.19	-0.022	0.78	4.01
C-Cutting Distance	-0.90	1	0.11	-1.13	-0.67	4.01

The second order model was used in specifying the relationship between the spindle speed, feed speed and cutting distance to independent variable. The model was based on the Box- Behnken design method. The developed second order mathematical model is given in equation below.

$$\text{Delamination} = +0.67 + 0.000 * A + 0.79 * B - 0.58 * C + 0.000 * A * B - 0.68 * B * C \quad (4.4)$$

The Table 4.7 shows the 95% confidence interval for the experiments. The analysis of variance of second order model is depicted in Table 4.8. For the second order model, the F-statistic is 267.45 (p<0.05). This alludes that the model could fit and that it is adequate. The fit summary recommends that both the (linear model) first order model and the interaction model (second order) are statistically significant to analyze delamination.

Table 4.7 Analysis of Variance Table of Delamination for Second Order Model

Source	Sum of Squares	df	Mean Square	F Value	p-value Prob > F	
Model	22.78	5	4.56	267.45	< 0.0001	significant
A-Spindle Speed	0.000	1	0.000	0.000	1.0000	
B-Feed per Tooth	0.65	1	0.65	38.11	< 0.0001	
C-Cutting Distance	0.84	1	0.84	49.45	< 0.0001	
AB	0.000	1	0.000	0.000	1.0000	
AC	0.000	0				
BC	0.57	1	0.57	33.55		
ABC	0.000	0				
Residual	0.22	13	0.017			
Cor Total	23.00	18				

As it can be understood from the coefficient estimates in the Table 4.8 for effect A reveals that A is aliased to AC and AB aliased to ABC. This observation would lead the experimenter to conclude that the variability is due to interaction AC and ABC not factor A or AB. Interaction of three factors was not calculated.

Table 4.8 Coefficient Table of Delamination for Linear Model

Factor	Coefficient Estimate	df	Standard Error	95% CI Low	95% CI High	VIF
Intercept	0.67	1	0.087	0.48	0.86	
A-Spindle Speed	0.000	1	0.17	-0.37	0.37	10.38
B-Feed per Tooth	0.79	1	0.13	0.51	1.07	5.82
C-Cutting Distance	-0.58	1	0.082	-0.76	-0.40	7.39
AB	0.000	1	0.29	-0.63	0.63	10.38
AC ALIASED A						
BC	-0.68	1	0.12	-0.63	0.63	1.91
ABC ALIASED AB						

The first order and second order models are found to be truly representative of delamination with experimental results. Yet, the second order model is more precise than the first order model in predicting the delamination.

The interaction plot by using 3D surface method was presented in Figure 4.20. Because only feed per tooth and cutting distance factors indicates an interaction, the 3D surface figure was presented for these factors. Other factors presented aliased with the same factors in the experiment. Spindle speed and cutting distance interaction were aliased to spindle speed, where interaction of three factor which are spindle speed, cutting distance and feed per tooth were aliased to interaction of feed per tooth and cutting distance. Aliased Matrix of analysis is given below;

Alias Matrix;

- [Intercept] = Intercept
- [A] = A + AC
- [B] = B
- [C] = C
- [AB] = AB + ABC
- [BC] = BC

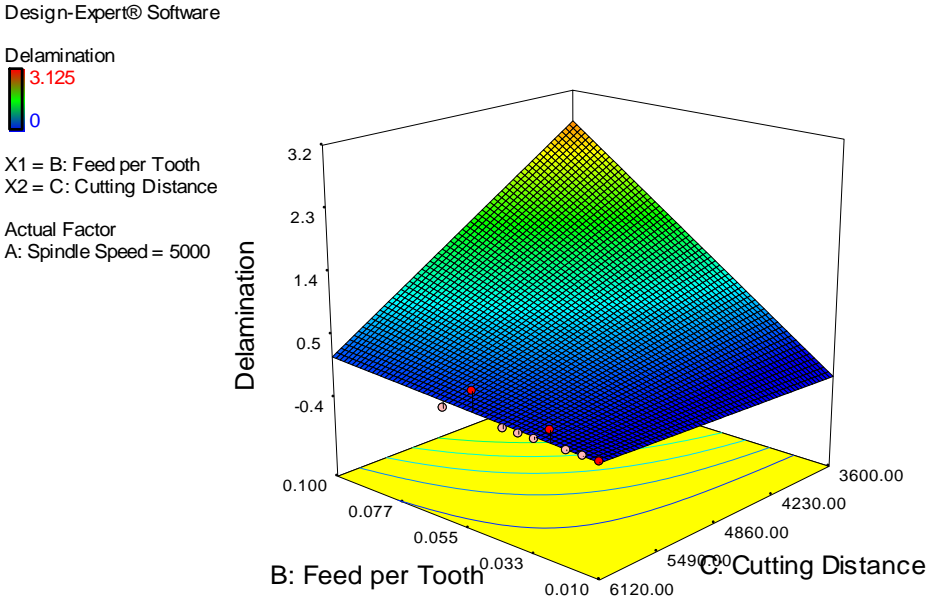


Figure 4.20 Interaction Effect Plot of Feed per Tooth and Cutting Distance for Delamination

3D surface plot displays the predicted response as a 3<sup>rd</sup> dimension. In the 3D surface plot, the feed per tooth and cutting distance (input parameter) variables are shown on the horizontal axes. Delamination (solve for) variable is shown along the vertical axis. Thus, the surface plot presents that delamination minimum, high feed per tooth and low cutting distance.

The contour plot is given in Figure 4.21, the contour plot is formed by vertical axis; cutting distance, horizontal axis feed per tooth; response value delamination. The visual observation of contour plot presents that highest delamination is achieved at feed per tooth range between 0.077 and 0.100 mm/tooth, and cutting distance range between 4230 and 3600 mm.

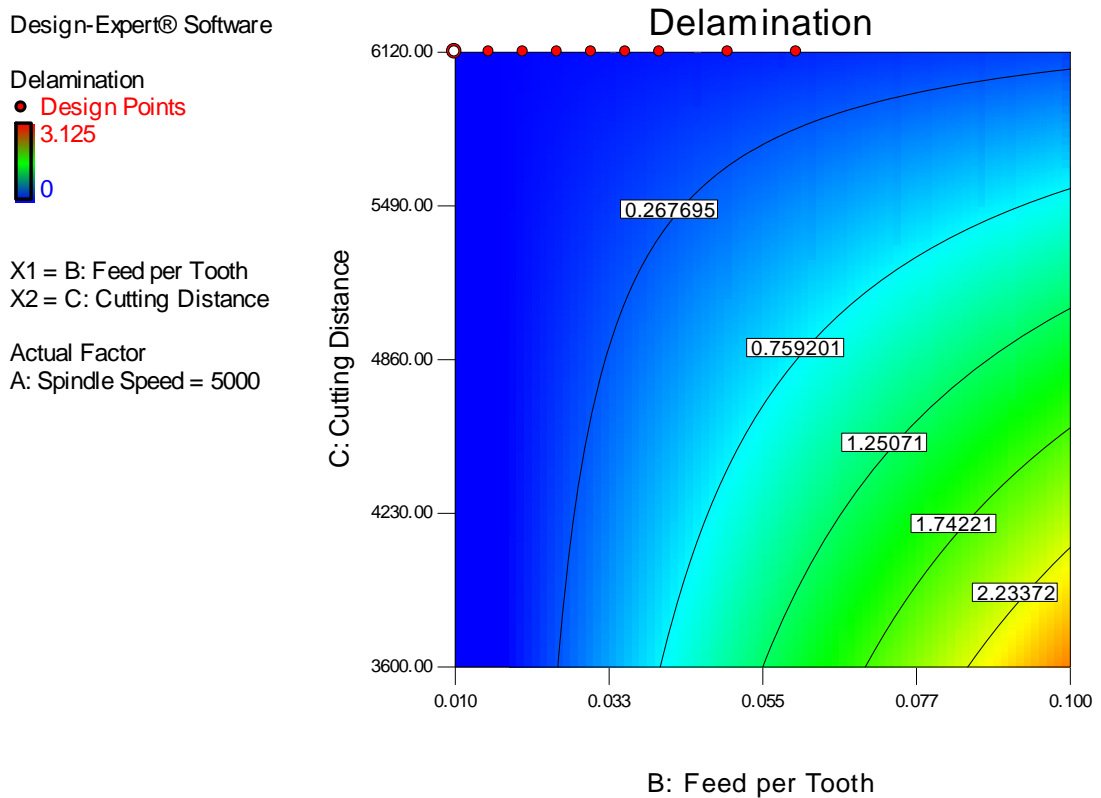


Figure 4.21 Contour Plot of Feed per Tooth and Cutting Distance for Delamination

## 4.6 Results and Discussions

The cutting forces samples which are shown in the figures 3.14, 4.1, 4.2, 4.3, 4.15, 4.18 and 4.19 were obtained during the machining operations with a rotary type dynamometer. The data sampling rate was 25000 Hz. The force signals appear in all measured data similar to sinusoidal wave and negative and positive direction in the graphs. Since, the dynamometer is attached on to the spindle and it rotates with the spindle simultaneously. It can be seen clearly, there are distinctive peaks in the cutting force measurements graphs corresponding to the engagement of the twelve flutes on the cutting tool. The force signals fluctuations are probably because of the inhomogeneous workpiece structure and omitting of the force measuring system.

The cutting forces increase in each cycle because of the rise on uncut chip thickness from zero at the cutting edge entry to a maximum exit. The effect of the fiber orientation which constantly changes from tool entry to tool exit is observed on the cutting force by Sheikh-Ahmad [25].

For the multidirectional laminate workpiece, there are two idiocratic peaks for each flute engagement in the cutting forces. These peaks again show the sudden changes in fiber orientation during the cutting edge transition from one laminate to another. Since, the cutting tool has two flutes, and the radial depth of cut is small, and only one single flute engages the workpiece at a time. While cutting tool rotates, the engaged cutting edge in the workpiece goes from one thickness laminate direction to another as expressed again by Sheikh-Ahmad [17].

Karpat et al [22] also examined different fiber orientations effects on the cutting forces. He found that  $45^\circ$  and  $135^\circ$  fiber direction laminate gave lower cutting forces than  $0^\circ$  and  $90^\circ$  fiber directions during machining. It is concluded that laminates with  $45^\circ$  and  $135^\circ$  fiber directions can be used as top and bottom layer fiber directions. Also, sine function represent the fiber angle and the cutting force coefficients in his study. He believes that, sine function yielded good estimations during machining multidirectional CFRP laminates.

In this study, to investigate the effect of the fiber orientations and the cutting tool geometry on the cutting force, some additional experiments also performed with two cutting edge tool which is non-complicated shown in the Figure 4.22 and only  $0^\circ$  laminated workpiece.



Figure 4.22 Two Fluted Cutting Tool

In the performed experiments, twelve fluted cutting tool causes shifting of the  $F_x$  and  $F_y$  cutting force components in the cutting force graphs can be seen in the Figures 3.14, 4.1, 4.2, 4.3, 4.15, 4.18 and 4.19. To compare the cutting tools, the cutting force was measured during machining the workpiece , has 28 different ply orientation, used all the experiments with the two fluted cutting tool which has simple geometry in contrast the twelve fluted cutting tool. The results show that while shifted force components occur in the twelve fluted cutting tool, there is no shifting in the cutting force components in the two fluted cutting tool as seen in the Figure 4.23.

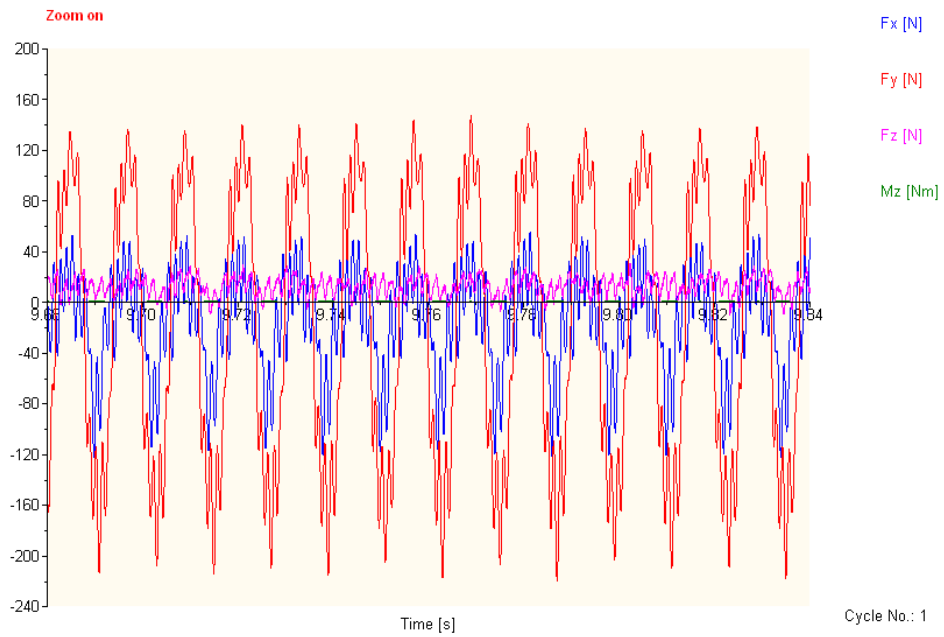


Figure 4.23 The Cutting Force Data with Two Fluted Cutting Tool on Original Workpiece

The same two fluted tool and the twelve fluted tool which is used in all the experiments were tested on  $0^\circ$  laminated workpiece. The cutting force data results are given Figure 4.24 and 4.25.

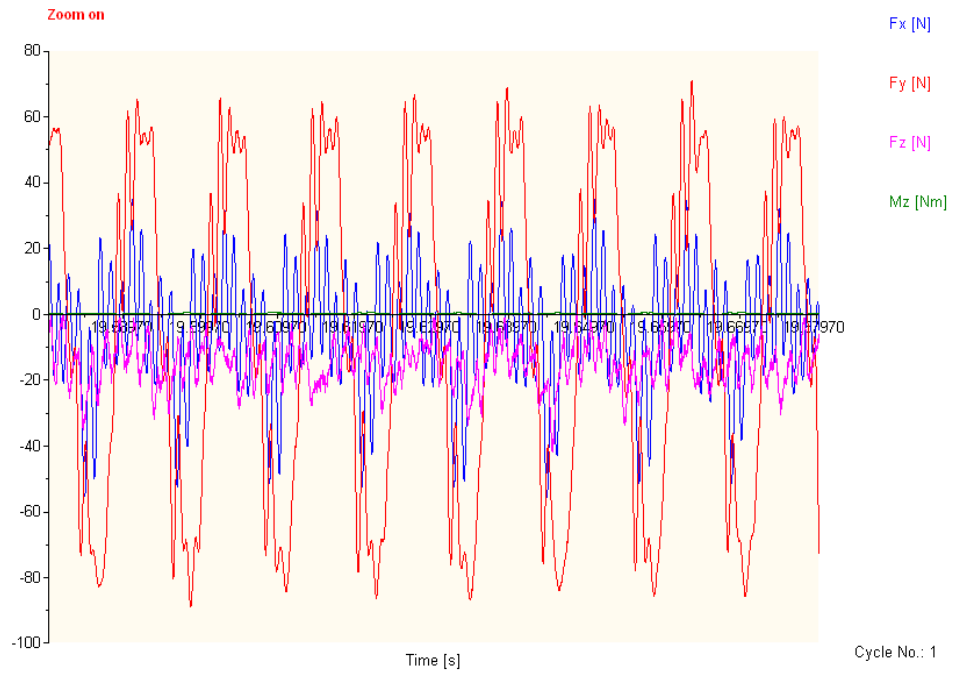


Figure 4.24 The Cutting Force Data with Two Fluted Cutting Tool on  $0^\circ$  Laminated Workpiece

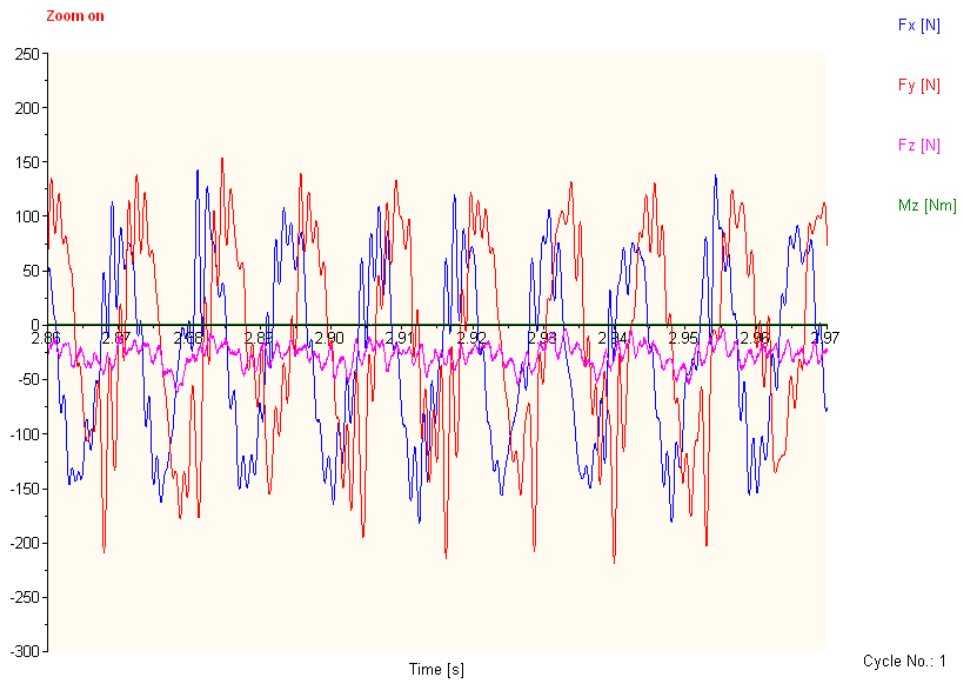


Figure 4.25 The Cutting Force Data with Twelve Fluted Cutting Tool on  $0^\circ$  Laminated Workpiece

As seen in the figures, the laminate orientation does not affect the shifting issue. The important thing in shifting of cutting force components is the shape of the tool geometry. Shifting phenomena occurs when the tool geometry is complicated; otherwise there is no shifting on the cutting force components,  $F_x$  and  $F_y$ .

In this thesis, the most appropriate cutting conditions are investigated at the same time. Different feed per tooth values were tested on the same workpiece material at 5000 rpm at the same cutting distance and the best cutting conditions which are 0.02, 0.03 and 0.04 feed per tooth values were determined according to tool wear and delamination depth. The same feed per tooth values were tested at 3000 rpm and 7000 rpm. The results of experiments are given collectively in the Figure 4.26 below.

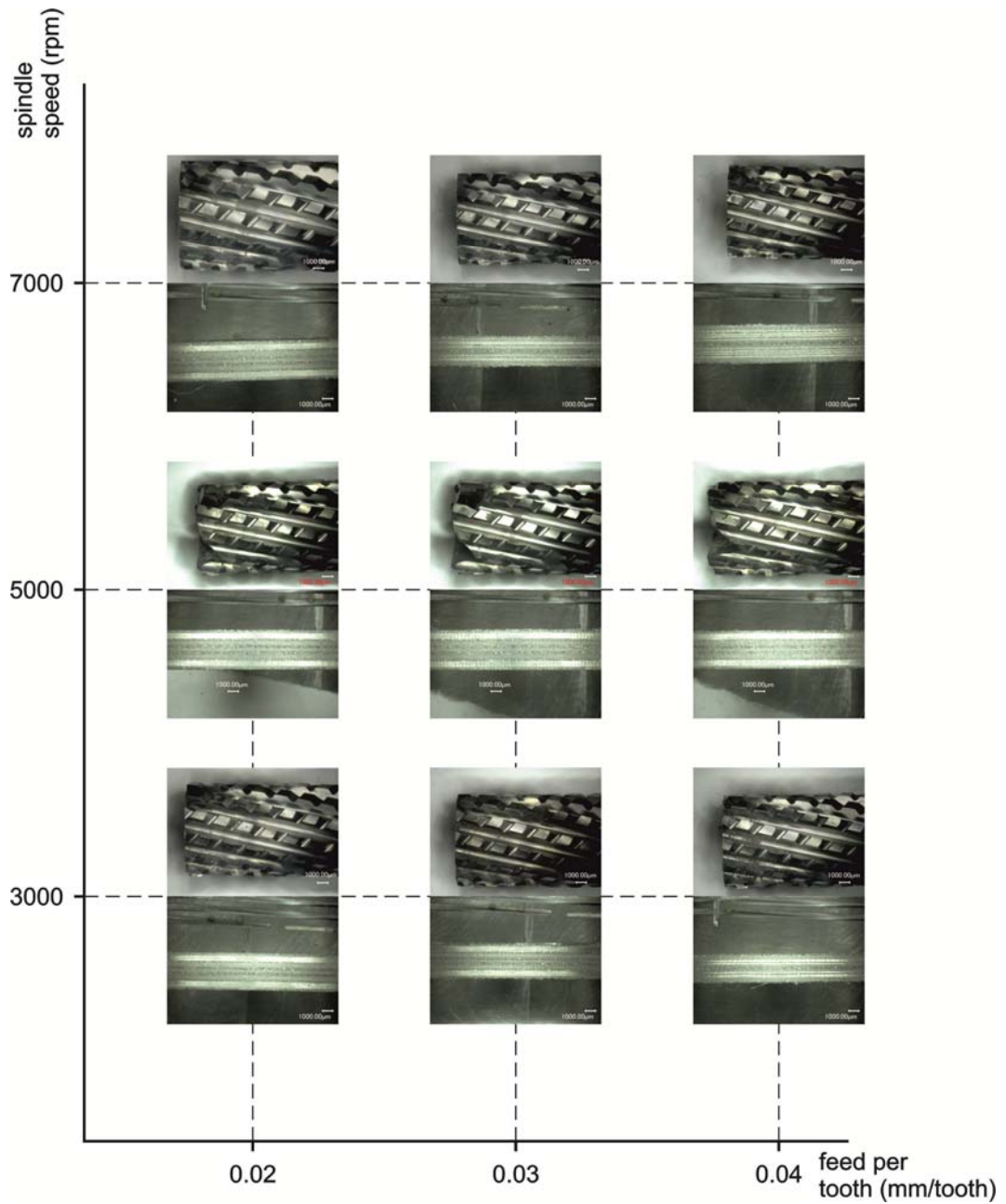


Figure 4.26 The Results of Experiments According to Spindle Speed and Feed per Tooth

As observed in the Figure 4.26, while delamination does not occur any feed per tooth and spindle speed values, there are edge chippings are seen on the cutting tool edges in 0.02, 0.03 and 0.04 feed per tooth values. Due to the machining time, the values at 3000 rpm is eliminated. In conclusion, the most appropriate cutting conditions are obtained at 5000 rpm.



## CHAPTER 5

### CONCLUSIONS AND FUTURE WORKS

#### 5.1 Conclusions

This research concentrated on the issue of developing a method for quantifying tool wear in diamond coated interlocked knurled tool, and of developing a method that would suggest the time for tool replacement during the edge trimming of CFRP composite material. The workpiece used was a 28-ply unidirectional CFRP panel with an overall thickness of 3.5 millimeter. Considering delamination damage as a controlling factor, the routing operation on CFRP panels was carried out on a 3-axis CNC machine router. An optical microscope was used to measure tool wear during the trimming operation of CFRP composite material for different combinations of machining parameters as spindle speed and feed speeds. In addition, cutting tool forces cutting tool wear and delamination were monitored and recorded at regular intervals of time.

The following conclusions are reached after the evaluation of the test results:

- Delamination on the workpiece occurs with a rise in feed speed and it is observed to decrease with an increase in the spindle speed. Feed speed is the most prominent factor affecting delamination.
- The cutting forces increases with a rise in spindle speed and feed speed.
- For high feed speeds, material adhesion occurs on the cutting tool at the beginning and then it causes edge chipping on the tool edges.

- The best cutting conditions for high surface quality are obtained for high spindle speeds and low feed speeds, and the worst cutting conditions are for low spindle speed and high feed speed.
- The workpiece material and its ply orientation play important roles for observing suitable cutting conditions. For the same ply orientation, when the workpiece material thickness increases, the cutting forces and the amount of edge chipping rises up.
- The ANOVA equation for the effect of spindle speed, feed per tooth and cutting distance on delamination was obtained.

## **5.2 Future Works**

- This thesis involved varying the spindle speed and feed speed, while the depth of cut was kept constant. The effect of varying the depth of cut could be investigated.
- The effect of cutting forces on surface finish might be studied in detail.
- Different tools with varying tool geometry can be used to study the effects of process parameters on tool life and surface quality.
- The wear characteristics of the knurled tool were determined only by examining it under an optical microscope. Better knowledge and measurement of wear propagation phenomenon could be acquired by analyzing it under a scanning electron microscope (SEM).
- The routing of CFRP panels was conducted under dry cutting conditions. The effect of using coolant on tool wear, surface quality and delamination might be examined.
- Different thicknesses and ply orientations could be chosen for workpiece material to investigate the effect of cutting parameters.

## REFERENCES

- [1] Mallick, P. K., 'Fiber Reinforced Composites', New York, Marcel Dekker, Inc., 1988.
- [2] Colligan K. & Ramulu M., 'Edge trimming of graphite/epoxy with diamond abrasive cutters', American Society of Mechanical Engineers Materials Division MD, Machining of Advanced Composites, 45, 97-115, 1993.
- [3] Ramulu M., Koshy P. & Jahanmir S., 'Machining of Ceramics and Composites', New York, Marcel Dekker, Inc., 1999.
- [4] Wern, C. W., 'Surface characteristics of machined graphite/epoxy composite', MS Thesis (University of Washington), 1991.
- [5] Konig W., Wulf P Ch., Grab P. & Willerscheid H., 'Machining of fiber reinforced plastics', Annals of CIRP, 34, 537-547, 1985.
- [6] Santhanakrishnan, G., Krishnamurthy, R., Malhotra, S.K., 'Mechanics of tool wear during machining of advanced fibrous composites', International Conference on Machining of Advanced Material, V 847, PP 489-500, 1993.
- [7] Ferreira, J.R., Coppini, N.L., Neto Levy, F., 'Characteristics of carbon-carbon composite turning', Journal of Materials Processing Technology, V 109, PP 65-71, 2001.
- [8] Komanduri, R., 'Machining of fiber reinforced composites', Machining Science, and Technology, V1, N1, PP-113-152, 1997.
- [9] Teti, R., 'Machining of composite materials', CIRP Annals-Manufacturing Technology, V 51, N 2, PP-611-634, 2002.

- [10] Ferreira, J.R., Coppini, N.L., Miranda, G. W. A., ‘Machining optimization in carbon fiber reinforced composite materials’, *Journal of Materials Processing Technology*, V 92-93, PP-135-140, 1999.
- [11] Hocheng H., Puw H. Y. & Huanh Y. ‘Preliminary study on milling of unidirectional carbon fiber reinforced plastics’, *Composite Manufacturing*, V 4, PP-103-108, 1993.
- [12] Koplev, A., Lystrup, A. and Vorm, T., ‘The cutting process, chips, and cutting forces in machining CFRP’, *Composites*, Vol. 14, No. 4, pp.371–376, 1983.
- [13] Puw, H.Y., Hocheng, H., ‘Machinability test of carbon fiber reinforced plastics in milling’, *Journal of Materials & Manufacturing Processes*, V 8, PP717-729, 1993.
- [14] Konig, W., Wulf, Ch., Grab, P., Willerscheid, H., ‘Machining of fiber reinforced plastics’, *Annals of the CIRP*, V 34, N2, PP 537-547, 1985.
- [15] Ramulu, M., ‘Machining and surface integrity of fiber reinforced composites’, *Sadhana*, 22 , 449-472, 1997.
- [16] Sadat, A. B. ‘Machining of graphite/epoxy material’, *SAMPE Quartely*, V 14, PP-1-4, 1988.
- [17] Devi Kalla, Jamal Sheikh-Ahmad, Janet Twomey, ‘ Prediction of cutting forces in helical end milling fiber reinforced polymer’, *International Journal Machine Tools and Manufacture* , 50, PP-882-891, 2010.
- [18] Ramulu M., Arola D. & Colligan K., ‘Preliminary investigation of machining effects on the surface integrity of fiber reinforced plastic’, *Proceedings of the Engineering System Design and Analysis Conference*, 2, 93-101, 1994.
- [19] Ramulu M. & Arola D., ‘Manufacturing effects on the impact properties of graphite/epoxy composites’, *Proceedings of the American Society for Composites Tenth Technical Conference*, 239-248, 1995.

- [20] Colligan K. & Ramulu M., ‘Delamination in surface plies of graphite/epoxy caused by edge trimming process’ *Processing and Manufacturing of composite materials*, 49, 113-126, 1991.
- [21] Yiğit Karpat, Naki Polat, ‘ Mechanistic force modeling for milling of carbon fiber reinforced polymers with double helix tools’ , *International Journal Machine Tools and Manufacture* , 62, PP-95-98, 2013.
- [22] Yiğit Karpat, Onur Bahtiyar, Burak Değer, ‘ Mechanistic force modeling for milling of unidirectional carbon fiber reinforced polymer laminates’ , *International Journal Machine Tools and Manufacture* , 56, PP-79-93, 2012.
- [23] Wolfgang Hintze, Dirk Hantman, Christoph Schütte, ‘Occurrence and propagation of delamination during the machining of carbon fiber reinforced plastics (CFRPs)’ , *Composite Science and Technology* , 71, PP-1719-1726, 2011.
- [24] H.Y. Puw, H. Hocheng, ‘Milling of Polymer Composites’, PP-267-294, 1999.
- [25] J. Sheikh-Ahmad, J. Twomey, D. Kalla, P. Lodhia, ‘Multiple regression of and committee neural network force prediction models in milling FRP’, *Machining Science and Technology* 11, 3, 391-412, 2007.